Master Thesis
TVVR 17/5003

Potentials and limitations of 1D, 2D and coupled 1D-2D flood modelling in HEC-RAS

A case study on Höje river

Alexander Betsholtz
Beatrice Nordlöf

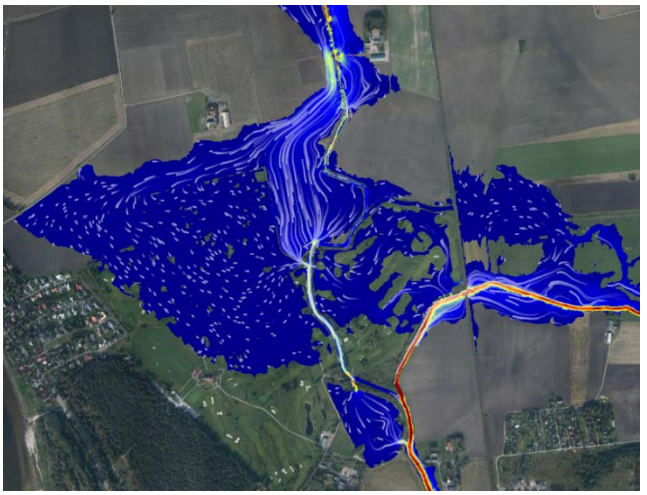

Division of Water Resources Engineering
Department of Building and Environmental Technology
Lund University

Potentials and limitations of 1D, 2D and coupled 1D-2D flood modelling in HEC-RAS

A case study on Höje river

By:
Alexander Betsholtz
Beatrice Nordlöf

Master thesis

Division of Water Resources Engineering
Department of Building & Environmental Technology
Lund University
Box 118
221 00 Lund, Sweden

Water Resources Engineering
TVVR-17/5003
ISSN 1101-9824

Lund 2017

www.tvrl.lth.se

Master Thesis

Division of Water Resources Engineering

Department of Building & Environmental Technology

Lund University

Swedish title: Begränsningar och möjligheter med 1D, 2D och kopplad 1D-2D modellering i HEC-RAS - En fallstudie av Höje Å

English title: Potentials and limitations of 1D, 2D and coupled 1D-2D flood modelling in HEC-RAS - A case study on Höje river

Author(s): Alexander Betsholtz, Beatrice Nordlöf

Supervisor: Rolf Larsson, Håkan Persson

Examiner: Magnus Larson

Language: English

Year: 2017

Keywords: Hydraulic modelling; HEC-RAS; 1D; 2D; 1D-2D; flooding; sub-grid

Acknowledgements

To our supervisor at SMHI, Håkan Persson, thank you for taking your time to talk every week and discuss hydraulic modelling and HEC-RAS specifics.

We would also like to thank our supervisor at Lund University, Rolf Larsson, who helped developing the project and providing us with important background information about the study area. To our examiner, Magnus Larsson and opponents, Julia Wallden and Josefin Tollgren, thank you for valuable feedback on the report.

Thanks also to doctoral student Björn Almström, who provided us with valuable information and tips regarding hydraulic modelling in Höje river.

Lastly, thanks to student and friend Hampus Nilsson for fruitful discussions around the dinner table.

Abstract

Hydraulic models can be used to predict the consequences of flooding events. In this project, three hydraulic models were constructed using the software HEC-RAS, and compared through a case study on Höje river catchment. The models include (i) a 1-dimensional (1D) model, where river and floodplain flow is modeled in 1D, (ii) a coupled 1D-2D model, where river flow is modeled in 1D and floodplain flow is modeled in 2D, and (iii) a pure 2D model, where river and floodplain flow is modeled in 2D. Important differences between data requirements, pre-processing, model set-up and results were highlighted and summarized, and a rough guide that may be used when deciding the appropriate type of model for a project, was presented. In addition, the sub-grid technique used in 2D HEC-RAS modelling was studied by investigating the influence of computational mesh structure and coupling between 1D and 2D areas. The results showed that all three models could successfully reproduce a historic flooding event. The 2D and 1D-2Ds model could also provide more detailed information regarding flood propagation and velocities on the floodplain. The results from the 2D mesh analysis show that model result is very sensitive to mesh alignment along barriers. In rural floodplains with clear barriers, computational cell alignment is more important than computational cell size. With regards to the 1D-2D model, the results showed that the parameters describing the coupling between the 1D and 2D domain have large impact on model results.

Sammanfattning

Hydrauliska modeller kan användas för att förutsäga effekterna av översvämningar. I detta projekt har tre hydrauliska modeller konstruerats med modellverktyget HEC-RAS. Modellerna har jämförts genom en fallstudie av Höje Å avrinningsområde. Modellerna inkluderar: (i) En 1D-modell, där flöde i flodfåran och på flodplanet modelleras i 1 dimension, (ii) en kopplad 1D-2D modell där flödet i flodfåra modelleras i 1 dimension, och flödet på flodplanet modelleras i 2 dimensioner samt, (iii) en ren 2D modell där både flödet i flodfåran och på flodplanet modelleras i 2 dimensioner. Viktiga skillnader mellan modellerna vad gäller dataunderlag, förbehandling, modelluppbyggnad och resultat har lyfts fram och sammanfattats, och en enkel guide har presenterats som kan användas för att välja lämplig typ av modell för ett givet projekt. Utöver detta har programmets sub-grid teknik för 2D modellering studerats genom att undersöka hur konfigurationen på beräkningsnätet samt kopplingen mellan 1D och 2D påverkar modellresultaten. Resultaten visar att alla tre modeller kunde användas för att reproducera en historisk översvämning. 2D och 1D-2D modellerna kunde dessutom beskriva översvämningens dynamik mer i detalj. Analysen av beräkningsnätets påverkan visade att modellresultaten påverkas mer av hur beräkningscellerna är orienterade än av storleken på beräkningscellerna på flodplan med tydliga barriärer. Analysen visade också att resultaten i hög grad påverkas av hur kopplingen mellan 1D och 2D modellen beskrivs.

Table of contents

1 Introduction

Flooding events are some of the worlds most significant natural hazards. Between 1998 and 2009, the 216 largest european flooding events caused a total of 1126 fatalities and an estimated economical loss of 52.2 billion euros (European Environment Agency, 2010). Meanwhile, an increase in floods is expected in the future. The mean global sea water level is expected to rise by up to 0.98 meters by 2100, threatening coastal areas (Church et al., 2013). In urban areas, the damage from heavy rain is expected to increase as a result of urbanization and increases in the intensity and frequency of heavy rainfall (Olsson and Josefsson, 2015).

Flooding events are often separated based on their characteristics. The three most commonly types of floodings are (1) Fluvial floods, (2) pluvial floods, and (3) coastal floods. Most common are *fluvial* floods, caused when the water surface of a river is rising above its river banks, flooding nearby areas. Fluvial floods are controlled by hydrological processes (such as precipitation, evaporation and infiltration) occurring over large temporal and spatial scales, and typically occur after periods of sustained rainfall. On the other hand there are *pluvial* (urban) floods, occurring when the intensity of the rain exceeds the infiltration capacity of the ground, resulting in overland flow and, when the stormwater system is insufficient, flooding. Pluvial floods do, in contrast to fluvial events, occur on a significantly smaller temporal and spatial scale, making them harder to predict (Olsson and Josefsson, 2015). Lastly, *coastal* floods are caused by increases in sea water levels due to set up from winds, waves, climate change etc. affecting low-elevation land next to seas.

In order to try to predict the consequences of flooding, different modelling techniques are typically applied. River flow is estimated using *hydrological modelling*, while *hydraulic modelling* is required to compute water depths and velocities in order to assess the actual consequences of a certain river flow or overland flow.

Over the last decades, the performance of hydraulic models have improved tremendously as a result of more powerful computers, while techniques such as remote sensing and radar has improved the detail of the input data (e.g. rainfall, topography and land use). As promising as new technology seems to be, modellers still face problems with lack off reliable data. In addition, current models are still far from able to correctly represent the complexity of natural and urban environments. Important trade-offs have to be made between the performance/detail of the model and the time (and money) spent setting up and running the model (Salvadore et al., 2015).

Fluvial flooding can be modelled in many different ways. Traditionally, the river and the surrounding floodplains are represented by a set of cross sections, in between which the flow is modeled only in one dimension (*1D-models*). While such models seem to perform well in straight rivers where the flow is restricted in a mostly 1D direction also during elevated water levels, rivers that have flat and/or complex floodplains require a 2-dimension (2D) flow representation to account for the many individual 2D flow paths that will arise when the river is flooded (e.g. Horritt and Bates (2002) and Tayefi et al. (2007)). This has led to the development of *coupled 1D-2D models*, where the river is represented by 1D flow between cross sections, and the floodplain is represented by

a computational mesh where flow modeled is in 2D. *Pure 2D models* also exist, with both river and floodplain flow is modelled in 2D. However, such models require detailed representation of the river bathymetry, which increases computation times. In addition, rivers are often manipulated with bridges, weirs and culverts, and methods for presenting such structures are only well developed for 1D modelling purposes (Babister et al., 2012). While coupled 1D(river)-2D(floodplain) is favoured in literature, the connection between the two model descriptions is problematic with respect to set-up, stability and description of the flow (US-ACE, 2015). Furthermore, by using models that incorporate terrain representation that are smaller than the computational mesh (so called *sub-grid models*), such as the hydraulic modeling software HEC-RAS, computation times for pure 2D applications might be reduced substantially, making pure 2D modelling a potentially interesting alternative to 1D-2D.

The performance of sub-grid models are not well studied, neither in rural, nor urban areas. Important questions regarding suitable mesh size and mesh orientation remains, including software specific considerations for 2D modelling in HEC-RAS.

Overall, comparisons between the use of 1D, 1D-2D and 2D models are rarely done in literature. In addition, most studies target calibration and validation of the models and do not incorporate important differences and considerations during model set-up.

With this background, this study aims to investigate important differences between 1D, 2D and coupled 1D-2D modelling in HEC-RAS. The study is constructed as a case study on the lower part of the Höje river catchment, including considerations for Lomma city.

1.1 Aim

The general objective with this project is to study and compare different methods for flood modelling and inundation mapping. The aim is to identify differences, potentials, and limitations of 1D, 2D and 1D-2D HEC-RAS models for the modelling of fluvial flooding events. Furthermore, the study aims at investigating model specific aspects regarding the use of 1D, 2D and 1D-2D models in HEC-RAS.

More specifically, the following questions will be addressed:

- How do the models differ in terms of data requirements, pre-processing, model set-up, and output?
- For what applications could 1D, 2D or 1D-2D models be suitable?
- How sensitive is flood inundation to computational mesh construction?
- How should the computational mesh be designed around the river and on the floodplain respectively?
- Can pluvial flooding events be modeled using HEC-RAS 2D?
- How does the parameters describing the 1D-2D connection affect model results and stability?

1.2 Method

The study is conducted through a case study on Höje River catchment where the following three models will be constructed:

- A 1D model, where flow is modeled in one dimension both inside the river and on the floodplains.
- A coupled 1D-2D model, where river flow is modeled in one dimension and floodplain flow in two dimensions.
- A pure 2D model, where both river and floodplain flow is modeled in two dimensions.

The models are calibrated against the flooding event of July 2007 and compared with respect to data-requirements, construction and capabilities to model flood dynamics.

A literature study, targeting important theory regarding hydraulic modelling of rural and urban areas, mathematical background of equations and solution schemes as well as general theory and methodology of the HEC-RAS software, is presented chapter 3-4. Case specific information, as well as data collection and pre-processing is presented in chapters 5-6.

Model set-up and result is presented separately for each of the models in chapter 7-9, and a comparison is shown in chapter 10. Model-specific design considerations are investigated in the sensitivity analysis of respective model chapter. The 2D model will, in addition to the fluvial modelling, include a brief study targeting geometric set-up in urban areas.

1.3 Limitations

This study aims at comparing the performance of 1- and 2-dimensional hydraulic models developed using HEC-RAS. No other hydraulic simulation software are used, and the study does not aim at comparing HEC-RAS with other hydraulic models. The models are not compared with respect to their ability to match validation data, simply because no such data existed.

No hydrological simulations are performed in this study. HEC-RAS does not have the capability to model infiltration, evaporation, groundwater flow or snow melt. Small scale rainfall-runoff simulations are performed, these are limited to modelling surface runoff. Flow in pipe networks or infiltration on green surfaces cannot be modeled using HEC-RAS.

The study does not look into details of the modelling of hydraulic structures. The bridge modelling options will be presented and tested briefly, to contribute to the the comparison between 1D, 2D and 1D-2D capabilities.

The study will not investigate geometric sensitivity when modeling fluvial events in urban areas, as no urban areas in the study area showed to be significantly impacted by fluvial flooding, even during extreme events.

2 Hydraulic modelling in 1D and 2D

For decades hydraulic models has been used to asses potential effects of fluvial and pluvial flooding events. There is a broad variety of models available today that are being used both in research and in commercial applications. The types of model vary both in the way that the governing equations are formulated, in the numerical solution of the governing equations, as well as in the way that the geometric properties of the system are described. This section aims at giving an introduction to the types of models that are being used, highlight potentials and limitations with different modelling approaches, and to present some challenges that remains to be addressed within the field of hydraulic modelling.

Traditionally, 1D river models have been used to model fluvial flooding events. 1D models are made up of a series of cross sections describing the topography of the river and floodplain, and water levels are calculated using the 1-dimensional form of the governing equations. 1D models only require topographical data to be collected at the cross sections that make up the model, which was a major advantage when access to topographic data was limited.

While 1D models perform well when flow is restricted between channel banks, 2D modelling have shown to better estimate flows in topographically complex floodplains, where the flow is considered largely 2-dimensional (e.g. Andersson and Bates (1993), Tayefi et al. (2007), Cook and Merwade (2009), Vojinovic and Tutulic (2008)). In these applications, 1D models may underestimate frictional losses, inundation extents and fail to capture flood dynamics (Tayefi et al., 2007).

2D models hydraulic models consist (most often) of a 2D computational mesh/grid, representing the underlying topography by connected cells/elements. In contrast to 1D, 2D models need continuous topographical data, covering the whole area that is to be modeled in 2D. Thanks to the development of Light Detection And Ranging (LIDAR) techniques for land surveying, the availability of high resolution topographic data has increased significantly in recent years, favouring the development of 2D hydraulic models.

Although floodplain flow is best represented in 2D, river channel flow is considered highly 1-dimensional, and 1D river modelling has been standard practice for decades. The importance of correct river representation has been highlighted in many articles (e.g. Horritt et al. (2006),Cook and Merwade (2009). For pure 2D modelling, it i suggested that the channel width is represented by at least 5 cells (Babister et al., 2012), something that might substantially increase computation times without improving model results. Furthermore, techniques for representing hydraulic structures (such as bridges, culverts and weirs) are based on empirical relationships derived for 1D applications. 2D representations may be able to incorporate some of the energy losses generated by contraction and expansion, although smaller scale phenomena, such as the formation of eddies around piers are much smaller than reasonable mesh sizes. Overall, there are less guidelines as how to handle energy losses around structures in 2D than in 1D (Babister et al., 2012). A final aspect of 2D river modelling is the lack of continuous river bathymetry data, shown to be very important for model results

(Cook and Merwade, 2009). This is because the LIDAR is incapable of penetrating the water surface. As a result 2D river models need to interpolate bathymetry from existing cross sectional data, resulting in additional work and uncertainty (Costabile and Macchione, 2015).

In order to benefit from the strengths of both 1D and 2D models, coupled 1D-2D models, where channel flow is represented using a 1D approach, and overbank flow is modeled in 2D, were introduced. However, these types of models require some kind of description of the coupling between the 1D and 2D domain. One solution is to run the 1D model separately to generate a boundary condition to the 2D domain of the model, this is referred to as loose coupling, and has been applied in many studies (e.g. Yu and Lane (2011), Yu and Lane (2006b),McMillan and Brasington (2007)). Yu (2005) compared the loose coupling technique with a so called tight coupling technique, where the 1D and 2D domains are coupled on a time step basis. The study showed that the choice of coupling technique can impact modeled inundation extent. Furthermore, they showed that loose coupling can lead to continuity errors since water cannot flow back into the 1D domain of the model. Tight 1D-2D couplings are often calculated using lateral weir equations, where flow is calculated from the water levels differences. Recent studies by for example Morales-Hernández et al. (2016) have proposed 1D-2D coupling techniques where both mass and momentum is conserved. The version of HEC-RAS used in this project allows for 1D-2D coupling on a time step basis. Flow between the domains can be calculated using a lateral weir equation (US-ACE, 2015), or by imposing 1D water levels onto the 2D domain as a stage boundary condition (US-ACE, 2016).

The main issue with 2D modelling are the often large computation times. In many areas, performing computations on the same resolution as the topographic detail generated by LIDAR techniques will result in unreasonable computation times. Thus, the effect of spatial resolution of 2D hydraulic models is a topic that as been explored extensively in literature (e.g. Yu and Lane (2006a) and Horritt and Bates (2001)). Yu and Lane (2006a) showed that decreasing the spatial resolution will, by smoothing the topography, (i) increase the rate of flood propagation of the inundation (overestimate flooding extents) and, more importantly, (ii) that it may change the direction of the propagation. While the first may be compensated by increasing the friction parameter, the latter cannot. In order to address these issues, Yu and Lane (2006b), amongst others (e.g. McMillan and Brasington (2007), and Casulli (2008)), have developed models that can represent the topographical data on a sub-grid level, capturing important features while keeping the computational grid large, reducing computation times. In the study by Yu and Lane (2006b), this was done by changing the stage-volume representation as well as introducing a porosity representation of the flux between cells, considering whether all sub-grid cells along the face of the larger computational cell are wet or not. The sub-grid representation was shown to produce a better result than could be attained by using a non-sub-grid approach and calibrating using the friction parameter: The sub-grid approach was both better at validating the extent at a certain point in time and produced a more similar extent over time as when using a higher resolution computational mesh.

Still, work remained regarding the optimization of resolution on computational grid scale and sub-grid scales. This issue was partly investigated by Yu and Lane (2011) - comparing inundation extent for various computational mesh sizes for a fluvial flooding in a rural area, with several clearly defined barriers in the floodplain. The study showed that sub-grid representation improves the results for all tested computational cell sizes in terms of producing more similar inundation extents as generated by a higher resolution mesh. Using 8m computational cell size with sub-grid (4m) representation heavily improved the result compared to the 8m - non sub-grid results. However, corresponding improvements were much smaller for larger cell sizes, indicating that sub-grid representation won't necessarily lead to large improvements for any given computational cell size. McMillan and Brasington (2007), did a similar study on fluvial flooding in an urban area. Using a 10m computation mesh size with sub-grid representation, they were able to produce similar inundation extent as using a 2m computational mesh, whereas a 10 m computational mesh (without sub-grid representation) overestimated the extent.

The development of sub-grid representations has increased the scale over which 2D models can be applied. For example, Neal et al. (2012a) used a pure 2D model with a sub-grid representation of both channel and floodplain flow over a 800km reach of the Niger river, Mali. The sub-grid representation had better agreement with satellite data than corresponding coupled 1D-2D (non sub-grid) model, indicating that representation of small channels, falling within the computational grid cell size, can be very important.

The literature study highlights several lacks of research and investigations when it comes to the use of 1D, 1D-2D and pure 2D modelling. Overall, there is a lack of studies looking at the use of sub-grid models for river channel modelling. The ones found have mainly targeted large scale applications (reaches of several 100 km) where topographical data is sparse (e.g. Neal et al. (2012b)) and the river width falls well within the size of the mesh. The use sub-grid models for river and floodplain representation for smaller applications in data rich environments thus still needs research. No studies looking at 1D models tightly coupled to sub-grid 2D models were found during the review. A question that remains to be addressed more in detail is how 1D-2D approaches differ from pure 2D approaches when modeling channel flow and channel-floodplain interaction.

Most of the studies found in the literature focused on model performance and accuracy of model results. In non-research applications, factors such as model set-up time, data requirements, computation times, and robustness will impact the model choice. Thus, this study aims at modeling channel and floodplain flow using 1D, 2D and 1D-2D modeling techniques, and comparing not only model performance, but also looking at factors presented above, relevant from a user perspective.

3 Theoretical background

This chapter will introduce the basic equations governing 1- and 2-dimensional (1D and 2D) unsteady flow, as well as a simplification of these equations, and some basics regarding the numerical solution of these equations.

Unsteady fluid flow varies in both space and time. The flow is governed by the conservation of mass and momentum, which can be described by a set of equations referred to as the *Shallow Water Equations* (also referred to as the St Venants equations). The following sections presents the 1D and 2D formulations of these equations.

3.1 Assumptions

The 1D and 2D Shallow water equations are based on a set of assumptions that may be more or less suitable depending on the application, and understanding their implications are therefore important. These assumption are the following.

- The fluid is incompressible: The volume is proportional to the mass since the density is assumed constant.
- The pressure distribution is hydrostatic: vertical accelerations are neglected
- The flow is one- or two-dimensional, vertical variations in flow and velocity are neglected.
- The wave lengths are much larger than the water depth.
- The average channel bed slope is small.
- Bed friction can be calculated using Manning's equation, which has been derived for steady flow conditions.
- The flow can be described as continuous functions of the velocity and the water surface elevation H.

3.2 1D unsteady flow

In many river modelling applications it is assumed that the flow is 1D. The flow is then calculated using the 1D formulation of the St Venants equations, which will be presented below.

3.2.1 1D continuity equation

The continuity equation describes the preservation of mass in a given control volume. It states that the net mass flux equals the change in storage. The 1D form of the St.

Venant continuity equation can be written in the following form:

$$\frac{\partial(Q)}{\partial x} + \frac{\partial A}{\partial t} + q = 0 \tag{3.1}$$

Where Q is the flow rate, A is the cross sectional area and q is the lateral inflow.

3.2.2 1D momentum equation

The momentum equation is based on Newtons second law of motion, stating that the sum of the forces acting acting on an element equals the rate of change of momentum. The formulation of the momentum equation will be different depending on what forces that are being considered. Taking pressure, gravity and frictional resistance into account, the 1-dimensional continuity equation can be written as:

$$\frac{\partial V}{\partial t} + g\frac{\partial}{\partial x}\left(\frac{V^2}{2g} + h\right) = g(S_0 - S_f) \tag{3.2}$$

Where V is the flow velocity, g is the gravitational acceleration, h is the water depth, S_0 is the bed slope and S_f is the friction slope.

3.3 2D unsteady flow

When studying flow over complex floodplains the assumption that flow is 1D may no longer be valid. 2D unsteady flow varies in time and along two spatial dimensions. The governing principles of 2D unsteady flow are the same as for 1D flow, the conservation of mass and momentum.

3.3.1 2D continuity equation

The 2D form of the continuity equation states, just as the 1D form, that the net mass flux into the control volume equals the change in storage in the control volume. The difference is that the mass fluxes are now calculated in 2 dimensions. The 2-dimensional continuity equation can be written as:

$$\frac{\partial H}{\partial t} + \frac{\partial(hu)}{\partial x} + \frac{\partial(hv)}{\partial y} + q = 0 \tag{3.3}$$

Where H is the water surface elevation, h is the water depth, u and v are the depth averaged velocities in the x- and y-direction, and q is the source term, representing inflow from external sources such as precipitation. (Chaudhry, 2008)

3.3.2 2D momentum equation

As in the 1D case, the momentum balance is based on the principle that the sum of forces acting on an element equals the rate of change of momentum. Considering forcing from gravity, eddy viscosity (momentum exchange), friction and the Coriolis effect, the 2D momentum balance equations can be written as follows.

Momentum balance in the x-direction:

$$\frac{\partial u}{\partial t} + u\frac{\partial u}{\partial x} + v\frac{\partial u}{\partial y} = -g\frac{\partial H}{\partial x} + \nu_t\left(\frac{\partial^2 u}{\partial x^2} + \frac{\partial^2 u}{\partial y^2}\right) - c_f u + fv \tag{3.4}$$

The momentum balance in the y-direction:

$$\frac{\partial v}{\partial t} + u\frac{\partial v}{\partial x} + v\frac{\partial v}{\partial y} = -g\frac{\partial H}{\partial y} + \nu_t\left(\frac{\partial^2 v}{\partial x^2} + \frac{\partial^2 v}{\partial y^2}\right) - c_f v + fu \tag{3.5}$$

where H is the water surface elevation, ν_t is the eddy viscosity coefficient, c_f is the friction coefficient , f is the Coriolis parameter and v and u are depth averaged velocities in the x and y directions respectively (Brunner, 2016a). The first term in the momentum equations represents the local acceleration ($\frac{\partial u}{\partial t}$ in equation 3.4, corresponding term in 3.5), the second term ($u\frac{\partial u}{\partial x} + v\frac{\partial u}{\partial y}$ in 3.4, corresponding term in 3.5) is the convective acceleration, the following terms describes the forcing from gravity, eddy viscosity, bed friction, and Coriolis force. Using the Manning's formula, the friction coefficient c_f can be expressed as following (in the x-direction):

$$c_f = \frac{n^2 g|u|}{R^{4/3}} \tag{3.6}$$

where n is Manning's n, g the gravitational constant, u the velocity in the x-direction and R the hydraulic radius.

3.4 Modelling simplifications

In order to reduce the computation time and reduce numerical instability, the full Shallow Water Equations are often simplified by neglecting different terms in the momentum equation. These simplifications are most often applied in 2D models. These simplifications are only valid for certain flow conditions, meaning that the understanding of their respective use and limitations is necessary if they are to be employed (Babister et al., 2012) While several different simplifications exist, this report will only present the main simplification/approximation used in HEC-RAS, namely the *Diffusive wave approximation*. In HEC-RAS, this approximation can be used instead of the 2D full momentum equations.

3.4.1 Diffusive wave approximation

If gravity and friction are assumed to be the dominating forces acting on the control volume, the momentum equation can be simplified to the so called diffusive wave approximation of the momentum equation. The following derivation follows the HEC-RAS Hydraulic Reference Manual (Brunner, 2016a).

In the diffusive wave approximation of the momentum equation the acceleration terms as well as the eddy viscosity and Coriolis terms are neglected, and the momentum balance is written as a balance between gravitation and bottom friction forces. The momentum equation can now be written as:

$$g\nabla H = -c_f V \tag{3.7}$$

Where V is the flow velocity in vector form V=(u,v).

If the bottom friction is evaluated using the Manning formula, equation 3.7 can be rewritten as:

$$V = \frac{-(R(H))^{2/3}}{n} \frac{\nabla H}{|\nabla H|^{1/2}} \tag{3.8}$$

Where $R(H)$ is the hydraulic radius at the water surface elevation H, ∇ is the differential operator, and n is the Manning friction coefficient.

Inserting equation 3.8 into the continuity equation 3.3 and writing in vector form gives:

$$\frac{\partial H}{\partial t} + \nabla \bullet \beta \nabla H + q = 0 \tag{3.9}$$

Where

$$\beta = \frac{-(R(H))^{2/3}}{n}$$

Using the diffusive wave approximation of the shallow water equations the governing equations for 2-dimensional flow (3.3, 3.4 and 3.5) are thus simplified to expression 3.9. The diffusive wave approximation leads to shorter computation time and may reduce model instability. It may be used to describe varying flow in moderate to steep reaches. However, flow separation, eddies as well as momentum transfer cannot be modeled (Babister et al., 2012).

3.5 Solving techniques

The Shallow Water Equations make up a set of partial differential equations that cannot be integrated analytically. In order to obtain the values of the variables the equations need to integrated numerically. The water surface elevation and the flow velocity varies both in space and in time. For each model time step, the computation engine must determine the value of these variables throughout the model domain. This is done by discretising the equations in space and in time, and solving system of equations that arise for one time step at a time. Different numerical methods varies in the way that the governing equations are discretised in space and time, and how the system of equations that arise is solved. A numerical solution scheme can be either explicit, meaning that the values of the variables at time step $n+1$ step are calculated directly from the values provided at time step n, or implicit, meaning that the program iterates to obtain the solution for the next time step. Many hydraulic models are based on finite difference, finite element or finite volume methods (Chaudhry, 2008). The HEC-RAS 1D engine uses a semi-implicit finite difference scheme, and the 2D engine uses a hybrid finite difference-finite volume scheme, where different approximations are made depending on the orientation of the mesh. (Brunner, 2016b)

Numerical methods often put some restrain on the *Courant number* in order for the solution to be accurate and stable. The Courant number can be calculated as:

$$C = \frac{v * \Delta t}{\Delta x} \tag{3.10}$$

Where v is the flow velocity, Δt is the computation time step, and Δx is the spatial step, i.e. cross section spacing in 1D models, and cell size in 2D models. In many model applications, the Courant number must be smaller than 1, meaning that the water should not flow through two cells or between two cross sections within one time step. For 1D HEC-RAS modelling, a Courant number < 1 is recommended, although higher Courant numbers can provide accurate results (Brunner, 2016a). For 2D modelling, the Courant number should preferably be < 1 and no larger than 3 when using the full momentum equation, and < 2, no larger than 5, when using the diffusive wave simplification (US-ACE, 2015).

4 HEC-RAS

HEC-RAS (Hydraulic Engineering Centre River Analysis System) is a hydraulic modelling tool developed by the US Army Corps of Engineers. The software can perform 1D steady state water surface profile calculations, unsteady 1D and 2D flow simulations, water quality modelling and sediment transport modelling (Brunner, 2016b). In this chapter, the basics of HEC-RAS modelling is introduced.

4.1 1D HEC-RAS-modelling

The 1D unsteady computation engine solves the 1D continuity and momentum equations presented in section 3.3 using a semi-implicit finite difference solution scheme. In this section the basics of the HEC-RAS 1D program is presented, along with the data necessary to set up and run an unsteady flow model. A 1D HEC-RAS model consists of geometric data, describing the geometric properties of the study area and flow and/or stage data that makes up the boundary conditions of the model.

4.1.1 Geometric data

A hydraulic model can consist on one or several river reaches, which are connected in junctions. The geometry data required to describe the system is the river reach connectivity, cross section geometry data and data describing the hydraulic structures in the system. The cross sections consist of station-elevation data describing the terrain profile along a transect perpendicular to the flow direction. The cross sections can be divided in main channel and overbank sections with different roughness properties. The hydraulic properties of the system are much dependent on the cross sections, and these are key elements in the hydraulic simulations. Figure 4.1 shows an example of an HEC-RAS cross section.

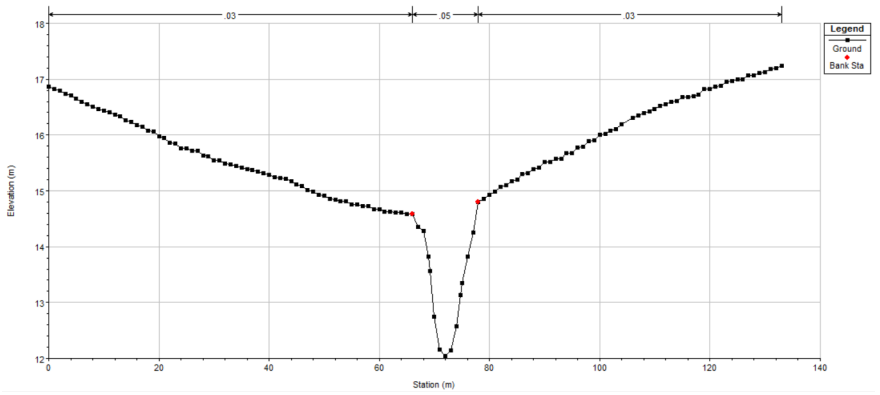

Figure 4.1: Example of a HEC-RAS cross section geometry. Red dots marks the location of the bank stations, separating the main channel from the overbanks.

Each cross section is associated with a hydraulic property table, describing how the cross sectional area and conveyance of the cross section changes with elevation (water level). An example of such a property table is shown in figure 4.2. (Brunner, 2016b). When the hydraulic computations are performed, the computation engine will look in the hydraulic property tables to find the properties corresponding to a given water surface elevation.

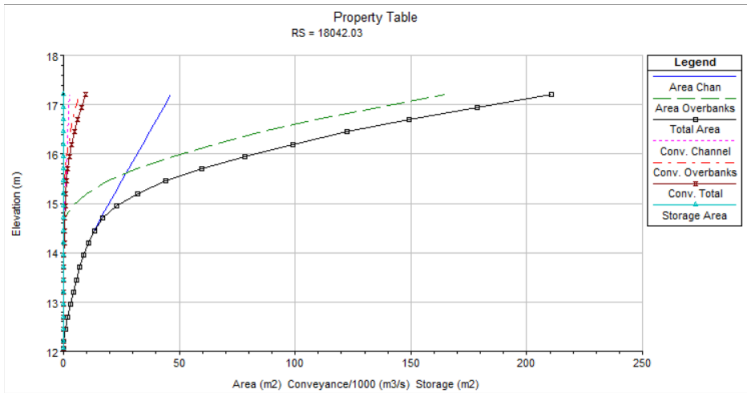

Figure 4.2: Example of property table associated with a cross section. The graph shows how the area and conveyance of the cross section changes with elevation

4.1.1.1 Bridges and hydraulic structures

The 1D HEC-RAS modelling tool is capable of modelling flow around bridges and through culverts. Such hydraulic structures may have large influence on flow dynamics due to the contraction and expansion of the flow around the structure . The program is capable of computing energy losses due to contraction and expansion of the flow, as well as due to submergence of the structure. It is also possible to model pressurized flow through through a culvert or under a bridge (Brunner, 2016b).

In 1D, flow passing a bridge is calculated based on four representative cross sections, two upstream and two downstream of the structure, and a geometric description of the bridge structure itself. The most upstream and most downstream cross sections should be placed at locations were flow is assumed to be fully expanded. The two cross sections in the proximity of the structure should represent the natural ground just upstream and downstream of the structure, to allow the program to compute energy losses due to contraction/expansion of the flow. The bridge structure is described by specifying the elevation of the bridge deck, the elevation of the lower chord of the deck, and the width of the bridge. In this project, flow through the bridge will be computed using the energy equation. However, there exists a variety of methods that can be used within HEC-RAS to compute bridge flow (Brunner, 2016a). This is not something that will be further investigated, as it goes beyond the scope of this project.

4.1.2 Modelling levees in 1D

The 1D computation engine computes a single water surface elevation for each cross section. The entire cross section area is available for flow at all times, and the water surface elevation changes homogeneously over the entire cross section. However, when floodplain flow is confined by a levee this may not be physically accurate. The image below shows a cross section were water is flowing both in the main channel and on the floodplain, without the high ground separating them having been over-topped.

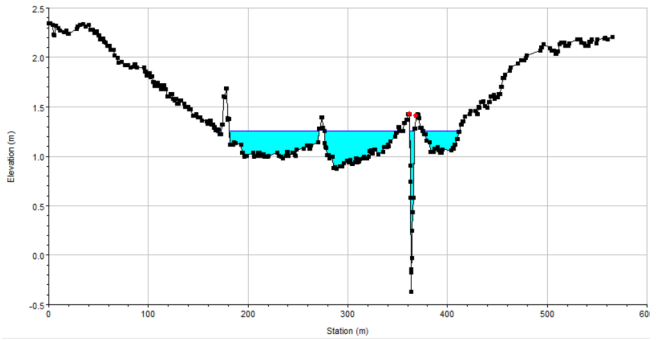

Figure 4.3: Flow in a cross section without levees. The entire cross section area is available for flow.

HEC-RAS 1D has the option to add levees to cross sections to make some regions of the cross section surface area unavailable for flow conveyance when the water level is below the levee level. However, the program can only compute one water surface for the cross section, when the levee is overtopped the entire area behind the levee will be filled with water instantaneously. The image below shows calculated water levels in a cross section for two consecutive time steps. The area to the left is instantaneously filled when the left levee is overtopped.

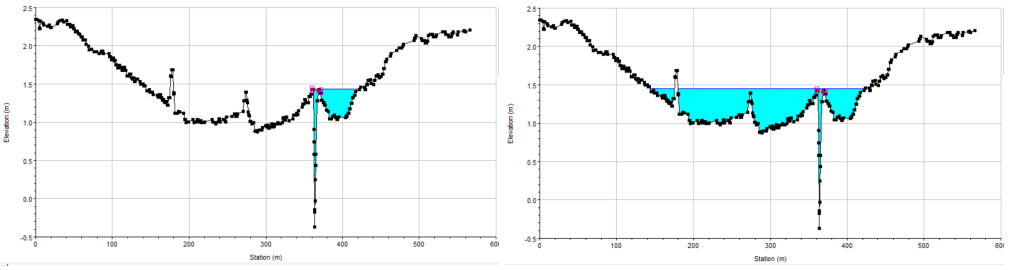

(a) Flow in cross section with levees, right levee is over-topped, left levee is not over-topped.

(b) Flow in cross section from a) one time step later when the left levee has been over-topped.

Figure 4.4: Flow in a cross section with levees.

Another option for modeling overbank flow and levee overtopping in 1D is using storage areas. Storage areas are 1D elements described by a water level - volume relationship. When the water level in a cross section exceeds a levee level, water will flow into the storage area, raising the water level in the storage area in accordance with the water level - volume curve. As the name suggests, the storage areas provide no conveyance of the flow, but simply acts as a sink where water is stored.

4.1.3 Boundary conditions

The HEC-RAS model requires boundary conditions to perform the hydraulic calculations. Depending on the flow regime, and whether the simulation is steady state or time dependent, boundary conditions are required in one or both ends of a reach. When unsteady flow computations are performed, boundary conditions must be specified at both ends of a reach. The upstream boundary condition can consist of either a flow hydrograph, a stage hydrograph or a combined stage and flow hydrograph. The downsteam boundary condition can consist of a stage or flow hydrograph, a rating curve, or as a normal depth assumtion. If normal depth is assumed, the Manning equation is used to calculate a water depth. In addition to the boundary conditions necessary to perform the calculations, flow hydrographs can be entered laterally along a reach. Lateral inflows can be added as a flow hydrograph entering at a single cross section, or as a hydrograph that is uniformly distributed over several cross sections. (Brunner, 2016a)

4.1.4 1D Hydraulic computations

The unsteady computation engine solves the continuity and momentum equations using a linearized finite difference approximation. For every cross section, a water surface elevation and flow velocities in the different compartments (overbank and main channel) is calculated. For a reach consisting of N nodes, the momentum and continuity equations make up a system of 2N-2 equations. Since there are 2N unknowns that need to be solved for, namely ΔQ and Δh in each cross sections, two more equations are required to solve the system of equations. These two equations are the upstream and downstream boundary conditions. The system of equations is solved iteratively until a satisfying solution is obtained in all cross sections, or until the maximum number of iterations is reached.

The user is required to specify the simulation time step Δt and the computation parameter θ. In the implicit solution scheme that is used in the computations the spatial derivatives are evaluated at an interior point $(n+\theta)\Delta t$, where $0.6 < \theta < 1$. The choice of θ can impact model stability and accuracy. In general, a higher value of θ increases model stability but reduces the accuracy of the numerical solution (Brunner, 2016a).

The user can chose to run a warm up period prior to the simulation. During warm up the model is run with the initial flows, allowing for the water surface to stabilize before the actual simulation starts. This may improve model stability in the beginning of the simulation. (Brunner, 2016b)

4.2 2D HEC-RAS modelling

Two dimensional modelling is a relatively new function in HEC-RAS (released in 2014), enabling pure 2D flow models as well as coupled 1D-2D modelling. In this section the features of 2D modelling in HEC-RAS is introduced. More detailed information can be found in the HEC-RAS hydraulic reference manual (Brunner, 2016a).

4.2.1 Mesh construction and features

The 2D geometry is built up by a computational mesh (or computational grid), illustrated in figure 8.3. Each mesh is built up by interconnected cells that may vary in size and shape, although one cell cannot have more than 8 cell faces (sides). Cell faces are similar to 1D cross sections and are used to compute flow between cells, except at the outer boundaries of the mesh (purple). Cell points (red), located at the connection between cell faces, are used used to connect the mesh to 1D structures and 2D boundary conditions. The cell center (blue) is where the water surface elevation is computed for each cell, but doesn't necessarily correspond to the cell centroid.

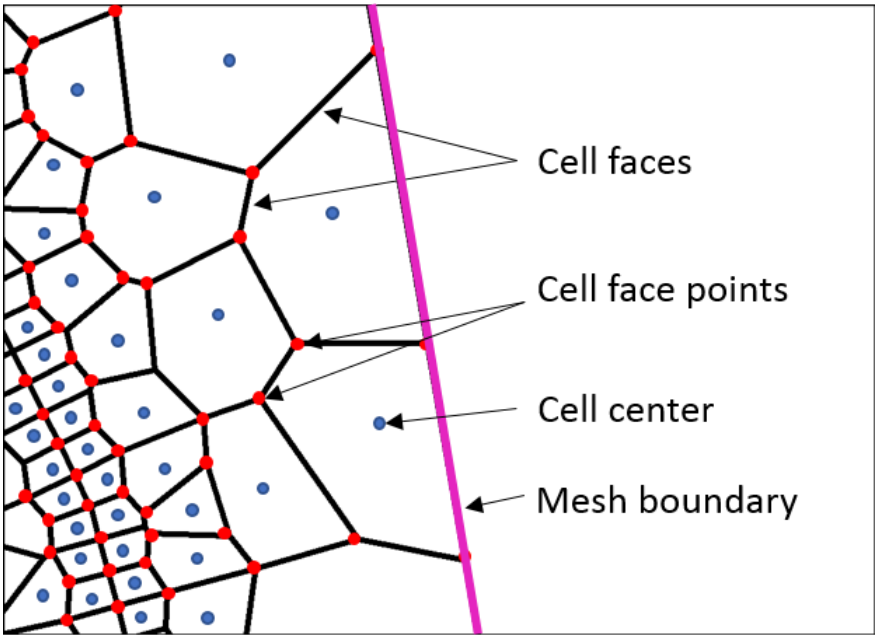

Figure 4.5: Illustration of a computational mesh/grid

4.2.1.1 Sub-grid terrain representation

Compared to many other 2D modelling software, HEC-RAS cells and cell faces are not restricted to contain only one elevation value. Instead, detailed geometric and hydraulic

property tables, based on the resolution of the underlying terrain, are created during pre-processing of the computational mesh. For each cell face, relationships between elevation and profile, area, wetted perimeter and Manning's n are computed. For each computational cell, a relationship between elevation and volume is computed. This is illustrated in figure 4.6.

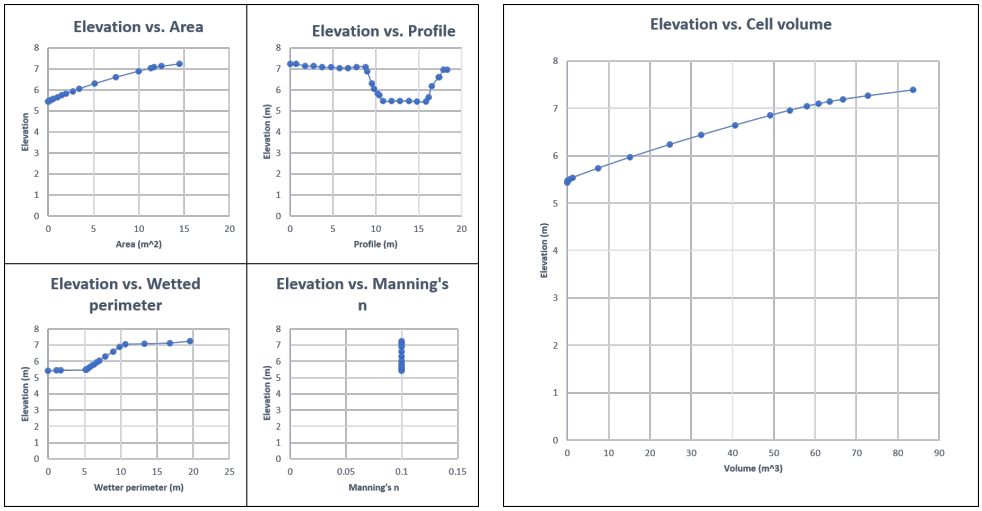

Figure 4.6: Hydraulic property tables generated for each cell face (left) and for each cell (right).

This method of representing the terrain is referred to as a "high resolution sub-grid model", a technique developed by Casulli (2008). The idea with this method is to be able to increase the cell size of the computational mesh (reduce computation times) without loosing too much important information regarding the underlying terrain.

One disadvantage of using the sub-grid representation is that only cell faces will capture the terrain profile. Features within the terrain will only be represented by the volume-elevation relationship of the computational cell. Thus, terrain barriers that are not aligned with cell faces will be missed in terms of their blocking ability which will result in an effect that, from now on, will be referred to as "leakage". This is illustrated in figure 4.7

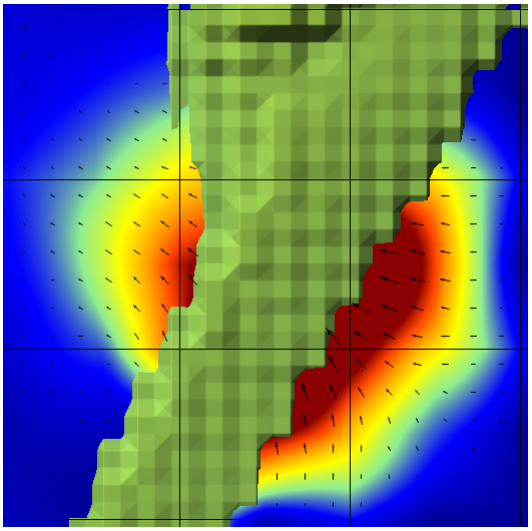

Figure 4.7: Flow velocity profile showing leakage through levee/barrier due to incorrect cell alignment. The arrows indicate the flow direction and size. The colors indicate the relative velocity where red is high and blue is low.

To get around this problem, "breaklines" can be used to force alignment of computational cell faces along barriers or other features that will significantly affect the flow situation. This is illustrated in figure 8.3.

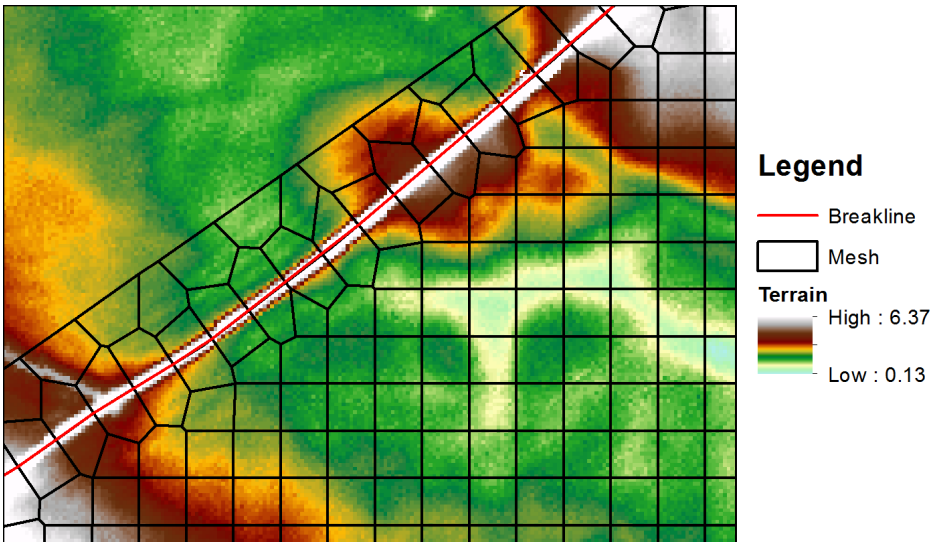

Figure 4.8: Illustration of a computational mesh with cells aligned along a breakline (red).

4.2.2 Hydraulic structures

Modelling structures in 2D is not as well developed and researched as in the 1D case. Weirs, culverts and gates can be added inside the 2D mesh and are modeled in 1D using the same equations as for the 1D case. No extra attention has to be added to cross section spacing and ineffective flow areas: the 2D equations will handle flow contraction and separation as long as the full momentum equations are used, and ineffective flow areas are considered as long as cell faces are aligned with the top of bridges and other barriers (US-ACE, 2015).

Bridges cannot be modeled in a similar fashion as in 1D. They can be incorporated by (i) modifying the terrain to capture bathymetry and banks underneath bridge. However, this option can not incorporate the bridge deck, meaning that it will fail to restrict the flow when the water surface reaches the bottom of the bridge deck. A more detailed representation of bridges can instead be done by expressing them as either (ii) culverts or (iii) gates. Using these options will likely require additional work during calibration since little reference with respect to reasonable parameter values is found. In addition, the geometry of bridge openings is often hard to capture using culverts and gates (US-ACE, 2015). This issue is highlighted in the 2D model set-up chapter. Ultimately modelling bridges using equations developed for other purposed poses a large uncertainty.

4.2.3 Boundary conditions

The same external boundary conditions that were presented in 1D (Flow hydrograph, stage hydrograph, rating curve and normal depth) can be used in 2D. In addition, precipitation can also as an internal boundary condition (see next paragraph).

In 2D, internal boundary conditions are set-up as BC (boundary condition) lines which are connected to one or more cells through the cell face points. With the exception of precipitation, boundary conditions can only be put at the perimeter of the mesh and not inside the mesh. Therefore, representing lateral inflow to a river, meant to represent for example infiltration or storm-water discharge, is more complicated than in 1D. Solutions to this issue is discussed during 2D model set-up (section 8.1).

4.2.3.1 Precipitation

A precipitation boundary condition can be set up for each 2D flow area as a time series of varying rain intensities. Rain is evenly distributed to all cells within the area and can thus not be varied within a single 2D mesh. Evaporation and infiltration cannot currently be modeled in HEC-RAS, meaning that the precipitation added should be an effective precipitation where the effects of evaporation/infiltration are removed (US-ACE, 2015).

4.2.4 2D hydraulic computations

The 2D solver can compute water surfaces, flows and velocities using either the full momentum equations (equation 3.4 and 3.5) or the diffusive wave wave simplification (equation 3.9). Each cell in the computational mesh makes up a control volume for which the water surface elevation and flow across the faces is to be solved. Integrating the continuity equation 3.3 and rewriting using Gauss divergence theorem yields the following integral form of the continuity equation:

$$\frac{\partial}{\partial t}\iiint_{\Omega} d\Omega + \iint_{S} V \bullet n dS + Q = 0 \tag{4.1}$$

Where Ω is the volume occupied by the fluid in the cell, S the cell boundary surface, n is the normal to the boundary surface and Q is the volume flux from external sources. This equation can be discretized in a way that incorporates the available sub-grid information:

$$\frac{\Omega(H^{n+1}) - \Omega(H^n)}{\Delta t} + \sum_k V_k \bullet n_k A_k(H) + Q = 0 \tag{4.2}$$

Where $\Omega(H)$ is a function describing the cell volume as function of the water surface elevation, and $A_k(H)$ is a function of how the area of the cell face k varies with water surface elevation (see figure 4.6). The summation in the second term of equation 4.2 is over all faces of the cell. This form of the continuity equation can be combined with the simplified form of the momentum equation to obtain a new formulation of the diffusive wave equation, or it can be solved together with the full momentum equations.

4.3 Coupled 1D-2D HEC-RAS modelling

HEC-RAS is also capable of coupled 1D-2D modelling, where some areas can be modeled in 1D and others in 2D. When developing a coupled 1D-2D model, the necessary required input data is the same as when developing a pure 2D model. A Digital Elevation Model (DEM) complemented with bathymetry measurements in the river is required to set up the model geometry, and flow and water level data is required to set up the boundary conditions. Coupled 1D-2D modelling can be performed in two different ways. The first option is to set up a lateral connection where 2D flow areas are coupled to 1D cross sections using lateral structures (used in this study). The second option is to model the upstream (or downstream) reach of the river in pure 1D and connecting the most downstream (or upstream) cross section with a 2D area. These two modelling approaches will be described more in detail in this section.

4.3.1 1D-2D model with lateral connections

Using this type of 1D-2D model coupling, flow in the main channel can be modeled in 1D while flow in the floodplain is modeled in 2D. The flow between the two models is calculated as flow over a lateral structure. The 1D part of the model consists of cross sections just as in a pure 1D model, but the width of the cross sections is reduced so that they do not cover areas that are part of the 2D model. The 2D part of the model consist of a mesh, which is set up in the same way as for a pure 2D model (US-ACE, 2015). Figure 4.9 shows an example of a 1D river reach that is connected to a 2D flow area on one side.

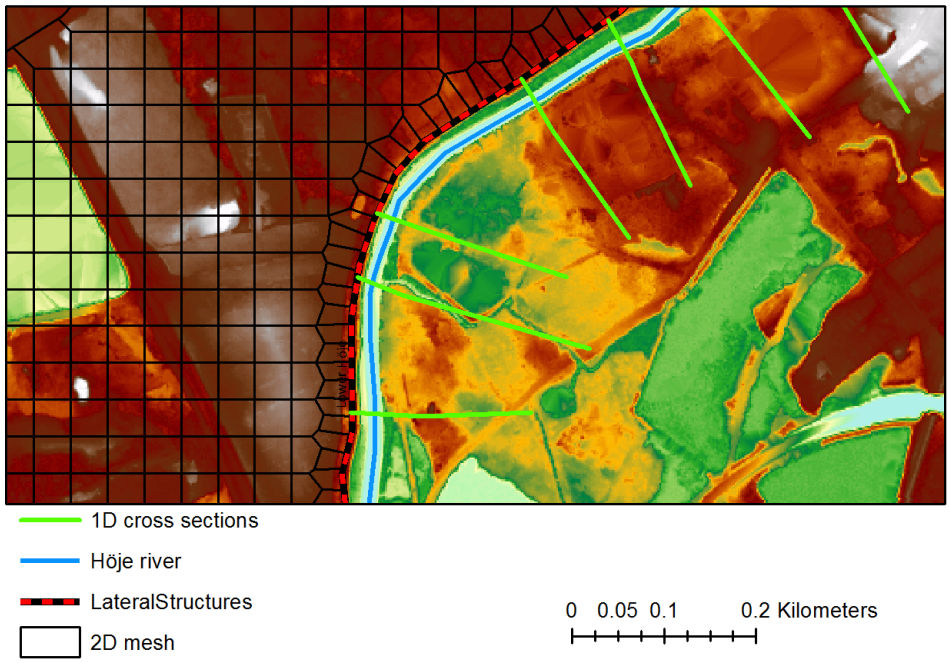

Figure 4.9: Example of a 1D river reach connected to a 2D flow area using a lateral structure

The lateral structure connecting the two models contains elevation data which can be extracted from the underlying terrain model. When the water level in the 1D cross section or 2D cell exceeds the elevation of the lateral structure, water flows over the structure. Flow over the structure can be calculated either using a weir equation or using the 2D flow equations (Brunner, 2016a). When the 2D equations are used, the 1D water surface profile is added as a stage boundary condition to the 2D cells (US-ACE, 2016). When the weir equation is used the flow is calculated based on the difference between water surface elevation and the elevation of the structure. Equation 4.3 is the

standard weir equation used to calculate flow over a lateral weir.

$$dQ = C(y_{ws} - y_w)^{2/3} dx \tag{4.3}$$

Where dQ is the flow over the structure over the length element dx, y_{ws} is the water surface elevation, y_w is the elevation of the structure, and C is the weir coefficient. When the water surface and the lateral structure are not parallel, HEC-RAS uses a modified version of this equation (Brunner, 2016a).

4.3.2 Direct connection of 1D river reach and 2D flow area

The second type of model coupling available in HEC-RAS allows 1D river reaches to be directly connected to 2D flow areas though connecting a cross section to a 2D area. Flow discharging from the 1D-model is distributed in the 2D-model based on the conveyance distribution in the connected cross section. Further flow propagation is thereafter modeled using the standard 2D equations. This type of connection should be set up where flow is highly 1D. (US-ACE, 2015)

5 Study area - Höje river

5.1 Catchment area

The catchment of Höje river is 316 km^2 large and is situated in western Scania. The main stream originates in the southeastern part of the catchment and flows in a mostly northwestern direction, passing the cities of Staffanstorp, Lund and finally Lomma, where it discharges into Öresund. Figure 5.1 shows an overview of the catchment area.

The catchment land use is dominated by farmland (62%), followed by open land (13%) and forest (12%) (Höje Å Vattenråd, 2016). Urban areas stand for 11%, which is considered a very high value for a catchment of this size, and suggests stormwater discharge could have large impact on the overall flow.

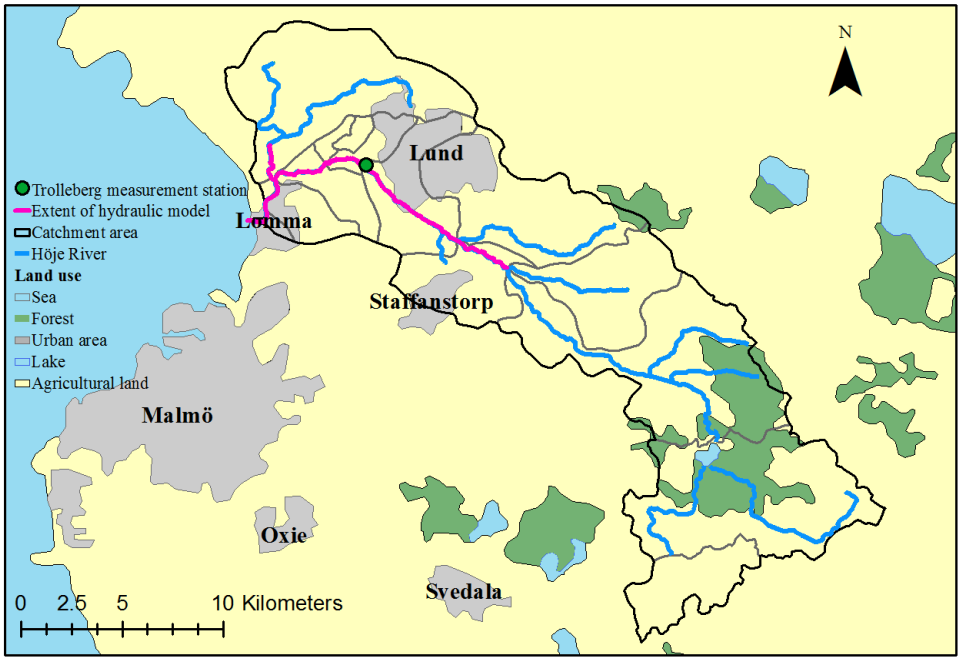

Figure 5.1: Höje River catchment and sub- catchments. The extent of the hydraulic model is highlighted in pink. Based on Sverigekartan ©Lantmäteriet.

5.2 Höje river

The Höje river main stream is approximately 35 km long, with an average discharge of 2.5 m^3/s at the outlet in Lomma. Höje river has several smaller tributaries, the tributary Önnerupsbäcken will be included in the hydraulic models set up in this project.

Önnerupsbäcken discharges into Höje river approximately 3 km from the outlet in Lomma, and has an average discharge of 0.3 m^3/s (Höje Å Vattenråd, 2016).

The high degree of anthropogenic activities is reflected in the management of the water courses. By replacing tributary streams with culverts, the total open channel stream lenghts has been reduced to half since the beginning of the 19th century (Höje Å Vattenråd, 2016). The main stream has also been manipulated extensively, in most parts consisting of a straightened stream or even a straight ditch. Some minor meanders exist, and some meanders have been reintroduced as part of the Höje river project (Höje Å Vattenråd, 2016).

The figure below shows the catchment area, Höje river and tributaries. The extent of the hydraulic model have been highlighted, as well as the location of the flow measurement station at Trolleberg.

5.3 Flooding history

Höje river has been exposed to several flooding events over the last decade. In July 2007, a large area in northern Lomma was flooded after a two week period of heavy rain. The area consists of Örestad golf course and nearby agricultural areas, located where the tributary Önnerupsbäcken connects to the main stream of Höje river, see figure 5.2.

Figure 5.2: Overview showing the area in Lomma municipality where the main flooding occurred in July 2007. Ortophoto ©Landtmäteriet.

A photo showing the extent of the event was taken by the coastguard the 8th of July and is shown in figure 5.3. It should be noted that the time of the photo doesn't necessarily correspond to the time when the maximum extent occurred.

Figure 5.3: Flooding extent in northern Lomma the 8th of June 2007 viewed from southwest. The flooded land consist of farmland and Örestad golf course. Original photo taken by the coast guard.

5.4 Previous studies

Several hydraulic studies have previously been conducted in Höje river by the consultant company SWECO. In one report they analyzed four raingages in the area, showing that a total of 186-216mm fell between 21st of of June and 6th of July 2007, with a maximum volume the 5th of July. They concluded that it was the combination of 2 weeks of sustained rain in combination with the heavy rain recieved the 5th that resulted in the flooding of July 2007 (Sweco Environment AB, 2010)

SWECO used a 1D hydraulic model (MIKE 11) to study the flooding from different combinations of extreme flows and sea water levels. In a report from 2009 (Sweco Environment AB, 2009), their results show that only the houses situated next to the river in Lomma city are likely to be affected by fluvial events with 100 year return periods. Sea level rise might significantly increase the flooding extent. A combination of a 100-year river flow event with a sea level of +1.89m (RH2000), showed to increase the water level in Höje river several kilometers upstream.

Pluvial events have also caused damages in Lomma. The 31st of August 2014, 155 basements were flooded as a result of a heavy rain event (Boel Lindqvist, personal communication 2016-11-01).

6 Data collection and pre-processing

Reliable and detailed input data is a crucial part of all modelling in order to be able to produce trustworthy results. In this chapter, the background data used for the study is presented. In figure 6.1, an overview of the input data used for model set-up and boundary condition design is presented.

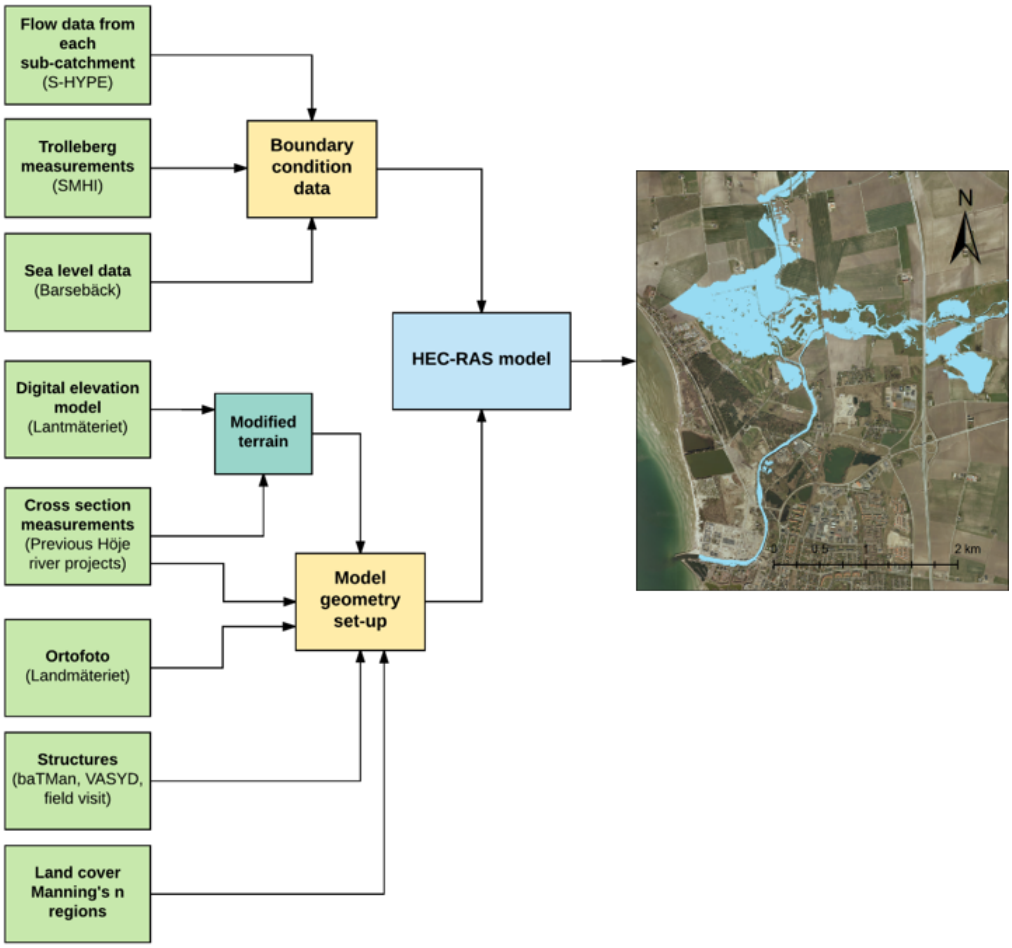

Figure 6.1: Flowchart illustrating the use of different input data in this study.

6.1 Cross section data

Detailed cross sectional data is essential for hydraulic modelling as the river bathymetry controls the characteristics of the flow. Cross sectional data is measured in field and represented by a set of points with x (longitude), y (latitude) and z (elevation) coordinates. Generally, measurements should be taken so that important changes in bathymetry are captured. This includes locations where the flow passes through bridges, culverts or other location where significant accelerations may occur.

In this study, cross sectional data was provided as a shapefile by Sweco, who have conducted several studies on Höje River. A total of 158 cross sections were used.

6.2 Elevation data

The digital elevation model (DEM) used in this report is developed by Lantmäteriet and is part of the national elevation model GSD-Grid 2+. The DEM consists of raster data with a resolution of 2x2 m and is interpolated from elevation points generated through aerial laser scanning, conducted between 2 April and 11 May 2010. The point density varies within the area but is mostly above 0.5 points/m^2 (corresponding to more than 2 points per 2x2 m grid). The main exception is within urban areas, such as Lomma, where the point density is mostly 0.25-0.5 points/m^2, but runs as low as 0.0625points/m^2. In these areas, the DEM might have a significantly diminished degree of detail (Lantmäteriet, 2015).

There are several limitations in the representation of the terrain which cause/may cause significant errors in the DEM supplied by Lantmäteriet. These include for example (Lantmäteriet, 2015):

- Houses are supposed to be removed from the terrain (so that the actual ground is represented) by removing laser points from rooftops before the terrain is interpolated. However, distinguishing houses in the laser point cloud is not easy, and thus the automatic and semi-automatic algorithms used to recognize and remove the buildings might miss to account for some of them. Similarly, dense vegetation can cause the terrain to be lifted compared to the actual case.
- Water cannot be penetrated by the laser, meaning that water surfaces are presented as ground levels, hiding important information regarding the bathymetry of water bodies. It should be noted that, even if the laser would be able to penetrate water, it does not provide the amount of detail generated by measurements.
- Bridges/viaducts hide water pathways and will incorrectly act as barriers if not accounted for when setting up models.
- Very steep terrain that might occur for example at cliffs, might be mistaken for houses and be incorrectly removed.

In order to account for the limitations/errors stated in bullet 2 and 3 several modifications has to be done to the terrain model to enable correct terrain representation for 2D modelling. Mainly, river bathymetry has to be incorporated using river cross

sectional data. The terrain modifications used in this study are presented in section 8.1.1.

6.3 Mannings' n values

Land use data and aerial photographs from Lantmäteriet were analysed visually in order to get an opinion on reasonable Manning's n intervals for the river and floodplain. Determining accurate n-values, especially for overland flow, include large uncertainties and often makes little sense for modelling purposes as the friction parameter often is the main calibration parameter. Still, for model reliability, it is useful to know that the used n-values are within reasonable intervals. In addition, in places where calibration data is not available, Manning values must be estimated. Below follows some suggestions of Manning's n values for channels/rivers and overland flow.

6.3.1 Overland flow

The vast majority of the Höje river catchment consists of agricultural land. However, the area where flooding has previously occurred consists to the largest extent of a golf course with open areas covered with short grass. For reference values Chow (1959) suggests using n values ranging between 0.02 (no crops) and 0.05 (fully mature crops) for cultivated land and 0.025-0.035 for a pasture with no shrubs and short grass. The latter was the alternative that was most similar to a golf course. However, when heavy shrubs are present, such as in the vicinity of the river, Chow (1959) suggests a Manning's n of 0.16, meaning that floodplain Manning's n might be much larger, and likely shows large variations in space.

For urban areas, n-values for hard surfaces are expected to be around 0.01 (Engman, 1986), while green areas may have n-values more similar to that of the golf-course (around 0.03).

6.3.2 Channel flow

Höje river is a highly manipulated river that is mostly straight and uniform with little vegetation. Chow (1959) suggest values ranging between 0.018 (uniform straight channel) and 0.04 (Stony bottom and weedy banks). Arcement and Schneider (1989) suggests 0.025-0.032 for firm, uniform, straight soil channel with little vegetation.

6.4 Flow data

Flow data is used as a boundary condition to the hydraulic model. Since the extent of the hydraulic model covers a large portion of Höje river catchment, the inflow will origin from several sub-catchments. Flow measurements are only available from one station along the river, and can therefore not be directly used as a boundary condition. To be able to distribute the inflow from contributing sub-catchments, modeled flow

from the hydrological model S-HYPE is used as boundary conditions to the model, and adjusted against the flow measurements.

6.4.1 Trolleberg measurements

Flow data is based on stage measurements from the station in Trolleberg located just downstream of Lund (see figure 5.1). The stage (pressure) is measured by SMHI and converted to discharge through a rating curve based on a weir located approximately 40 m downstream of the stage measurement station. The weir is shown in figure 6.2.

Figure 6.2: Trolleberg weir. Photo taken 31st of January 2017

The rating curve has been established using flows up to 21 m^3/s. Higher flows have thus been interpolated from the rating curve, adding uncertainty regarding the estimated 25.6 m^3/s peak of July 2007 (Maud Goltsis Nilsson, personal communication 21 dec 2016). In addition, at flows exceeding approximately 10 m^3/s, water is suddenly distributed over a much larger cross section, spreading into the low-lying terrain situated on the left side of the weir (see figure 6.2). Therefore, there are large uncertainties regarding the accuracy of the rating curve when predicting extreme flows in Höjer river.

Stage measurements were used during calibration where it was compared with the modeled stage. Some additional uncertainties regard the conversions between reference systems. The stage is measured and recorded in a local SMHI reference system, and thus had to be converted to RH2000 which was standard for the project. The relationship between the local reference system and RH70 could be attained, although there is an older and newer version of RH70, and the specific version used could not be determined. The difference between the two is approximately 5 cm in Lund. Thus, when converting stage data from RH70 to RH2000, there is an uncertainty of up to 5cm (Lantmäteriets kundtjänst, personal communication, 2017-01-15).

6.4.2 Modeled flow data from S-HYPE

The hydrological model S-HYPE, developed by SMHI, calculates the flow in each of the sub-catchments in Höje river. For each sub-catchment the S-HYPE model computes the total flow out of the sub-catchment including contributions from upstream catchments (hereafter referred to as total flow), as well as the local contribution from the sub-catchment (hereafter referred to as local flow). Where flow measurement data is available, the modeled data is replaced with measurements (SMHI, 2014). The flow data from S-HYPE is used as boundary conditions in the HEC-RAS models that are being developed in this project. The local flows from the contributing sub-catchments are distributed in the hydraulic models.

Figure 6.3 shows the measured flow in Trolleberg station (yellow), the total S-HYPE modeled flow from the sub-catchment where Trolleberg is located (orange), and the sum of the S-HYPE modeled local flow from the sub-catchments upstream Trolleberg (green), for the period 20th June-20th July 2007, covering the major flooding event that occured in Lomma in July 2007. The sum of the modeled local flows (green) in the sub-catchments aligns with the modeled total flow in Trolleberg (orange). This comparison is made to control whether there is a delay in peak flow between the sum of the local flows and the total modeled flow. When comparing with flow measurements it can be noticed that the model underestimates the peak flow occurring around 7th of July, which is the time when the major flooding event in Lomma occurred. To accurately model this flooding event the local flows that are used as boundary conditions in the HEC-RAS model must be rescaled to capture the peak. For each day during period 6th-17th of July 2007, a factor relating the modeled flow to the measured is calculated. The local flows are thereafter multiplied with this factor. The flows are thus only rescaled during the period when the major flooding event occurs. The blue line in figure 6.3 shows the sum of the rescaled local flows, which now adds up to capture the measured flow peak.

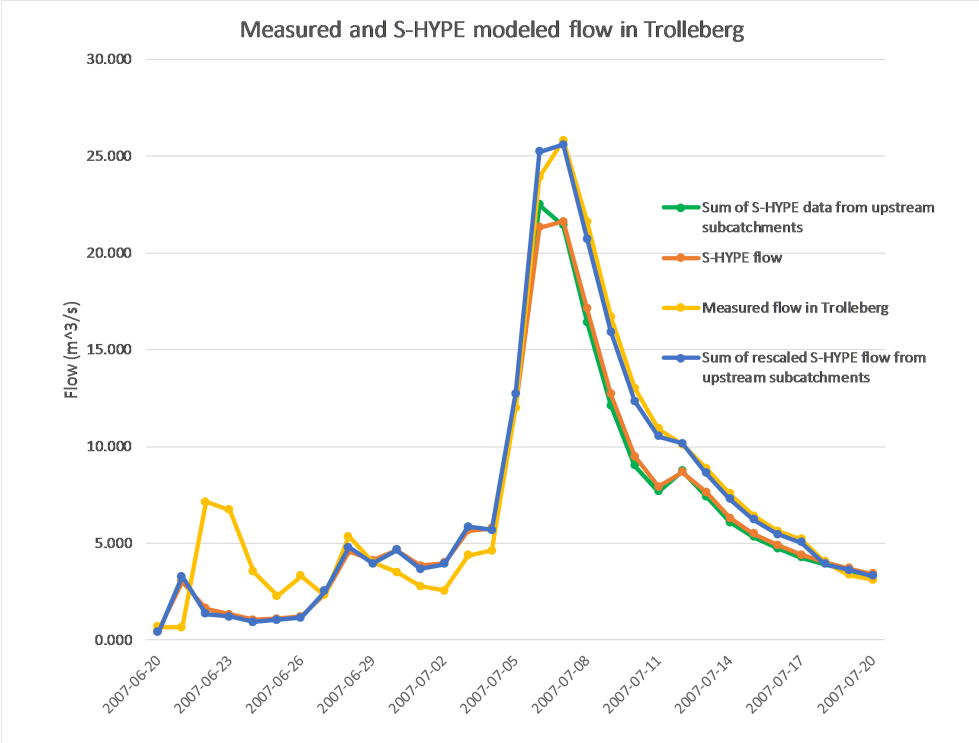

Figure 6.3: Measured flow from Trolleberg station and modeled flow from S-HYPE

All modeled local flow hydrographs are rescaled using the same factors, including the contributions from sub-catchments downstream Trolleberg. This adds some additional uncertainty to the input data.

It should also be noted that Önnerupsbäcken has been regulated with a culvert some kilometers upstream of the model domain. This has not been taken into account when the boundary flow hydrograph added to Önnerupsbäcken was calculated. It is hence possible that too much flow is added to Önnerupsbäcken than what was actually the case during the flooding event.

6.4.3 Frequency analysis

A frequency analysis of flow data from Trollberg was conducted, the calculations can be found appendix B.1. The table below shows flow with different return period calculated from a Generalized Extreme Value (GEV) distribution. The peak flow measured in Trolleberg in July 2007 was 25.6 m^3/s, which approximately corresponds to a 100-year flow.

Table 6.1: Results from frequency analysis of flow data from Trolleberg station.

Return Period (years)	Flow (m^3/s)
5	15.7
10	18.0
50	23.2
100	25.2
200	27.4

6.4.4 Climate change predictions

Average flow as well as extreme flows are expected to decrease as a result of climate change. The regional climate analysis of Scania region by SMHI predicts a decrease in annual average flow in Höje River by approximately 5-10%, and a decrease in 100-year flow by approximately 10%.

6.5 Sea level data

Sea water level measurements are conducted at a measurement station at Barsebäck, located approximately 13 km from the Höje River outlet at Lomma. The station is operated by SMHI, and the measurements are available as open data. The sea water level is used as a downstream boundary condition to the hydraulic model. Considering that Lomma is located inside a large bay, wind setup effects might be stronger than in Barsebäck. In the following frequency analysis, such effects are assumed to be negligible.

6.5.1 Frequency analysis

A frequency analysis was carried out for the sea water level measurements from Barsebäck. The calculations can be found in appendix B.2. Table 6.2 shows return period water levels calculated from a GEV distribution. The water levels are given in reference system RH2000. During the flooding event of 2007 the sea water level was between 20-35 cm. Comparing with table 6.2 it can be seen that this is not an extreme value.

Table 6.2: Results from frequency analysis of sea water level data from Barsebäck

Return Period (years)	Sea water level (cm)
5	126
10	137
50	158
100	165
200	171

6.5.2 Climate change predictions

According to the regional climate analysis for Skåne conducted by SMHI, sea water levels in Öresund are predicted to increase with 85-90 cm by the year 2100 as a result of climate change. By 2100 the 100-year return level is expected to have increased to 221 cm (Persson et al., 2011). The regional climate change report for Skåne also highlights the possibility to experience even higher water levels due to wave set up during storm events. These types of scenarios will not be addressed in this project.

6.6 Hydraulic structures

6.6.1 Bridges

The stretch of Höje river that is modeled in this project contains approximately 30 bridges of varying size. Sweco Environment AB (2010) identified structures that could limit the flow during high flow scenarios. A railway crossing near the junction between Höje river and Önnerupsbäcken, as well as a weir at Trolleberg, were, along with four other structures, found to be limiting during high flow. These two structures will be included in the hydraulic models constructed in this project.

Blueprints for many of the bridges are available from Trafikverket. The process of interpreting the blueprints and incorporating all present bridges in the hydraulic model would be very timely, and would likely require additional field measurements. It was decided to model only one bridge and thereby gain important insight on how bridge modelling is conducted in the 1D and 2D versions of HEC-RAS. Blueprints were collected from Trafikverket (Trafikverket BaTMan, 2016). During a field visit to the area additional measurement were taken.

6.6.2 Weirs

The measurement station at Trolleberg (see section 6.4) is located in the proximity of a weir structure. The water level over the weir is measured and converted to flow data. For the hydraulic model to be able to accurately reproduce flow and stage at this point, the weir must be represented in the model. The dimensions of the weir were determined during a field visit.

7 1D model results

This section will describe the set-up and running of the 1D model of Höje river. Initial data processing, sensitivity analyses, calibration and considerations regarding stability and accuracy will be addressed.

7.1 Model set-up

7.1.1 Geometry data

The extent of the 1D hydraulic model can be seen in figure 5.1, highlighted in pink. The channel and the overbanks are represented by cross sections, figure 7.1 shows the downstream part 1D model, covering the area around Lomma and the golf course.

Figure 7.1: Overview of the 1D hydraulic model

The geometric data is processed in ArcGIS using the extension GeoRAS, developed by US Army Corps of Engineers. The primary input data for developing the 1D geometry of the Höje River model is the DEM from Swedish Land Survey, an orthophoto over the area and measured cross sections provided as a point shapefile with depth measurements. The items that needs to be digitized are river centerline, following the center of the river, banklines following the river banks on both sides, overland flow pahts, and

cross section cut lines, determining where elevation data from the DEM is extracted. The image below shows the geometric elements developed in GeoRAS.

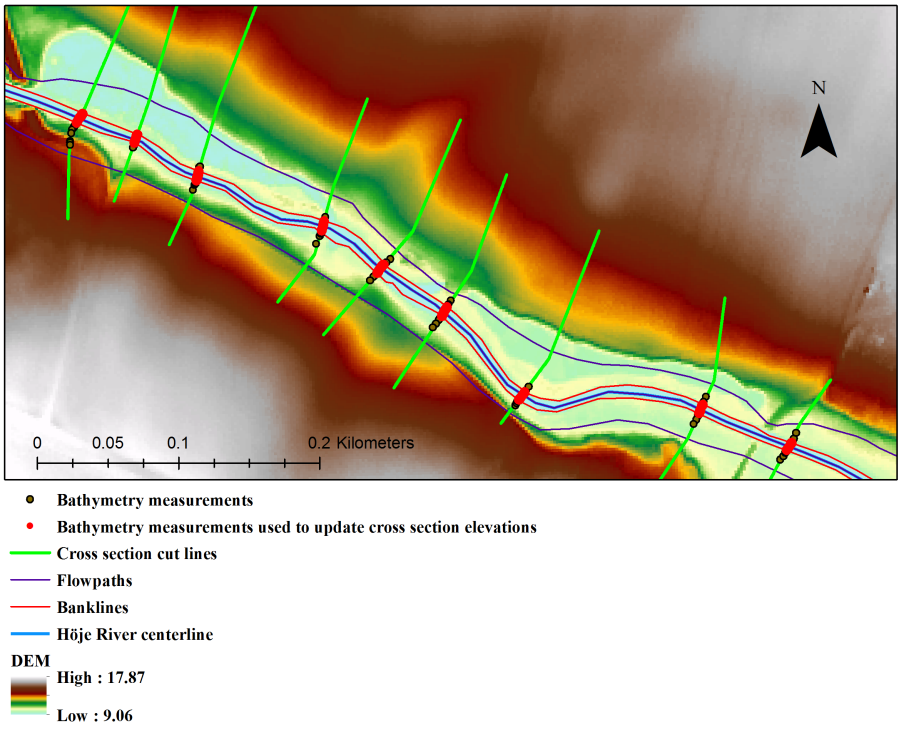

Figure 7.2: Digitizing river centerline, banklines, flowpaths and cross sections using GeoRAS.

The first step of creating the 1D geometry file is to digitize the river centerline, banklines and flowpath lines. The river centerline is used by the program to calculate the length of the river reach, the stationing of the cross sections as well as the the distance between consecutive cross sections. The bank lines are used to calculate the location of the bank stations for each cross section. The flow path lines are used to calculate the overbank reach lengths between consecutive cross sections. The stretch of the river, banklines, and flowpaths are determined based on the ortophoto and the DEM. The overland flowpaths are unknown prior to running the model, and therefore these has to be estimated by the modeller. The above-mentioned features are created as polylines in ArcMap. Using the available GeoRAS tools, the features are assigned all necessary attributes.

Next, cross section cut lines are digtized on all locations where depth measurements are available. A cross section cut line is a line describing the location of the cross section. Since the hydraulic computations are 1D, the cross sections should be perpendicular to the flow direction to accurately capture the hydraulic properties of the river. Since the

flow direction in the overbanks is not always known prior to running the model, the modeler must estimate the flow paths before laying out the cross sections. Each cross section is created as a polyline in ArcMap. The cross section polylines are thereafter converted to polyline Z features, which are essentially polylines containing elevation data. The elevation data is extracted from the DEM. Since the DEM does not contain any bathymetry measurements, the cross section elevations must be updated to include the available depth measurements. This is done using the GeoRAS tool "Update Elevations". This tool extracts elevation data from a specified shapefile (in this case the point shapefile containing the bathymetry measurements), and assigns this elevation data to the cross sections. Next, the geometry is exported to HEC-RAS. Using the 1D cross sections the river bathymetry can be interpolated and combined with the original DEM. This process will be described more in detail in section 8.1.1.1. When this is done, new cross sections can be added or removed directly within HEC-RAS and elevations can be cut directly from the new DEM.

Figure 7.3 shows the workflow for developing the 1D geometry.

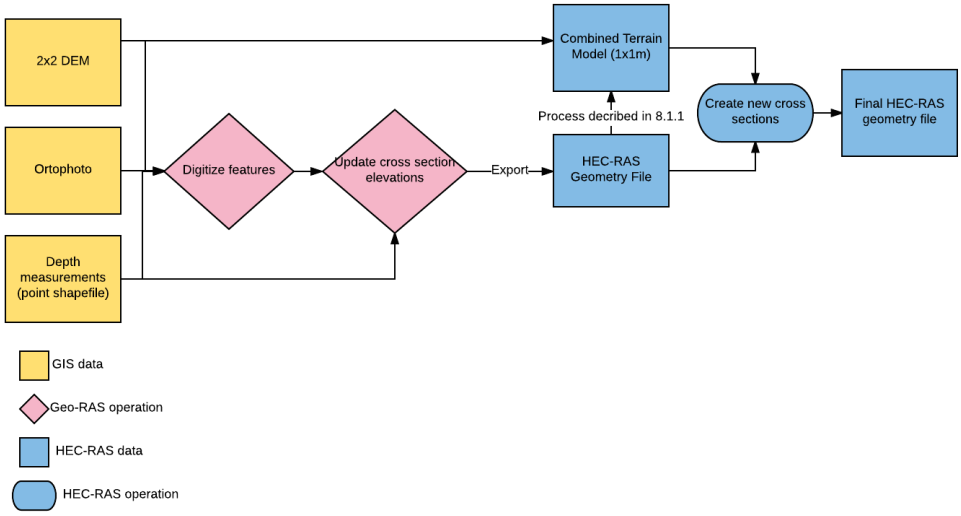

Figure 7.3: Workflow for developing the 1D geometry file

7.1.2 Modelling bridges and hydraulic structures

The railway crossing is modeled by entering the four necessary cross sections and specifying the geometry of the bridge deck. The dimensions of the bridge deck and the bridge opening are determined based on the blueprint, the DEM and from the findings during a field visit. Determining the locations of the cross sections posed some challenge since no information regarding contraction and expansion length was available. The placement of the cross sections is therefore somewhat arbitrary, and the model representation of this bridge should not be regarded as physically representative but rather as a qualitative example of how bridges can be modeled using the 1D

approach.

The weir close to the Trolleberg station was added as an inline structure. The elevation and width of the weir was specified, and the weir coefficient determined through calibration.

7.1.3 Boundary conditions

As boundary conditions to the 1D-model flow data from SMHI S-HYPE model, rescaled to capture the peak flow (see section 6.4), is used. Upstream boundary conditions consists of flow hydrographs at the upstream cross sections of the modeled reaches of Önnerupsbäcken and Höje River. Contributing flow from downstream sub-catchments are distributed in the model as lateral inflow hydrographs. Flow hydrographs from sub-catchments discharging into a single point in river are added as lateral inflows in a single cross section. Flow hydrographs from sub-catchments that the river flows through are distributed uniformely over all cross sections within those specific sub-catchments. An illustration on the boundary condition distribution can be found in appendix A.1. As downstream boundary condition a stage-hydrograph with sea level measurements from Barsebäck from the same time period is used.

7.2 Sensitivity analysis

A sensitivity analysis was carried out for the 1D model to determine the impact of some geometric and computational parameters on model results and stability. The parameters that were investigated in the sensitivity analysis were cross section spacing, time step, θ-weighting parameter, and Manning's friction coefficient. The tested scenarios are summarized in table 7.1. Results and further description of the scenarios are presented in the following sections.

Table 7.1: Scenarios tested in the 1D-model sensitivity analysis.

Parameter changed	Standard value	Scenario ID	Tested value
Cross section spacing	Original spacing	XS1a	Max 100 m, new cross sections interpolated from original
		XS1b	Max 100 m between cross sections, new cross sections cut from terrain.
		XS2	Every other cross section removed from original geometry
Time step	1 min	T1	1 s
		T2	10 s
		T3	30 s
		T4	5 min
		T5	15 min
		T6	30 min
		T7	1 h
		T8	2 h
		T9	6 h
		T10	12 h
		T11	24 h
Theta weighting factor	1.0	Theta1	0.6
		Theta2	0.7
		Theta3	0.8
		Theta4	0.9
Channel Manning's n	0.05	M1	0.1
		M2	0.03
Overbank Mannings's n	0.05	M3	0.1
		M4	0.03

7.2.1 Cross section spacing sensitivity analysis

The cross section spacing sensitivity analysis was performed to determine if the model would produce different results if cross sections are added or removed. This gives an indication if the geometry is sufficiently detailed to describe the hydraulic situation of the study area, and if the distance between the cross sections is suitable. Cross section spacing can impact the stability as well as the accuracy of a model. The cross sections must be laid out at representative locations so that important changes is geometry are captured. If this is not the case, the hydraulics of the river system cannot be accurately modeled. In addition, cross section spacing will impact the accuracy and stability of the numerical solution. Cross sections must be placed at a distance close enough to avoid the numerical diffusion that may arise from averaging the spatial derivatives of the governing equations over long distances. Numerical diffusion would lead to reduced

peak flow and a slower rise of the hydrograph. Too long distances between cross sections can also cause model instability. A too short distance between cross sections can lead to an overestimation of the spatial derivatives, which can cause the floodwave to steepen. This too may cause model instability. (Brunner, 2016a).

Scenario XS1a where interpolated cross sections are added in between original, is thought to reflect the impact of the spacing alone. Scenario XS1b where the additional cross sections are cut from the terrain is though to reflect the impact of representing the geometry more in detail. However, it should be noted that the terrain model has been modified to include main channel bathymetry which has been interpolated using the original cross sections. The cross section elevations in scenario XS1b has been extracted from this modified DEM, and thus, scenario XS1b will not provide a more detailed description of the channel bathymetry compared to the original geometry.

7.2.1.1 Results

Scenario XS2 where cross sections were removed to increase spacing between cross sections was not stable, the following analysis therefore only contains results from scenario XS1a and XS1b.

Decreasing the cross sectional spacing slightly increased peak flow in all selected cross sections, in the range of 0.05 m^3/s. Peak water level was increased with approximately 1 cm in both XS1a and XS1b compared to the default scenario. The general shape of the hydrographs was not affected by the change in geometry. Peak flow timing was only affected in a cross section in the upper reach of Höje river, were it occurred approximately 2 hours earlier in the scenarios with decreased cross sectional spacing. The maximum inundation extent was slightly reduced in both scenario XS1a and XS1b compared to the default scenario.

These results show that the model output is affected by cross sectional spacing, but only to a small extent. The default cross section spacing was kept for further simulations.

It is possible that the cross section layout will have larger impact on model output in another type of catchment. The terrain of the Höje river catchment is rather flat and homogeneous, especially around the flooded areas. If a more complex terrain was to be modeled it is possible that the impact of cross section spacing would be larger.

7.2.2 Time step sensitivity analysis

The time step of the hydraulic computations will affect how the temporal derivatives of the governing equations are approximated. If the computation time step is too large the change in hydraulic properties between two consecutive time steps might be too large, causing instability. A too small time step can also cause instability issues. The rule of thumb in 1D modelling is to chose a time step that gives a Courant number smaller than 1 (see section 3.5). The time step sensitivity analysis was carried out in order to investigate how the choice of time step influences stability and simulation results.

7.2.2.1 Results

The results from the time step sensitivity analysis are presented in table 7.2. For each model time step, the maximum and minimum Courant number, and magnitude and timing of the peak stage in a Höje river cross section close to the junction between Höje river and Önnerupsbäcken are compared.

Table 7.2: Results from time step sensitivity analysis

Time step	Maximum Courant number	Minimum Courant number	Stability	Peak stage	Peak stage timing
1 s	-	-	No	-	-
10 s	0.37	0.0005	Yes	1.53	7jul 0545
30 s	1.1	0.0013	Yes	1.53	7 jul 0545
1 min	2.2	0.0025	Yes	1.53	7 jul 0545
5 min	11.0	0.01	Yes	1.53	7 jul 0545
15 min	32.9	0.03	Yes	1.53	7 jul 0545
30 min	65.7	0.08	Yes	1.53	7 jul 0600
1h	131.5	0.15	Yes	1.53	7 jul 0600
2h	263	0.31	Yes	1.53	7 jul 0600
6 hr	786	0.96	Yes	1.51	7 jul 0600
12hr	1570	1.85	Yes	1.48	7 jul 1200
24hr	3127	3.7	Yes	1.44	7 jul 0000

The difference between maximum and minimum Courant number is very large. The low Courant numbers are found in Önnerupsbäcken, were the cross sections are very large and the flow velocities are low (approx. 0.01 m/s). The highest Courant numbers are found in closely spaced cross sections in the upper reach of Höje river. In this part of the model flow velocities are significantly higher (approx. 1 m/s) and flow is mostly contained within the main channel. The fact that the flow conditions differ so much between different parts of the model domain it will not be possible to choose a time step that produces Courant numbers close to 1 in all parts of the model. The results from the cross section spacing sensitivity analysis showed that increasing the distance between cross sections caused model instabilities, thus this would not be a good way to decrease the Courant numbers in Höje river.

It can be noticed that maximum and minimum Courant number varies linearly with the time step. The calculated velocities are hence the same regardless of model time step.

The model does not crash or produce oscillating stage of flow hydrographs when the model time step is increased to as high as 24 hours. However, when the model time step is too small, the model crashes. This is likely due to the very small Courant numbers in Önnerupsbäcken, causing instabilites when the derivatives are approximated and the difference between consecutive time steps becomes too small. It can be concluded that

the Höje river model is more sensitive to time steps and Courant numbers becoming too small than too large.

Peak stage is reduced when the time step is increased, but the change is not noticeable until the time step exceeds 2 hours. The reduction of peak stage reflects a general flattening of the hydrograph, which could be a result of numerical diffusion due to the time step being too large (Brunner, 2016a). The timing of the peak is delayed when the time step is increased. This is due to the fact that variations on a smaller time scale than the model time step cannot be captured, a model with a 1 hour time step cannot capture a peak occurring at given half hour.

The conclusion from the time step sensitivity analysis is that the 1D model is not sensitive to the choice of time step. The time step 5 min was chosen for further simulations. This time step produced the same peak stage and peak timing as both smaller and larger time steps, it allows for output to be stored often, and the computation time is fast.

7.2.3 Theta-parameter sensitivity analysis

When the hydraulic computations are performed the governing differential equations are solved using numerical approximations of the derivatives. The spatial derivatives are evaluated at an interior point $(n + \theta)\Delta t$, with $0.6 < \theta < 1$. Generally, a lower θ-value will produce a higher accuracy but may reduce model stability. (Brunner, 2016b). In order to investigate how the choice of θ-value impacts the model results, a sensitivity analysis was carried out.

7.2.3.1 Results

When θ is reduced to values smaller than 0.9 the model is no longer stable. However, comparing the the results from scenario Theta4 (where $\theta = 0.9$) with the default scenario where $\theta = 1$, no difference in output was detected. It was therefore concluded that the increased level of accuracy associated with reducing the θ-parameter was insignificant in the Höje river model. Since no improvement was seen, the default value of $\theta = 1$ was kept to enhance model stability.

7.2.4 Manning's n sensitivity analysis

Manning's n is a friction parameter reflecting the resistance against flow from the bottom surface. A high Manning's n value reflects a high frictional resistance, and will thus produce a slower flow and higher water levels, whereas a lower Manning's n will allow more rapid flow and lower stage. The impact on stage and flow hydrograhs and inundation extent of changing Manning's n was investigated. Manning's n is often used as a calibration parameter, and it is valuable to have an approximate idea of the magnitude of the response to a change in Manning's n.

7.2.4.1 Results

The results from the sensitivity analysis show that the model is very sensitive to the choice of Manning's n. Reducing Manning's n will decrease magnitude of peak and stage, and reduce the total inundation extent. Figure 7.4 shows the response of changes n-value in a cross section in the upper reach of Höje river.

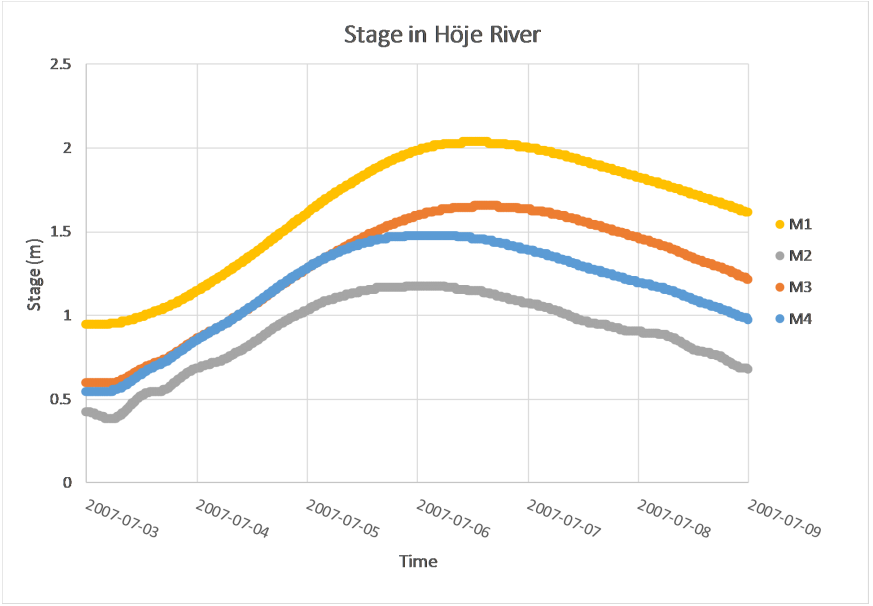

Figure 7.4: Stage in a cross section in Höje river for scenarion M1-M4

The value of Manning's n can be estimated based on the land use of the area, but its exact value for a given river is unknown. This, combined with the fact that Manning's n has such large impact on flow dynamics makes it valuable calibration parameter. During model calibration, the value of Manning's n can be altered within a reasonable range (see section 6.3) until model output match measured values.

It can also be noted that the change in output as a result of changing Manning's n was significantly larger than the changes due to changes cross section spacing, time step and θ-parameter. This indicates that the choice of friction coefficient can to some extent overshadow the uncertainties related to insufficient geometry data and the numerical solution of the equations, given that the model has been thoroughly calibrated.

7.3 Calibration

Stage measurements from Trolleberg and the aerial photograph from the flooding event of July 2007 (see figure 5.3 and 7.6) from the coast guard were used to calibrate the 1D model.

Initially, the weir coefficient was calibrated. During the field visit the drop over the structure was estimated to approximately 15 cm. The model was calibrated by running the model with the flow that was recorded the same day, and adjusting the weir coefficient until a drop of 15 cm was obtained. The weir coefficient was determined to 1.25.

Secondly, the model was calibrated against the stage measurements and the aerial photograph though adjustment of Manning's n. A good correlation between modeled inundation extent and the aerial photograph from July 2007 could easily be obtained by setting Manning's n to 0.03 in the main channel and 0.05 on the floodplains.

Obtaining a good correlation between measured and modeled water levels in Trolleberg was difficult. It was not possible to obtain a good correlation between measured and modeled stage and simultaneously reproduce the inundation extent of July 2007 if the Manning's n was changed homogeneously over the area. However, when increasing Manning's n in the upper part of Höje river, a fair correlation was achieved, but the resulting n-values were out of range (0.13 on floodplain, 0.07 in river). Using such high n-values also led to large areas being inundated in the upper reach of Höje river. It was concluded that the difficulties with calibration were due to the way that the weir is modeled in HEC-RAS. The weir is defined over one-cross section, and flow through that cross section will be calculated using the weir equation. For the Trolleberg station, this representation is accurate when flow is low. When flow is high, water will flow on the floodplain beside the weir, and should hence not be calculated using the weir equation. Using the weir equation when water flows on the floodplain will cause unrealistic acceleration of the flow, causing water levels to decrease. The damming effect of the weir will hence be modeled incorrectly when flow is high. This is the reason why unrealistically high Manning's n values had to be used to match the stage measurements. Replacing the weir with a cross section with bottom elevation corresponding to the weir elevation made it possible to match the measured peak stage using more reasonable n-values in the upper reach of Höje river (0.08 on floodplain, 0.05 in river). However, the agreement was poorer for low-flow compared to when the weir was present. Since the main purpose of the model was to model high flows it was decided to replace the weir with a cross section, as this option provided the best agreement with measurements of high flow. The agreement between measured and modeled flow in Trolleberg can be seen in figure 7.5.

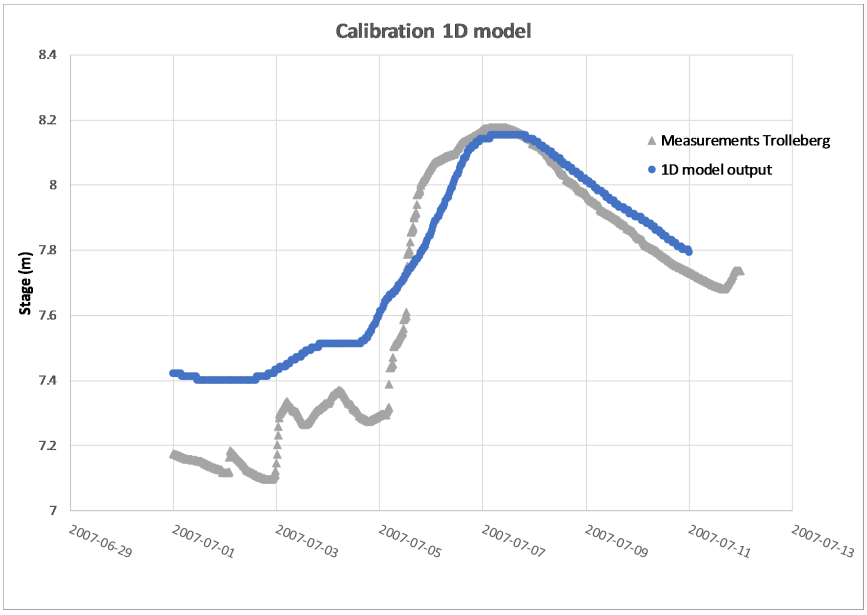

Figure 7.5: Measured and modeled flow in Trolleberg.

A comparison between 1D model output and the documented inundation extent on 8th of July 2007 is shown in figure 7.6.

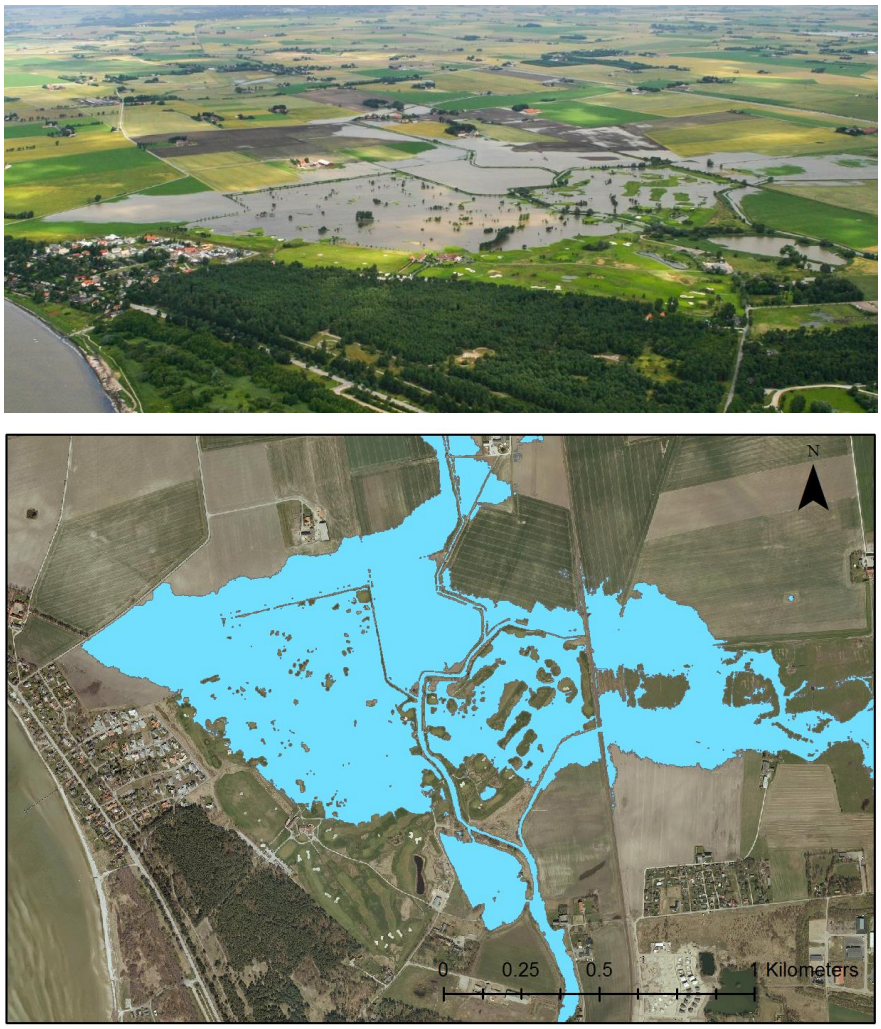

Figure 7.6: Upper: Önnerupsbäcken golf course 8th of July 2007 (Photo: Swedish Coast Guard). Lower: Result from 1D model, inundation extent 8th of July 2007. Background image: GSD-Ortofoto, 1m color ©Lantmäteriet

7.4 1D model stability

The stability of the numerical solution of the governing equations depend on the geometric set-up of the project as well as on the computational settings such as time step and theta-parameter. 1D HEC-RAS modelling has been widely used and is well studied, and therefore there also exist many different kinds of solutions to the stability issues that may arise.

As discussed in the cross section spacing sensitivity analysis, the spacing between cross

sections can greatly influence the stability of 1D HEC-RAS models. If the spacing between cross sections is too short the approximation of the spatial derivatives might be overestimated, causing unrealistic hydraulic gradients and instability. On the other hand, if the spacing is too large, the change in hydraulic properties between two cross sections might be too big, which could also cause the model to become unstable. (Brunner, 2016b). Some initial stability issues with the 1D Höje river model were overcome by removing closely spaced cross sections.

Another thing that might cause stability issues when modelling in 1D is low flow conditions. The numerical solution engine does not allow cross sections to go dry during any point of the simulation. Instabilities due to low flow can be overcome by for example increasing the number of points in the hydraulic property tables, or by inserting a pilot channel to the river.

7.5 Discussion

The main advantage with the 1D model approach is that the computation times are very fast, a month long simulation period can be calculated in less than a couple of minutes. It is possible to set up very large models without ending up with long computation times. Since the boundary conditions can be distributed and lateral inflows can be added it is possible to set up models on catchment scale.

Another advantage is the many options available for modelling hydraulic structures. Modelling bridges and other hydraulic structures is relatively easy in 1D. There exists a variety of different methods for modelling flow under bridges, through culverts and gates and over weirs. Adding the required data is fairly simple, given that the modeler has access to blueprints and elevation data. The modelling of bridges and structures was not studied in detail in this project. The aim with the bridge modelling was to compare the different options for bridge modelling in the 1D and 2D version of HEC-RAS, and not to give a detailed description of the flow around the bridges in Höje river.

Many of the disadvantages with 1D modelling arise from the much simplified description of reality. Overland flow is often 2D in nature, and it is difficult to represent these accurately using a 1D approach (Andersson and Bates, 1993). For example, studying results from the 2D and 1D-2D models developed in this project it can be seen that during high flow water flows from Höje river to Önnerupsbäcken via overland flow paths. This phenomenon cannot be modeled using the 1D approach.

The fact that a single water surface is calculated for the cross sections is a simplification that will have significant impact on the inundation dynamics. The option of using levees to confine some areas of the cross section was presented in the 1D HEC-RAS background (section 4.1.2). When levees are used to confine the overbanks from the main channel, the channel flow will likely be more accurately modeled up until the point when the levees are over-topped. If a low-flow scenario is modeled where flow is predicted to be maintained within the main channel the use of levees would probably lead to a more accurate water surface profile. However, when the water level reaches above the levee elevation the entire overbank area will be flooded instantaneously. If

levees are used it might also happen that the levee elevation is over-topped in one cross section but not in the next one. This can result in very odd inundation maps, such as the one showed in figure 7.7. If the timing of levee over-topping is of interest, the levee option should not be used on its own, but rather in combination with a storage area. Otherwise, inundation maps like the one in figure 7.7 may be the result.

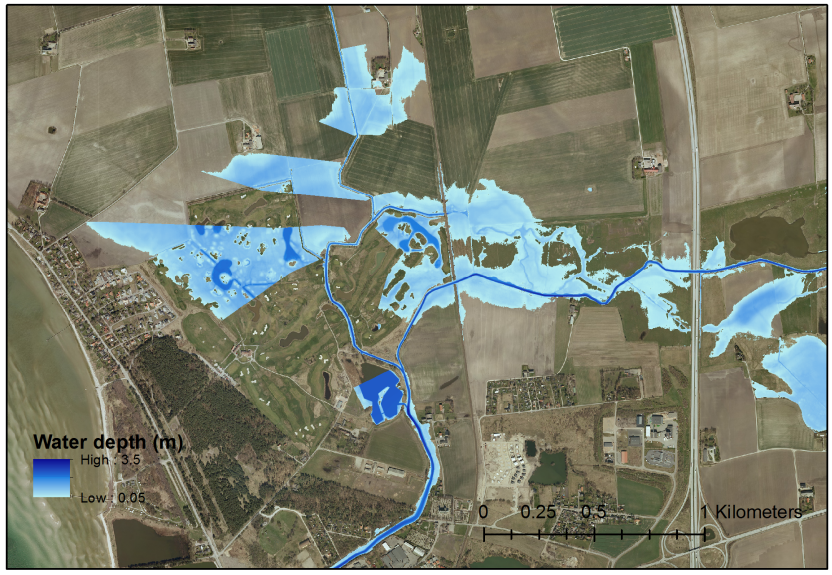

Figure 7.7: Inundation extent when the main channel is separated from the overbanks by adding levees to 1D cross section. Background image GSD-Ortofoto, 1m color ©Lantmäteriet.

Using levees can hence lead to non accurate results. On the other hand, when no levees are added, the water levels will rise simultaneously in the main channel and in the areas behind the barriers. Depending on the topography of the area and the geometry of the cross sections, areas behind barriers could hence be modeled as flooded before they actually should be, and the water level in the main channel could rise slower than it actually should. The 1D Höje river model predicts inundation on the golf course already during very low flow. The 1D model is hence not suitable for modelling channel-floodplain interaction and inundation dynamics. The issues with weir flow discussed in the calibration section is another example of how the 1D model fails to capture channel-floodplain dynamics. If such information is of interest the 1D approach is hence not very suitable. In the 2D and 1D-2D chapters that follows, modelling of channel-floodplain interaction will be further discussed.

When the computed 1D results are displayed in RAS-mapper or in a GIS, the results has to be interpolated to a continuous surface, and displayed on a terrain model. In literature it has been suggested that the method used for mapping 1D results will have much impact on the final inundation maps, especially when the terrain is complex (Vojinovic and Tutulic, 2008). When mapping velocity distribution based on 1D results

is should be emphasized that the velocity maps are based purely on interpolation of 1D results (Brunner, 2016b), and that it is not possible to map velocities around features represented between cross sections. This is illustrated in figure 7.8, showing the mapped velocity between Önnerupsbäcken and Höje river. The figure highlights the limitations of using a 1D approach to model overland flow. To the left, velocities are interpolated based on calculated velocities in Önnerupsbäcken, to the right velocities are interpolated based on calculated velocities in Höje river. The velocities differ in magnitude and direction, and the mapped velocity distribution is not realistic. It can also be seen that the water appears to flow straight through the barriers in terrain. In 1D features between cross sections can only be represented implicitly through increasing the friction coefficient. It is not possible to obtain detailed information of flow velocities around such features, since no such results are calculated using a 1D approach.

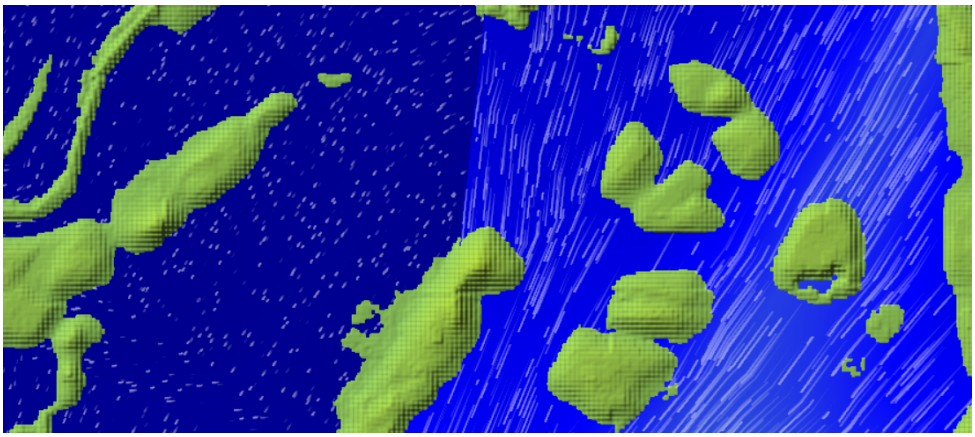

Figure 7.8: Velocity map created in RAS mapper based on interpolated 1D results.

The issues discussed above are inherent to 1D modelling and well established in literature. When modelling flow in complex terrain or urban areas limitations of 1D modelling becomes even more evident (see for example Vojinovic and Tutulic (2008), Tayefi et al. (2007)). Despite the apparent issues with much simplified 1D approach, it should be highlighted that the developed Höje river model could reproduce the flooding event from July 2007 accurately without much effort having to be put into the calibration. If the purpose of the model is to produce a map of inundation extent, and more detailed information is not of interest, a pure 1D model is sufficient.

8 2D model results

Constructing a 2D model in HEC-RAS differs from 1D set-up both with respect to terrain representation and overall geometric set-up and possibilities. This chapter will first introduce river bathymetry interpolation and other terrain modifications that should/could be used to enable a more correct representation of reality. After this, the set-up of the 2D model is shown. A comprehensive sensitivity analysis is conducted to find suitable cell sizes and cell configurations and time steps, as well as investigating sensitivity of model parameters. Finally, urban 2D modelling in HEC-RAS is discussed in terms of geometric set-up, possiblities and current limitations.

8.1 Model set-up

Setting up the 2D-model requires some additional work compared to the 1D-model. As discussed in section 6.2, rivers and other water bodies are not correctly represented in the original elevation data. Depending on the application, these may be accounted for through modification of the DEM. In this section, the elevation model modifications used for the 2D modelling is presented.

8.1.1 Elevation model modifications

8.1.1.1 River Bathymetry Interpolation

In order to correctly represent the river, cross section (XS) data can be used to interpolate the river bathymetry, incorporating it into the terrain model. Cross sections must first be digitized and updated to incorporate river bathymetry using "update elevation" in Geo-RAS, as described in the 1D set-up. The interpolation was done in HEC-RAS using the "XS-interpolation surfaces" function. Due to current bugs in the interpolation tool in HEC-RAS 5.0.1 and 5.0.3, flat banks are created outside the channel in parts with heavy meanders. After exporting the bathymetry to Arc-GIS, these were removed in using the tool "Extract by Mask", using a polygon covering the river only. The river bathymetry was finally combined with the original raster using conditions in the raster calculator. The river bathymetry resolution was set to 1x1m when created in HEC-RAS. In order to keep this resolution, the original raster had to be converted from 2x2 to 1x1 m resolution using the function "RESAMPLE", where the four new 1x1 cells were given the same value as their mother cell (2x2 m). It should thus be noted that this only resulted in an effective 1x1 resolution inside the the river and not in the surroundings floodplain. A summarized flowchart is shown in figure 8.1.

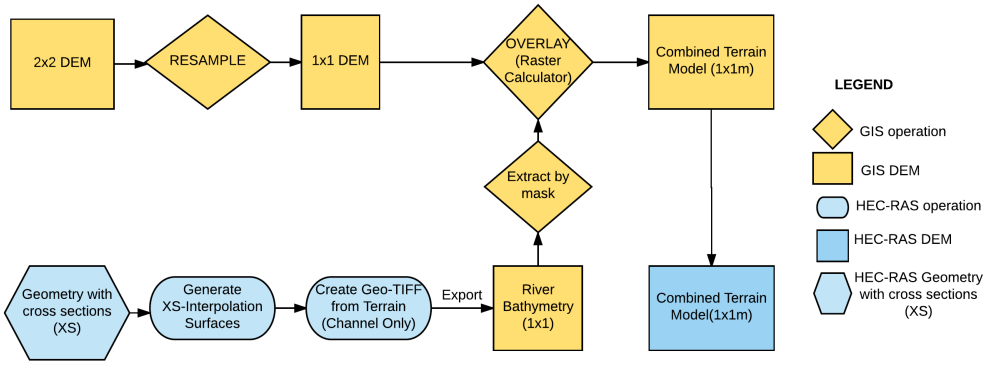

Figure 8.1: Workflow for incorporation of river bathymetry into the DEM.

8.1.1.2 Other terrain modifications

A set of further modifications of the DEM were done to account for terrain features that are suspected to significantly influence the flow pathways and inundation. All DEM modifications were performed in Arc-GIS by drawing/importing polygon features covering the area to be lowered/elevated, converting these to (1x1) raster files and using conditions to either lower the ground relative to the current elevation, or set the elevation to a specific value. All given values are in A flowchart of the work is shown in figure 8.2.

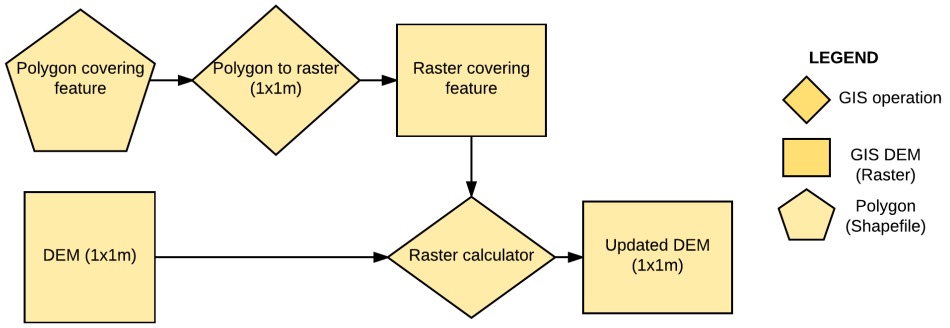

Figure 8.2: Workflow for changing the ground level within the elevation model.

A pond is located where Önnerupsbäcken meets up with Höje river. Due to the evident connections between the pond and the rivers, flow through the pond was incorporated by lowering the DEM inside the pond by 1 m. The inflow and outflows were lowered by adjusting their elevation to an average depth of -1.1m (RH2000) estimated from the available cross section data.

In order to model flooding in urban environments, houses were incorporated into the terrain model by raising them by 5m, using the polygon layer "Fastigheteskartan", acquired from Lantmäteriet. This modification only had impacts on the pluvial investigations, since the urban part of Lomma was shown not be significantly affected fluvial events (shown in later chapters), and is further discussed in the section 8.4.

8.1.2 2D Geometry set-up

A 2D flow area was designed to cover the extent of the flooding during all events, a process that was modified during calibration. Breaklines were introduced along ridges, bridges, banks and other features that may act as important barriers to the flow.

In order to set suitable cell sizes for the breaklines and the overall 2D area, a geometric sensitivity analysis was conducted (see section 8.2). One Manning's n value was assigned to the river and the floodplain respectively, using polygons created using the bankline polylines. The final geometry and parameters used are presented in the calibration section (8.3).

In figure 8.3, the mesh structure around one part of the river is shown, illustrating cell alignment and cell size differences between the river and the floodplain. The location of one of the point inflow boundaries is also presented (discussed in the following section).

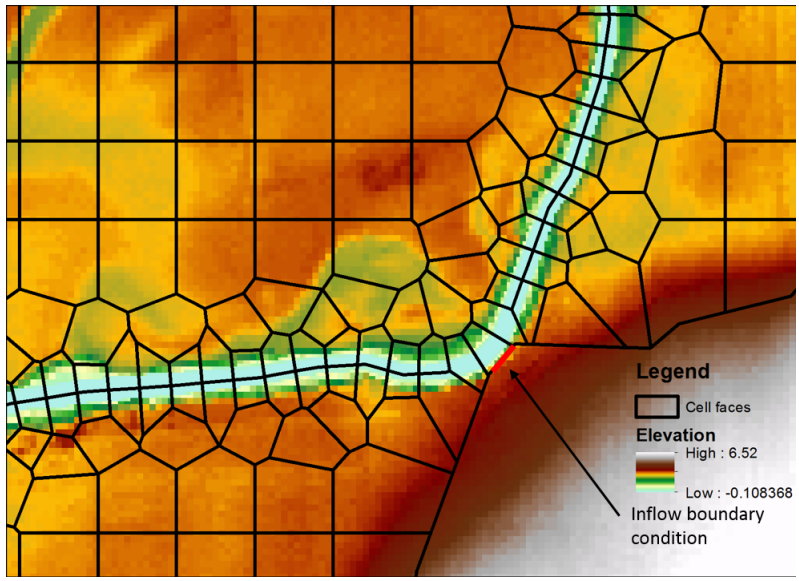

Figure 8.3: Mesh structure around one part of Höje river, illustrating cell structure generated around the river using a breakline, as well as a point inflow boundary condition.

8.1.3 Boundary conditions

For sub-catchments that the river passes through, there is no possibility of adding uniform lateral inflows along the river unless the outer boundary of the mesh is aligned with the river side, although this will prevent flood modelling on that side of the river. Instead, in this study, several point inflows were put along these reaches, the individual inputs summing up to the total inflow as calculated from S-HYPE data for each sub-catchment. The construction of the point inflow is illustrated in figure 8.3.

A map showing the location of all the inflow points is shown in figure A.2 in the Appendix.

8.1.4 Hydraulic structures

In the 2D HEC-RAS theory, the limitations in current 2D bridge modelling was introduced. Since the railway bridge was shown to be limiting during high flows, capturing the effect of the bridge deck will be important. Thus, in this study, a culvert was used to represent the railway bridge opening. The culvert geometry is illustrated in figure 8.4. It is seen that while the culvert captures the approximate area of the cross section (bounded by the terrain profile and the bridge deck) it will produce an incorrect elevation-area relationship for the opening.

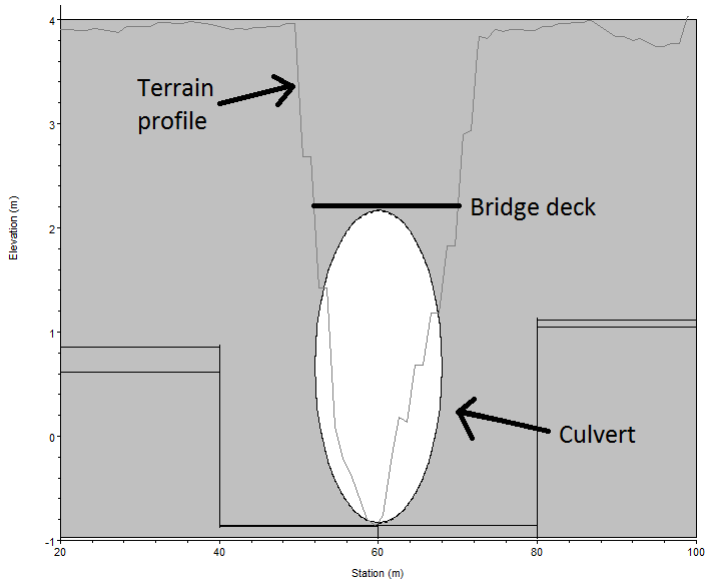

Figure 8.4: Approximating the railway bridge opening with a culvert in HEC-RAS 2D

The weir in Trolleberg was added to enable capturing of backwater effects which may have significant impact on the depth measurements. A weir coefficient of 1.25, generated by 1D-simulations, was used in the 2D model.

8.2 Sensitivity Analysis

A sensitivity analysis was carried out to determine the influence of mesh geometry, time step and other model parameters. Investigating mesh geometry is not truly a sensitivity analysis, mesh configuration should not be used as a parameter for calibration, but rather to find out the most suitable mesh configuration for the application.

8.2.1 Mesh construction

The aim of this geometric sensitivity analysis is to find the cell size and alignment needed to sufficiently represent the river and riverbanks while keeping cell sizes large enough to enable reasonable computation times. Mesh construction is site specific, although results from this analysis can help to draw more general conclusions regarding design considerations.

In the area around the golf course, water is retained within the river by man-made river banks, having a higher elevation than the surrounding floodplain. Thus, capturing the features of these banks are of great importance in order not to allow water to escape into the floodplain before the river water level reaches the top of the banks.

8.2.1.1 Method

In order to reduce the computation time, a smaller area was used for 2D sensitivity analysis than for the study. The area (shown in figure 8.5) was chosen since it captures the main flooding area. Still, it is assumed that the results from the sensitivity analysis is applicable for the whole area.

Figure 8.5: Area investigated during sensitivity analysis. Background image: GSD-Ortofoto, 1m color ©Lantmäteriet.

In the early stages of the study, the diffusive wave simplifications seemed to give almost identical results when using the full momentum equations. This was later shown not to be the case. Thus, the diffusive wave simplification was used for the mesh sensitivity analysis. Still, the analysis is only used to compare results between geometries. Preferably, they should have been conducting using the full momentum equations. The differences between results generated when using the diffusive wave simplification compared to the full momentum equations are presented and discussed in the next chapter (8.2.2).

A time step of of 5 seconds was used for all simulation, resulting in Courant numbers less than 2 for all simulations.

A total of 10 different geometries were used, presented in table 8.1. The overall cell size (CS) for the area was varied between 10 m and 40 m. The cell alignment was tested using breaklines along (i) the middle of the river, (ii) the river banks, and (iii) both. The breakline cell sizes were varied between 5 and 20 m. For the smallest cell sizes, a flexible cell size (indicated by "5min10max") was used since it reduced the amount of errors in the mesh and resulted in a smoother transition between the breaklines and the overall mesh. Geometry 1 was set to be the standard used for comparison between models, and many of the following results are displayed relative to those of geometry 1.

Table 8.1: Geometries tested in the sensitivity analysis.

Geometry	Overall CS (m)	Bank CS (m)	River CS (m)
1	20	5min10max	5min10max
2	40	5min10max	5min10max
3	10	5min10max	5min10max
4	20	-	-
5	20	20	-
6	20	10	-
7	20	5min10max	-
8	20	-	20
9	20	-	10
10	20	-	5min10max

The different geometries were analysed with respect to the (i) maximum water surface elevation (WSE) generated on the golf course, (ii) time needed to reach a water depth of 40cm at observation point (see figure 8.5), (iii) peak flow near discharge in Lomma, (iv) corresponding peak time and (v) computation time. Furthermore, the flow inside the river was compared for a cross section at the golf course. Flows at the golf course and in Lomma were analyzed along the flow control lines shown in figure 8.5. Finally, visual inspections were done to (vi) compare differences in flooding extent over time as well as (vii) differences in velocity distribution.

8.2.1.2 Results

The results of analysis (i-iv) is shown in table 8.2. All results are relative to geometry 1 except for the peak flow in Lomma. The maximum relative water surface elevation is regarded representative for the whole golf course.

Table 8.2: The result of the geometric sensitivity analysis. All results are relative to geometry 1 except for Lomma peak flow. The difference in time for the water level to reach 0.4 m was compared at the observation point at the golf course. Negative values in column 3 and 5 indicate that these happened before the time of the standard geometry.

Geometry	Max. rel. WSE (%)	ΔTime when D=0.4 at obs. point (hrs)*	Lomma Peak Flow (m^3/s)	Rel. Peak Delay (hrs)
1	0%	0	30.79	0
2	-1.23%	0	30.73	0
3	-0.79%	3	30.78	0
4	20.21%	-16	31.09	- 1
5	18.36%	-8	30.67	0
6	11.74%	-6	30.64	0
7	9.00%	-10	30.92	-1
8	26.03%	-16	30.49	0
9	17.52%	-12	30.92	0
10	-0.51%	-2	30.95	0

8.2.1.2.1 River and river bank representation It is shown that representing both river and banks with breaklines results in largest reductions in maximum water level in golf course compared to using no breaklines (geometry 4). As expected, representing only the banks with breaklines (geometry 5-7) gave a larger reduction in the water depth compared to using only river breaklines (8-10), except for geometry 10. Also, the reduction in water level is larger when smaller cell sizes are used along the breaklines. Inspecting the geometries (not presented) show that using larger cell sizes often results interference between breakline cells, preventing some of the cells to be correctly aligned along the breaklines, resulting in barrier leakage.

The results further show that incorrect use of breaklines may worsen river bank representation compared to using no breaklines (geometry 8). Geometry 10, giving a surprisingly large reduction in maximum water level, had a cell size that well matched the distance from the middle of the river to the bank, and thus managed to (accidentally) capture the river banks.

The differences in dynamics is illustrated in column 3 showing the differences (relative to geometry 1) in time needed for the water level to reach a depth of 0.4 meter at the observation point. A large difference between results was seen also here, the depth of 0.4m reached 16 hours earlier when no breaklines are used compared to geometry 1. This result should not be used to compare floodplain cell size (varied in geometry 1-3),

as the propagation of flooding depends on floodplain representation and is discussed later in this section.

The differences in dynamics between various river representation is illustrated in figure 8.6, comparing inundation extents for geometry 1(River+Banks), geometry 7 (Banks) and geometry 10 (River) after 12 hours of simulation. Overall, differences in extent were large during the first 24 hours of simulation, but decreased as the golf course became increasingly flooded (result not presented).

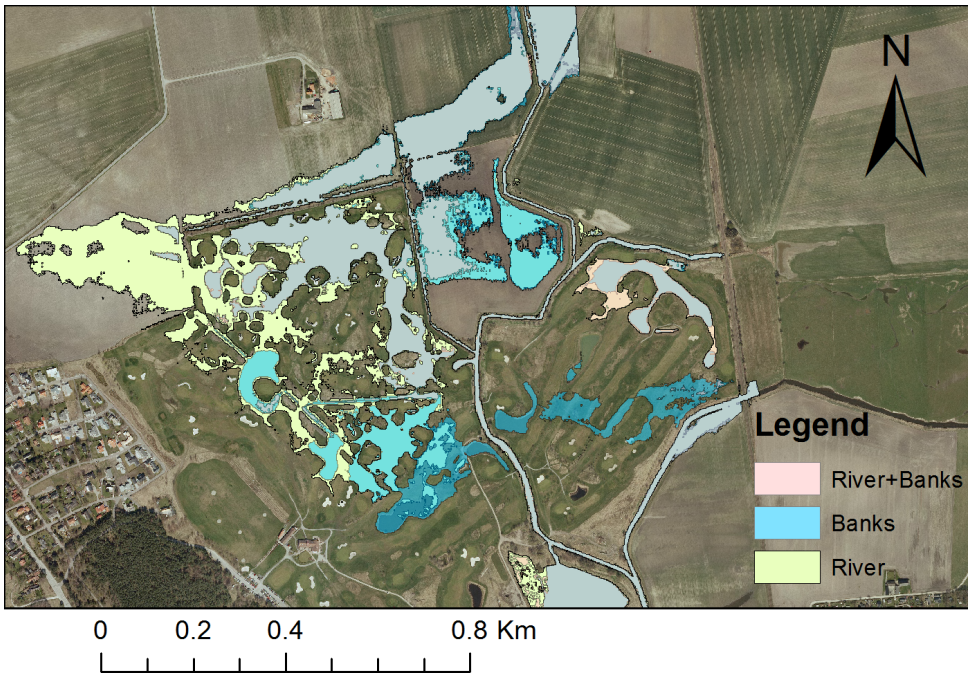

Figure 8.6: Inundation extent after 12 hours of simulation generated by different river representation. Background image: GSD-Ortofoto, 1m color ©Lantmäteriet.

In figure 8.7, the flow in Önnerupsbäcken (measured across the flow line) is presented for geometry 1-10. The results show that geometry 1-3 (river and bank breaklines) are able to retain highest flow rates within the river, followed by geometry 5-7 (bank breaklines), while geometry 4 (no breaklines) and geometries 8-10 (river breaklines) generate the lowest flows.

The additional river cells generated when having both river and bank breaklines seems to enable additional detail of the river that significantly reduced throughflow compared to representation of banks only.

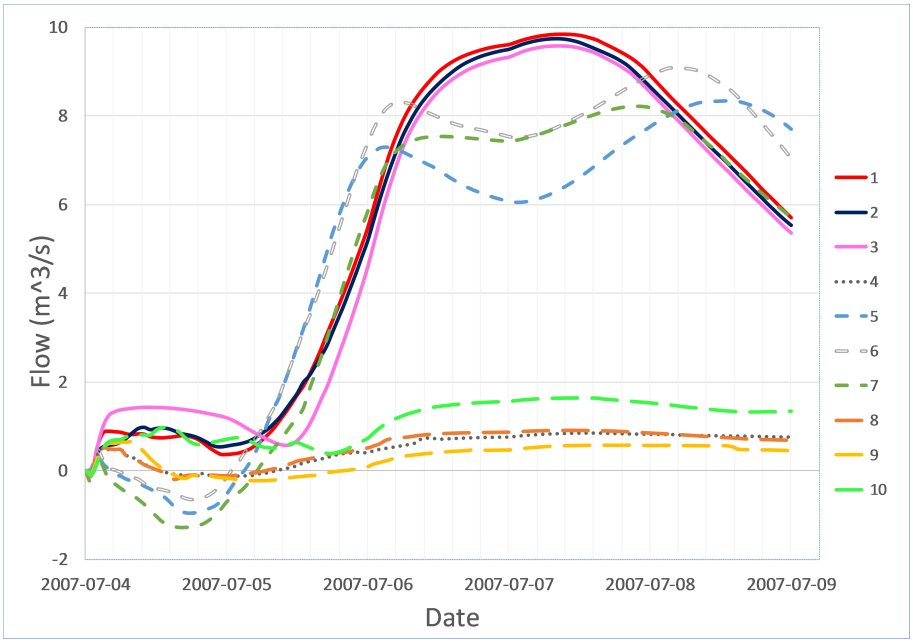

Figure 8.7: Flow hydrograph in Önnerupsbäcken generated for geometry 1-10. Location shown in figure 8.5.

Looking at the peak flow and relative peak delay at the profile line in Lomma, the differences are interestingly very small (column 4 and 5). It may be that when the largest flows arrive, the water levels in the river and surrounding floodplain are already high enough so that correct representation of the banks does not matter much since most of the banks are under water.

One potential effect of using river breaklines, except for introducing more cells inside the river, is that the cells are aligned so that the cell faces become perpendicular to the flow direction. The opposite might occur if less detail is used for the river. An example of possible implications is displayed in figure 8.8 showing the velocity distribution generated by geometry 10 at a location in Önnerupsbäcken. For geometry 10, the velocity profile form a zigzag pattern where velocities are slightly higher (brighter color) along the cell faces. In contrast geometry 1 generates a much smoother and natural looking velocity profile. Due to the large importance of bank representation in this area, it is hard to draw any conclusions regarding the impact of this phenomena. However, it is possible that the zigzag pattern may result in an extended flow path length, overestimating frictional losses and river depths.

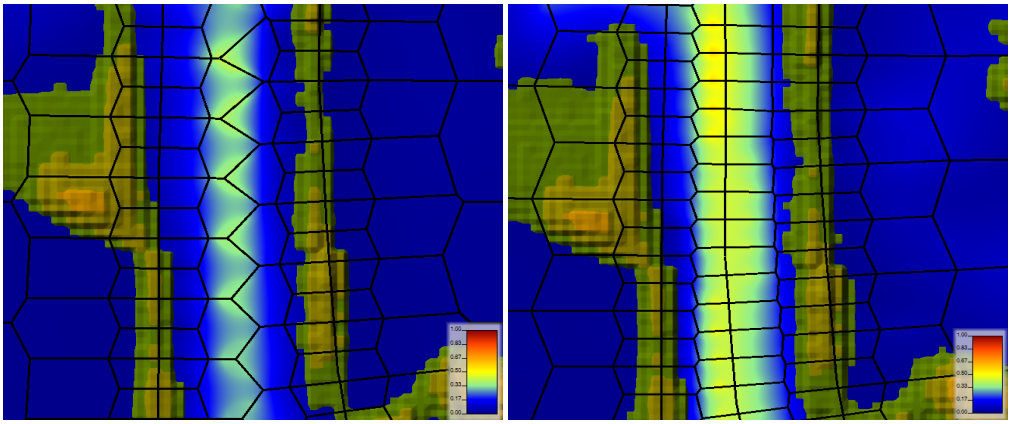

Figure 8.8: River velocity profiles shown for geometry 10(left) and geometry 1(right)

8.2.1.2.2 Floodplain representation In order to address the influence of floodplain cell size, the flood propagation was compared over time. The results showed that the inundation extent varies a lot during the first 24 hours of simulation, but decreases as the golf course becomes increasingly flooded (not shown). The result is illustrated in 8.9, showing the difference in flooding extent after 12hrs of simulation for geometry 1 and 2.

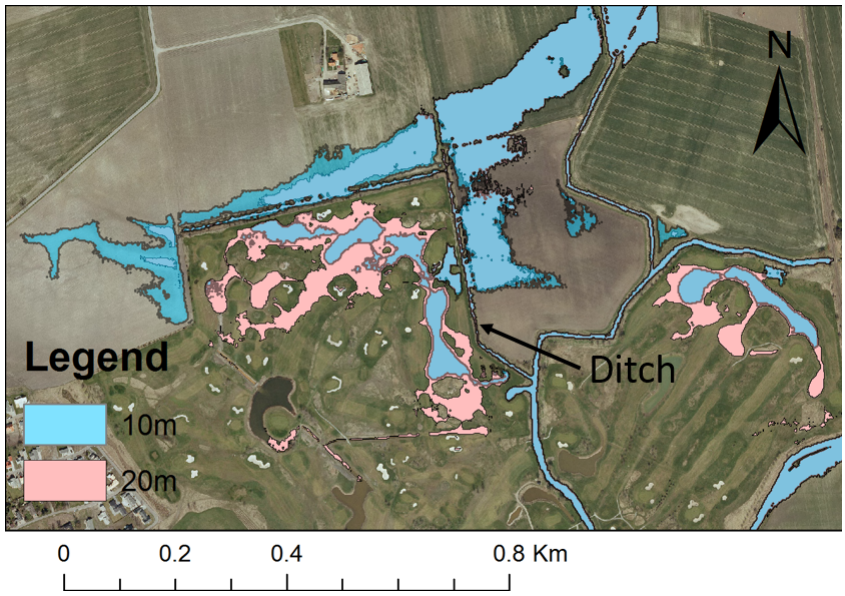

Figure 8.9: Difference in flooding extent after 12 hours of simulation when using a floodplain mesh resolution of 10m (blue) and 20m (pink). Background image: GSD-Ortofoto, 1m color ©Lantmäteriet.

The difference in extent between 10 and 20 m resolution seems to be caused by the ditch (see figure 8.9), separating the northern parts of the golf course from surrounding farmland. In 10 m resolution, this ditch is well represented, forcing the water to stay north of the ditch and flow in a westerly direction. For the 20 m resolution however, the cells do not capture the banks of the ditch, resulting in leakage into the golf course.

The effect of the ditch is further shown in figure 8.10, presenting the flooding for the same computational mesh sizes and time, although now the 20m mesh has its cells aligned along the ditch using a breakline. It is clearly seen that the extents are matching much better than without the breakline, suggesting that the use of breaklines can give the same effect as reducing cell sizes, but without significantly increasing computations times (there was no notable difference in computation times between models with and without the golf ditch breakline).

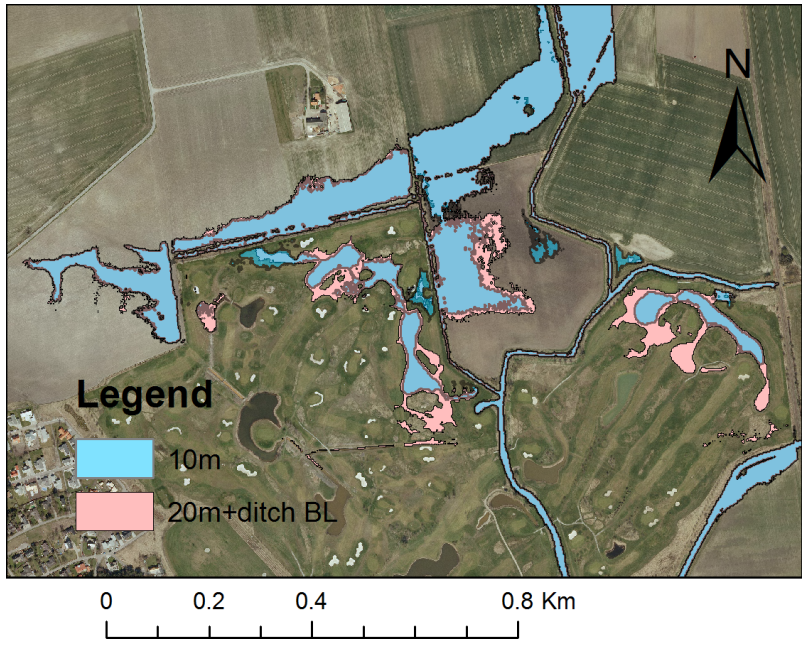

Figure 8.10: Difference in flooding extent after 12 hours of simulation when using a floodplain mesh resolution of 10m (blue) and a mesh of 20m with a breakline along the ditch (pink). Background image: GSD-Ortofoto, 1m color ©Lantmäteriet.

8.2.1.2.3 Computation times A final comparison was made between computation times for the different geometries. The result is shown in table 8.3. Geometries 1-3, which have the most complex river mesh, also have the largest computation times per cell. However, with the exception of geometry 3, there is little difference in computation time per cell compared to geometry 4 (where cells are rectangular). It should be noted that other work was conducted on the computer at the time of the simulations. This is expected to be the cause of the large computation time needed for geometry 3.

Considering the results presented earlier in this section, using geometry 3 will lead to a large increase in computation times without significantly improving the result.

Table 8.3: computation times for geometry 1-10.

Geometry	Comp. time (hh:mm:ss)	Comp. time per cell (seconds/cell)
1(Standard)	00:45:19	0.2
2	00:30:44	0.2
3	02:52:51	0.38
4	00:15:21	0.17
5	00:17:13	0.18
6	00:22:25	0.18
7	00:33:50	0.18
8	00:16:48	0.18
9	00:16:59	0.16
10	00:26:31	0.19

8.2.2 Parameter sensitivity

In the mesh sensitivity method it was highlighted that there first seemed to be little difference between the using the full momentum equations vs. the diffusive wave simplification. This was found to be incorrect at the end of the study, and thus the diffusive wave simplification has been used for most of the 2D modelling in this report. However, in this chapter, some differences between the results generated by the full momentum equations vs. the diffusive wave simplification will be highlighted and discussed.

In table 8.4, the results from the overall sensitivity analysis is shown. The parameters tested were (i) Manning's n inside the river, (ii) Manning's n for the floodplain(fp), (iii) time step, (iv) governing flow equations (diffusive wave simplification (D.W.) or Full momentum St. Venant (F.M.). Geometry 1 was used for the analysis. Column 2 shows the original parameters values/conditions used, and column 3 the changes made to these parameters. The results in column 4 and 6 are relative to using the diffusive simplification with the standard (Changed from) parameters.

Table 8.4: Parameters tested in sensitivity analysis. All parameters are changed relative to geometry 1 using the diffusive wave simplification

Parameter	Changed from	Changed to	Max. rel WSE(%)	Lomma Peak Flow (m^3/s)	Rel. Peak Delay (hrs)	Comp. time (hh:mm:ss)
Manning's n (river)	0.04	0.02	-32.8	31.4	-2	45:19
Manning's n (floodplain)	0.06	0.03	-5.0	31.0	-1	46:00
Time step	5	3	0	30.8	0	1:04:03
Governing eq. and time step	D.W. 5s	F.M. 3s	43.7	-	-	3:24:31

The results show that changing Manning's n in the river has the largest effect on the maximum WSE, followed by Manning's n in the floodplain. As expected, a reduction in Manning's n reduces WSE and results in a slightly earlier peak. As for the geometric analysis, little difference was seen between peak flows.

More interestingly, changing governing equation from diffusive wave simplification to the full momentum equations increased the water surface elevation on the golf course by 43.7%. Results from the 1D-2D modelling (presented later in the report), showed no difference between the two governing equations, suggesting that acceleration terms generated in the river might cause this large increase in water level. The importance of Manning's n within the river channel was thus investigated when using the full momentum equation. The results are presented in table 8.5. the maximum water surface elevation is here relative to using the full momentum equation with the standard (Changed from) parameters.

Table 8.5: Parameters tested in sensitivity analysis. All parameters are changed relative to geometry 1 using the full momentum equations

Parameter	Changed from	Changed to	Max. rel WSE(%)
Manning's n (river)	0.04	0.02	-1.89
Manning's n (floodplain)	0.06	0.03	-8.0
Time step	3	5	UNSTABLE

Surprisingly, decreasing Manning's n in the river had very little impact on the water surface elevation at the golf course. Changing floodplain Manning's n, however, had a larger effect than when using the diffusive wave simplification. Manning's n was further lowered both within the river and on the floodplain (not presented), although a water level as low as the one generated with the diffusive wave simplification could not be

generated since the model crashed at low Manning's (at Manning's n of 0.01 in both river and floodplain).

8.3 Calibration

The final 2D model was run with a floodplain representation using a 20m computational cell size. The river was represented with breaklines along river banks and the river centerline in areas with clear river barriers. In areas without such barriers, the river was represented with breaklines along the river centerline only.

The diffusive wave simplification was used in the final model since a reasonable match could not be attained using reasonable Manning's n values. The railway bridge was in the end excluded from the model due to instabilities.

The calibration was performed through adjusting Manning's n inside the river as well as on the floodplan upstream and downstream the railway bridge respectively. Post-calibration values of Manning's n were set 0.025 for the whole river reach, 0.05 for floodplain areas downstream the railway bridge and 0.065 for floodplain areas upstream the railway bridge.

Despite these issues, a good agreement between the aerial photograph and the modeled inundation extent could be obtained (8.11), while an acceptable match between model data and measurements was produced at the Trolleberg station (8.12).

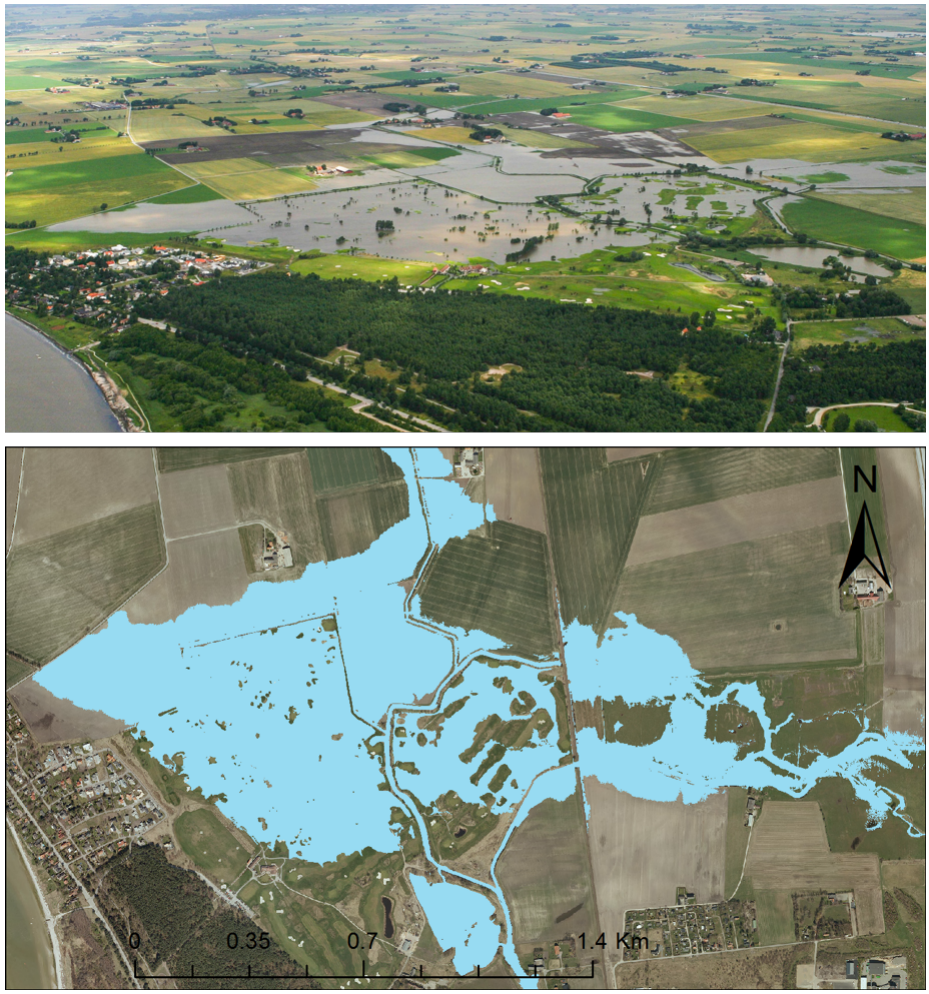

Figure 8.11: Upper: Önnerupsbäcken golf course 8th of July 2007(Photo: Swedish Coast Guard). Lower: Result from 1D-2D model, inundation extent 8th of July 2007.

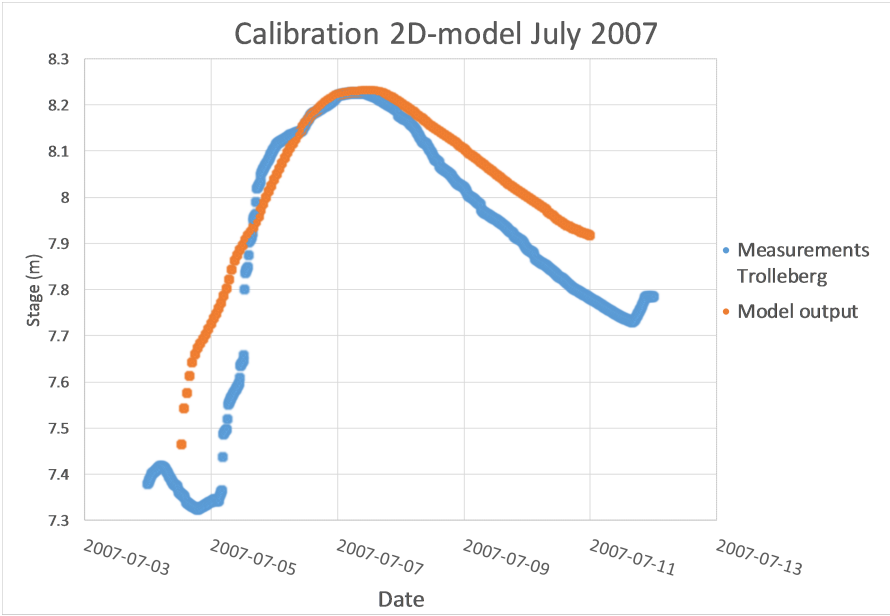

Figure 8.12: Modeled stage vs. Trolleberg measurements

8.4 Modelling of rapid flow events in urban areas using HEC-RAS

With the addition of 2D modelling in HEC-RAS, precipitation can now be added as a boundary condition. As highlighted in the introduction, pluvial events differ from fluvial events: they are much more rapid events, with time scales of hours rather than days.

The focus of this chapter was originally to investigate the importance of computational mesh size and governing equations when modelling pluvial events in Lomma city. Unfortunately, a current bug in HEC-RAS prevents detailed information to be exported from rainfall simulations. In order to better study the effects of rapid flood events in urban areas, the propagation of a flood wave in Lomma will be also investigated. It should be noted, however, that these events differ in characteristics, meaning that the results from the flood wave study might not be directly applicable to rain events.

The study can thus be divided into two parts: (i) Investigating the use of the precipitation boundary condition and (ii) investigating rapid flows in urban areas.

8.4.1 Method

The two studies use the same set-up, although the boundary conditions will vary. In this chapter, the model set-up is first introduced, before describing the details of the boundary conditions used for the rain and wave study respectively.

8.4.1.1 Data pre-processing and model set-up

Houses were incorporated into the elevation model by raising them 5 m according to the methodology presented in section 8.1.1. The resulting DEM for Lomma city is shown in figure 8.13, along with corresponding Ortophoto. Manning values of n=0.02 were assigned to buildings and roads using polygons acquired from the layers "Fastighetskartan" and "Oversiktskartan vector" aquired from Lantmäteriet. Manning's n=0.03 was assigned to Höje River. Remaining areas, consisting mostly of open areas and gardens were given n=0.06. The DEM had a resolution of 2 m.

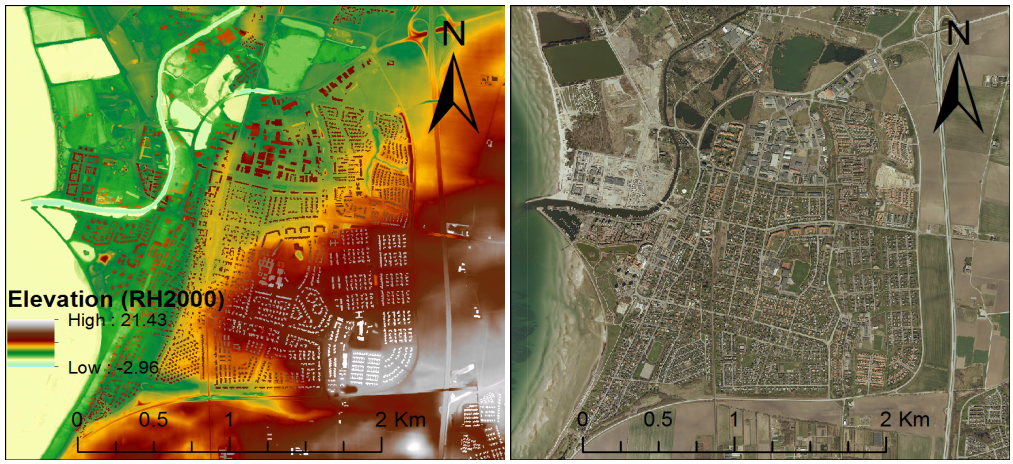

Figure 8.13: Lomma DEM with raised buildings (left) and corresponding Ortofoto (right).Based on GSD-Grid 2+ and GSD-Ortofoto, 1m color ©Lantmäteriet

Four computational cell sizes: 4, 8, 16, and 32m, were used. The cell faces coincided between geometries, illustrated in 8.14. One 8m cell shares computation cell faces with four 4m cells, although the 4m cells will also capture additional information regarding topography.

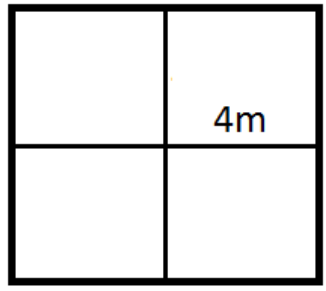

Figure 8.14: Alignment between 8 m cell (outer boundary) and four 4m cells.

8.4.1.2 Precipitation boundary condition

A 100 year CDS design rain with a duration of 6 hours was calculated according to Dahlström (2010) and Svenskt Vatten (2011). The stormwater system was compensated for by removing the capacity of a 10year rain with 30 min duration, which is considered as a standard design consideration in Sweden (MSB, 2014). This resulted in an effective rain occurring over 18 min with a total volume of 23.5 mm. The hydrograph is shown in figure B.3 in the Appendix. The same rain intensity was distributed over the whole area. Infiltration cannot currently be modeled in HEC-RAS and was neglected assuming saturated ground during the simulation period. The simulation was run for a total of 4 hours.

8.4.1.3 Flood wave boundary condition

A flood wave was released in the southeastern part of Lomma using an inflow boundary condition, see figure 8.15. The inflow size was set to $10 m^3/s$. The simulation was run for a total of 2 hours.

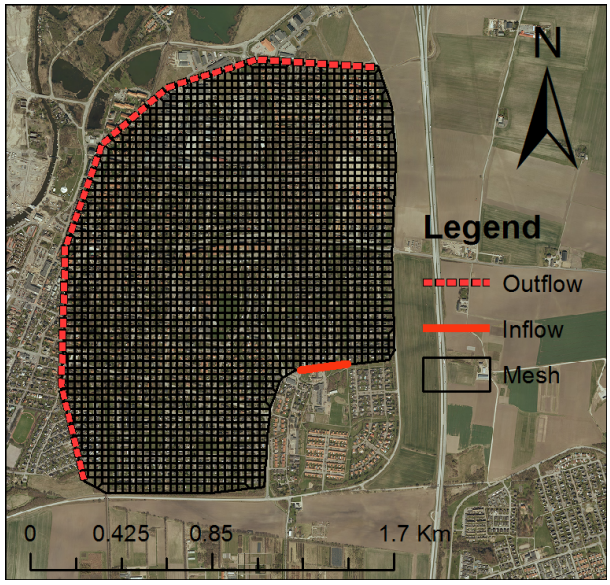

Figure 8.15: Boundary conditions used in the flood wave simulation.

8.4.2 Design rain results

The results of the rain simulations are shown in figure 8.16, presenting areas where depths exceeds 20cm for the 4m (blue) and 16m (red) resolutions respectively.

Figure 8.16: Areas with inundation depths larger than 0.2m, generated after 2 hours of simulation using 4m(blue) and 16m (red) computational mesh sizes respectively. Results are shown for the whole area (left) and for a smaller (zoomed in) part (right).

Overall, little difference was observed. Two areas where larger differences were seen are circled in the overview (left figure). However, the maps don't show the differences in water depths between the two cell sizes, making it hard to draw conclusions regarding the actual differences between estimated depths. The 8 m resolution gave an almost identical result as for the 4 m resolution, whereas the 32 m resolution differed slightly more than the 16m resolution (result not shown in figures).

The rain simulations were run with the diffusive wave simplification. The full momentum equation was shown to be unstable and caused unreasonable computation times. The instability was likely caused by the interaction between roofs and ground. For example, the equations used are based on assumptions regarding low bed slope and neglect vertical accelerations.

8.4.3 Flood wave results

In figure 8.17, maximum velocity profiles are shown for cell sizes of 4,8,16 and 32m respectively. All simulations were run with the diffusive wave simplification with a time step of 4s. The courant number was estimated to be less than 2 for all simulations. Water flows from southeast to northwest, following the general slope of the area.

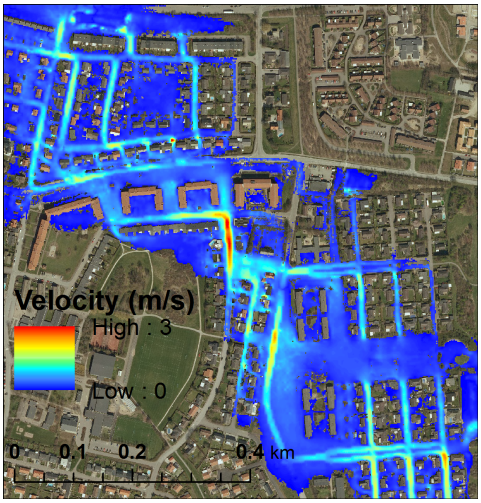

(a) 4m

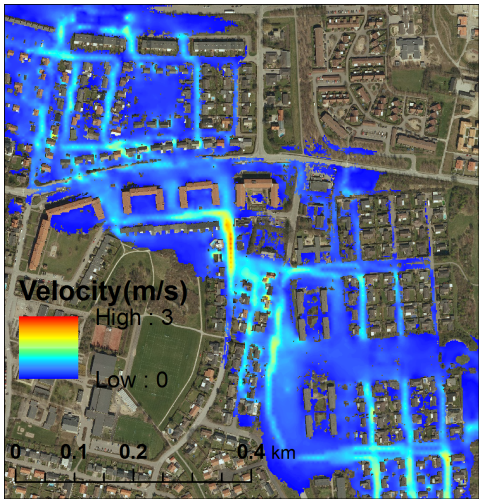

(b) 8m

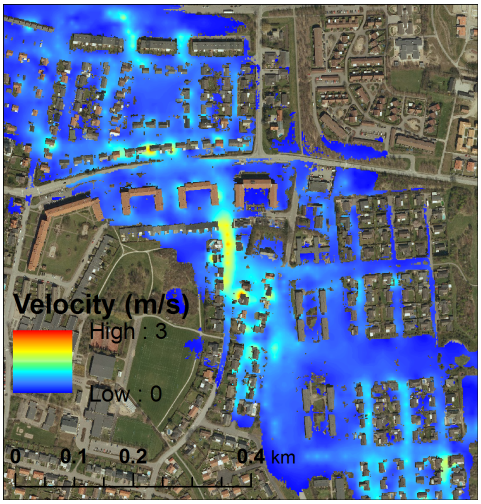

(c) 16m

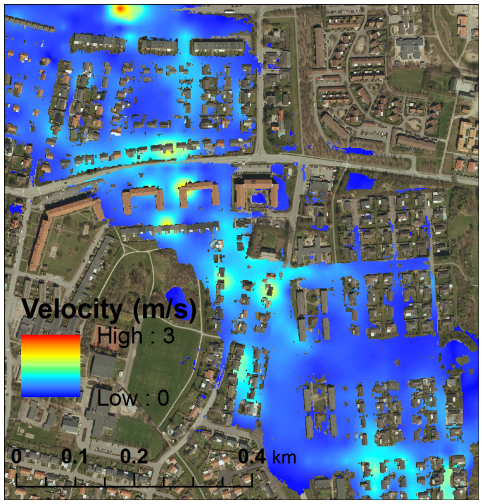

(d) 32m

Figure 8.17: Maximum velocity profiles at urban area in Lomma, generated by different computational mesh size.

The results show that smaller cell sizes are better at restricting flow to the streets and estimate higher maximum velocities compared to the larger cell sizes. The result is expected as larger cell sizes are more likely to allow shortcuts/leakage through houses and other barriers. Overall, the 8 meter cell size gave a similar result as to the 4 m cell size, suggesting that it might be used for rough estimations of flow velocities in urban areas similar to Lomma. When inspecting the average size of the houses in Lomma (visually), most of them have a minimum width of about 9-10 meters. Thus, the 8m

grid will capture most of the larger flow barriers consisting of houses. However, many of the smaller barriers will likely be missed. Generally, this should lead to quicker overall flood propagation and a lower mean depth for larger cell sizes. This hypothesis was investigated by looking at the inundation extent and depths after 1 hour of simulation. The results are shown in table 8.6 and visually in figure 8.18. In table 8.6, the inundated area (relative to 4m), mean and maximum depth are shown for computational cell sizes of 4,8,16 and 32 after 1 hour of simulation.

Table 8.6: Relative inundated area, mean depth and maximum depth, generated for computational cell sizes of 4,8,16 and 32 m respectively at 1hr after start of simulation.

Cell size (m)	Rel. Area (%)	Mean depth (m)	Max. depth (m)
4	0	0.162	1.17
8	1.75	0.161	1.13
16	3.26	0.159	1.06
32	-2.83	0.161	1.31

The results shows an increase in inundated area and a decrease in mean depth when increasing the computational cell size from 4 to 16m. Using 32m cell size, however, generated the opposite picture. Meanwhile, when looking at at maximum generated depths, it is seen that a much higher maximum depth was generated for the 32m resolution. This suggests that flow in the 32 m resolution has found its way to depressions that were not captured by the other resolutions. Thus, less water was available for propagation, which might have resulted in the low inundation areas and high mean depths that deviated from the trend.

In figure 8.18, the difference between computed depths (calculated as depths in the 4m resolution minus the depths in 32m resolution) as well as the difference in inundation extents between these resolutions, are presented. The figure shows that while there might be small differences between calculated inundated area, clear differences can be seen in the spatial distribution of the flooding as well as projected depths.

The left figure illustrates that the areas where the 4m resolution produces a larger depth than the 32 m resolution (blue), seems to be larger than for the opposite scenario (red and orange). In contrast, the 32m resolution will generate areas where it produces a much higher depth compared to 4m resolution, than the other way around (compare high scale= 0.63 and low scale=-1.22).

Based on these results, it is concluded that larger computational cell sizes are likely to underestimate overall depths, although larger depths might be generated in depressions. In addition, it might change the direction of propagation.

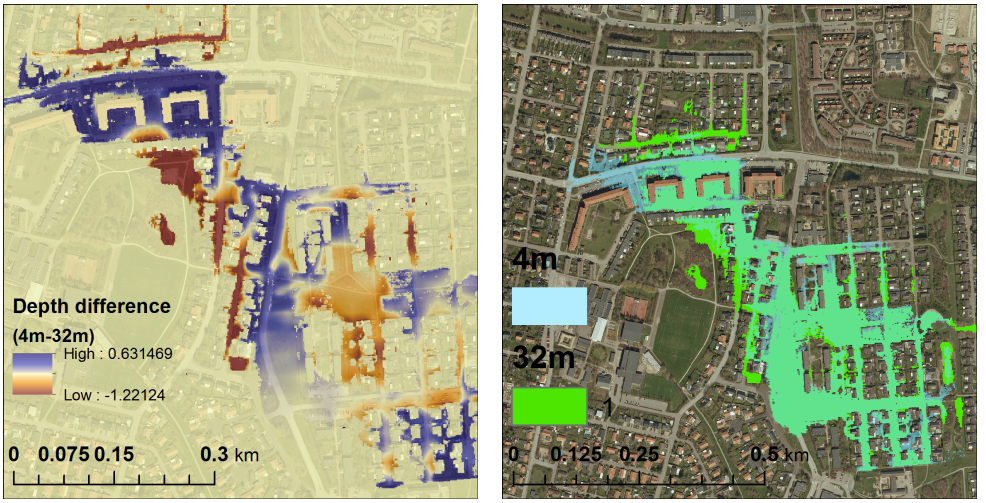

Figure 8.18: Difference in computed depths between 4m and 32m resolution (left) and computed extent (right).

Lastly, the differences between results generated using the diffusive wave and the full momentum equations was investigated for a computational cell size of 4m.

In figure 8.19, the maximum velocity distributions are compared when using the diffusive wave simplification compared to the full momentum equation. The time step was set to 1s for both simulations, reducing Courant numbers below 1.

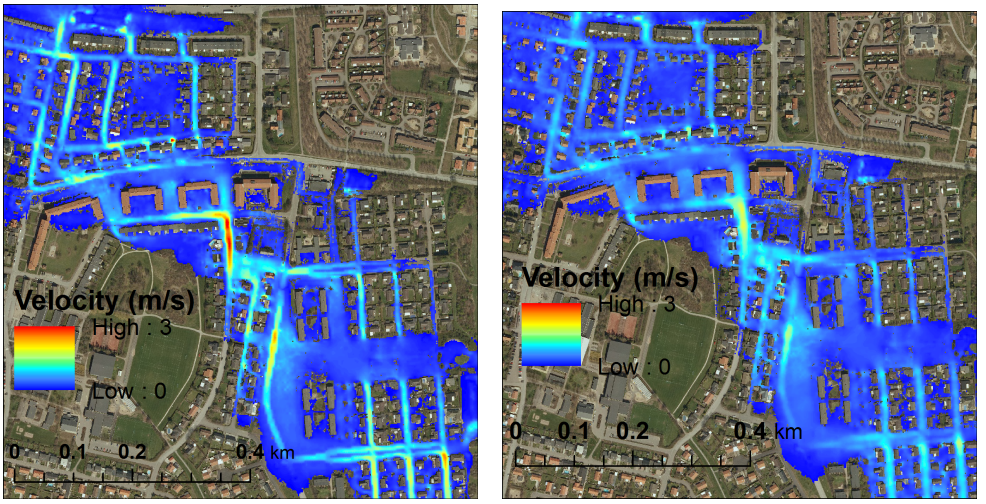

Figure 8.19: Velocity distribution generated with the diffusive wave simplification (left) and full momentum equations (right).

The results show that the full momentum simulation generates lower maximum velocities (1.9 m/s compared to 3 m/s for diffusive wave simplification) and a less clear velocity pattern along streets. Using the simplified model, local and convective acceleration terms are neglected, neglecting effects of contraction and expansion, turbulence and momentum transfer from streets to nearby garden/pavements. This might be one reason for the decrease in estimated velocities.

In figure 8.20, depth differences and area extent are compared between simulations with the diffusive wave simplification and full momentum equations.

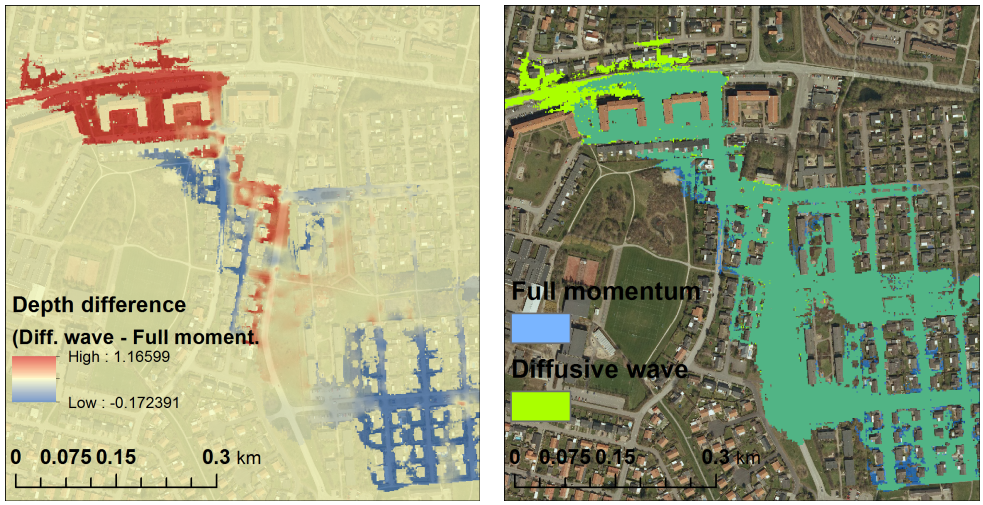

Figure 8.20: Difference in generated depths (left) and flooding extent (right) between results generated with the diffusive wave simplification and full momentum equations.

It is shown that the diffusive wave simplification allow further propagation of the design wave than for the full momentum scenario, while producing less inundation extent (and depths) in the upper (southeastern) parts of Lomma.

The results suggests that the local and convective acceleration terms in the momentum equation may play an important role for pluvial modelling in areas similar to Lomma, where using the diffusive wave simplification could neglect important energy losses, leading to an underestimation of depths and overestimation of velocities and the rate of flood propagation.

8.5 Discussion

8.5.1 Model construction

Pre-processing of data for 2D modelling is relatively easy. Using river bathymetry measurements, the river can be incorporated into the DEM using a few simple steps in HEC-RAS. Meanwhile, large uncertainties remains regarding the interpolation technique used by HEC-RAS, and current bugs require additional work using GIS software. Another consideration regarding pure 2D modelling are boundary conditions. Adding uniform lateral inflow to river reaches where floodplain flooding is to be modelled is not possible, and may be hard to get around for certain applications.

Modelling structures seems to be one of the largest current issues for pure fluvial 2D modelling in HEC-RAS. While bridges can be modelled using gates or culverts, this will likely introduce additional work during calibration and uncertainty for validation. In addition, the bridge representation made the model unstable, even when using the diffusive wave simplification.

Mesh construction was shown to be very important regarding the model outcome. Result sensitivity to mesh construction should thus be investigated in all projects. Results from this study highlight the importance of correct river representation in flat, rural areas. Important barriers, both next to river and in the floodplain, has to be correctly represented using breaklines.

When barriers are thin, steep and long (such as the barriers at the golf course), capturing the highest part can be difficult and requires precise work. It also requires high precision elevation data, and field surveys may have to complement LIDAR data. As a result, modifications may have to be done to the DEM in a GIS-software. Being familiar with GIS software and the many uncertainties included in GIS-operations is thus of great importance when constructing a pure 2D model.

Floodplain cell size is likely much less important than breakline placement if reasonable computation times are to be kept.

8.5.2 Mesh sensitivity

From the geometric sensitivity analysis it was shown that representing both banks and rivers with breaklines allow the best river representation for this area. This method produced 4 cells between the banks, compared to 2-3 cells when using bank breaklines and 1 cells when using river breaklines.

Based on this observation, a minimum of four cells between river banks is suitable, enabling both capturing of breaklines and aligning cell faces perpendicular to the main direction of the flow. However, the use of smaller river cell sizes should be investigated to find out if further reductions in cell size are needed. Meanwhile, large uncertainties lie within the representation of the banks. When inspecting the bank breaklines (not presented), they do not seem to be correctly placed on the top of the barriers in the DEM at all locations. Thus, the large difference in results generated by different river

representations might be due to the fact that more cells within the river will increase the chance of the cell faces correctly capturing the actual top of the banks. Still, this highlight the fact that using smaller cells increases the chance of capturing important topographical elements that might be missed when placing breaklines. It also highlight the importance of careful breakline placement. In future studies, investigations targeting the importance of river representation should be conducted in reaches where barriers are clearly defined so that there are no uncertainties to whether or not the highest elevation of the barriers have been captured by the breaklines.

Considering the velocity zigzag pattern generated in figure 8.8, it can be expected that the orientation of cells may play an important role for the result, although the magnitude of this effect should must also be investigated in an area where the effect of barriers can be eliminated.

While the use of bank and river breaklines is important in flat areas where flooding is controlled by clearly defined banks/levees, it will not be as important in areas where the river is surrounded by increasingly elevated terrain. In those situations, using only river breaklines with cell sizes similar to those in the floodplain might be sufficient.

Suitable floodplain cell sizes are likely to vary highly depending on the type of floodplain. For rural floodplains, the results from this analysis suggest that floodplain cell size has much less effect on the inundation extent compared to river representation. Instead, the most important design consideration regarding rural floodplains are to represent natural barriers with levees. Results from this study suggest that the use of breaklines could produce the same effect as reducing computation cell size, but without significantly increasing computation time.

It is likely that much larger cell sizes could be used in the floodplain as long as the ditch is represented with a breakline, although this study did not look into optimization of floodplain cell size.

While the use of breaklines seems promising in areas with clearly defined barriers, areas with complex terrain, such as urban areas, will have so many barriers that representation of them all will be impossible (each house can be considered a barrier). With this in mind, important design considerations remain regarding the trade off between the use of small computational cells versus the use of large computational cells and breaklines.

8.5.3 Pluvial modelling

Using HEC-RAS 2D for modelling of pluvial events could be promising when wanting to get an overview of risk-prone areas. Compared to other 2D programs, the sub-grid representation might allow larger computational grids to be used for pluvial overview modelling and might thus be used to scan larger areas in a shorter time. While computational cell sizes below 5m has been suggested for other models, results from this study suggest that 8m resolution can give very similar results as of 4m models. However, before HEC-RAS is used for modelling of pluvial events, several things should be investigated.

First of all, future studies investigating propagation of waves should use the full momentum equations. Acceleration terms are likely to increase in importance when maximum velocities are higher. Thus, since the results indicate that smaller computational mesh sizes generate larger velocities, the full momentum equations might generate larger differences between different computation cell size compared to what was seen when the diffusive wave simplification was used.

The effect that raising the terrain has should be further investigated. Currently, HEC-RAS cannot handle the flows from rooftops to the ground when using the full momentum equations. One possible solution could be to be to add rain only on the groud, althoguh spatially varied precipitation cannot currently be added in HEC-RAS. As of now, the diffusive wave simplification works better, but will neglect the momentum transfer of the water that falls from roofs. The importance of this effect might thus have to be further investigated.

Meanwhile, the results from this study suggest that the diffusive wave simplification will underestimate depths and overestimate flood propagation. Thus, a larger Manning's n will be needed compensate for the energy losses generated by the acceleration terms. Depending on the application, this might be a viable option, although differences between results must be compared more carefully.

Overall, a better building representation should be investigated. Rising the DEM by 5 meters to represent building will produce flat rooftops with corresponding ground depressions, causing water to get stuck of roofs. The effect is likely larger when using smaller computational mesh sizes, since more cells will have all sides on top of the roof. Thus, while smaller cell sizes will improve topographic representation, less water will be available to propagate.

Considering that elevated barriers are the main issue for sub-grid representation, it is suggested that the computational grid is smaller than common house sizes in order to avoid leakage. However, street representation should not be an issue, since these are normally low compared to the rest of the landscape. This fact may allow for larger cell sizes than in other applications.

Further studies are needed to make a more thorough investigation of computational cell sizes in urban areas. HEC-RAS sub-grid representation is likely to excel when very detailed topographical data is available. For many urban areas, topographical resolution of 0.5m can be generated. An interesting study would be to compare a 4m computational grid (using sub-grid resolution of 0.5m) with a software without sub-grid representation, having to interpolate the 0.5 m grid to 4m. Likewise, using the same 0.5 topographical resolution, a comparison between an 8m computational mesh using sub-grid information could be compared with a non sub-grid model with 4m resolution.

The importance of the full momentum equations likely depends on the slope of the area, since this will control velocities. In flat areas where velocities are lower, the acceleration terms are likely less important. A quick estimation of the slope between the start and ending areas gives a mean slope of 0.27°, although the actual average slope based on mean flow path lengths is likely much lower, since the streets will prevent the water from taking the shortest path. As highlighted in the introduction of this chapter, the characteristics of the flood wave differ significantly from that of an evenly distributed

rain event. Thus, further studies are needed to be able to draw conclusions regarding rain events.

9 Coupled 1D-2D model results

This chapter will describe the set-up and running of the coupled 1D-2D model. First, the process of setting up the model geometry is described. Thereafter, the results from the sensitivity analysis are presented. The focus of the sensitivity analysis is to investigate the impact of the parameters describing the model coupling. Thereafter, results from model calibration are presented, followed by a discussion on 1D-2D modelling in HEC-RAS.

9.1 Model set-up

The initial processing of the geometry data is performed in ArcMap using the GeoRAS extension.

If a 1D geometry has been developed in GeoRAS it is fairly simple to set-up the 1D-2D geometry using the 1D model as a base. It was decided to model the flooded areas around the golf course and areas east and west of Önnerupsbäcken in 2D, and the rest of the domain was model purely in 1D. The 2D areas are connected to the 1D model using lateral structures, which should ideally follow the high ground separating the river from the the floodplain (Brunner, 2014). The stretch of the lateral structures was determined using the DEM. Using GeoRAS, the structures were digitized and assigned elevation data from the DEM. Thereafter, the 2D flow areas were digitized as polygons, with the edge of the polygon following the lateral structure. The last step was to cut the original cross section cut lines layer and create a new layer with cross section that did not cover the extent of the 2D flow area. A flowchart describing the set up of the geometry is showed in figure 9.1.

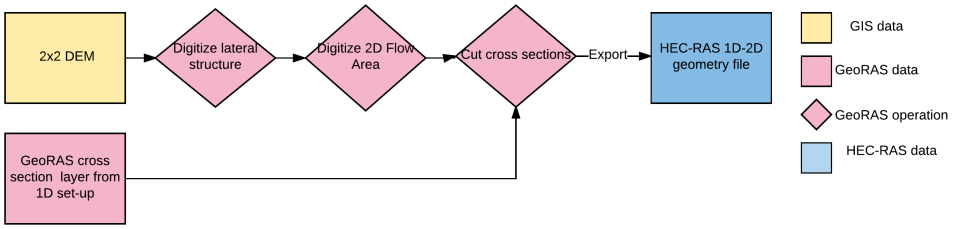

Figure 9.1: Workflow for developing 1D-2D geometry with lateral structures using GeoRAS and existing 1D geometry

Figure 9.2 shows the layout of the 1D-2D geometry. Once the geometry has been imported into HEC-RAS, modifications of the 2D model can be performed in the same way as described in chapter 8. Breaklines were added on important features in the 2D flow area to align the cell faces along these. The lateral structure was modified so that the elevation of the lateral structure did not exceed the elevation of the connected 2D cells, which is not allowed in HEC-RAS.

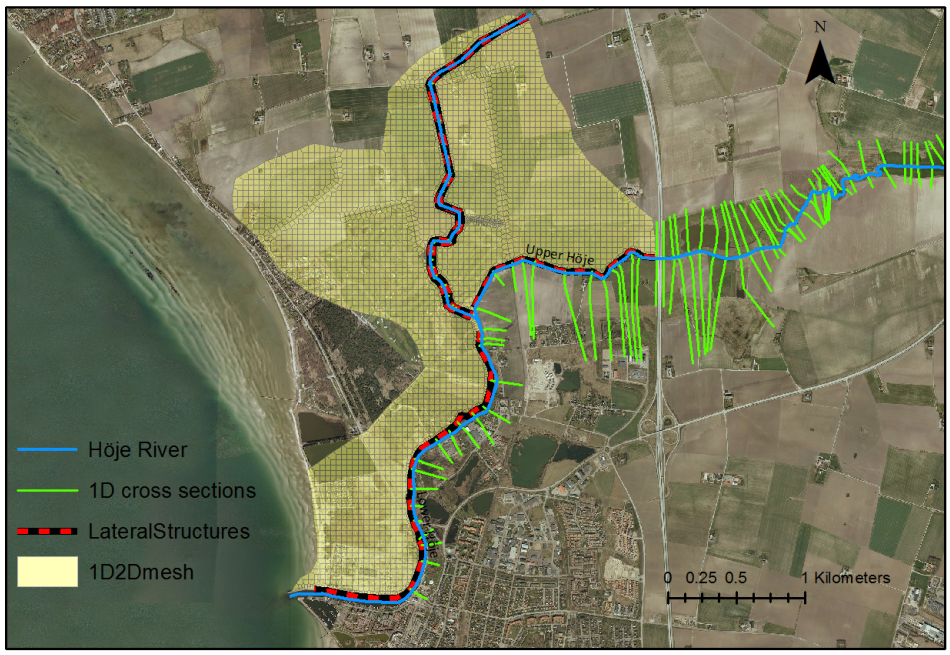

Figure 9.2: Overview of the coupled 1D-2D model, showing location of 1D cross sections, 2D flow areas and lateral structures. The entire model is not shown in the figure, the 1D domain reaches further upstream.

9.1.0.1 Hydraulic structures and bridges

Hydraulic structures can be added to the combined 1D-2D model in the same way that they are added to the pure 1D and 2D models. Due to the instability issues with the coupled 1D-2D model of Höje river, no attempts to model bridges or other structures were made.

9.1.1 Boundary conditions

The boundary conditions are added to the 1D cross sections in the same way as to the 1D model. No boundary conditions are added to the 2D areas of the model. See figure A.1 in appendix for a graphical illustration of the distribution of boundary conditions.

9.2 Model stability

The Höje river model was sensitive to all kinds of changes in flow dynamics. Changes in 2D geometry, boundary condition hydrographs, Manning's n-value, and lateral structure elevation all had impact on model stability. Based on stage-hydrographs and profile plots it was concluded that the model easily goes unstable when when the water

level in the river reach is approximately the same as the elevation of the lateral structure. Therefore the model goes unstable when modelling slowly rising hydrographs, or when modelling scenarios where the difference in water level between the 1D and 2D domains of the model are very small.

The geometry of the lateral structures had big impact on the stability of the Höje river model. The barrier separating the river from the overbanks was small, making it was difficult to determine the the stretch of the lateral structures. Due to smaller tributaries entering Önnerupsbäcken the elevation profiles of the structures become very irregular. The very low elevation of the structure at the location where the tributary enters causes a lot of water to flow out of the 1D reach at this point. The irregular shape of the lateral structures likely contribute to the issue of 1D water levels becoming very close to the level of the structure. When the elevation profiles of the lateral structure are smoothed through filtering the elevation data, the model stability increased significantly. However, this process means that the representation of the terrain is modified, and the accuracy of the model result can be questioned.

Model stability will be discussed further in the sensitivity analysis, where stability issues related to model time step and other calculation parameters will be addressed.

9.3 Sensitivity analysis

A sensitivity analysis of the parameters describing the coupling between the 1D and the 2D model was carried out. HEC-RAS has two options for calculating flow over the lateral structure connecting the 1D and 2D domains of the model, the weir equation and the 2D equations, sensitivity analyses were performed using both calculation methods to identify differences between the two. The default form of the 2D equations is the diffusive wave approximation. The effect of using the 2D full momentum equations was also investigated. The tested scenarios are presented in table 9.1. Findings from the sensitivity analyses of the 1D and 2D model are applied to the coupled 1D-2D model. Therefore, no sensitivity analysis regarding cross sectional spacing, general mesh cell size or friction parameters are performed.

Due to issues with model stability the sensitivity analysis was carried out for a simulation period for which the majority of the simulations were stable. The aim with the sensitivity analysis was to investigate how the model parameters affected not only model stability but also model results. Performing the sensitivity analysis for the shorter time period for which the majority of the simulations were stable will hopefully provide more general information of the impact of different parameters.

Table 9.1: Scenarios tested in the 1D-2D sensitivity analysis

Calculation method	Changed parameter	Scenario ID	Parameter Value
Weir equation	Time Step	W-TS1	1s
		W-TS2	3s
		W-TS3	5 s
		W-TS4	10 s
	Weir coefficient	W-W1	0.1
		W-W2	0.3
		W-W3	1.1
	2D equations	W-FM	Full Momentum
		W-DW	Diffusive wave
Normal 2D	Time step	N-TS1	1 s
		N-TS2	3s
		N-TS3	5s
		N-TS4	10 s
	2D equations	N-FM	Full Momentum
		N-DW	Diffusive wave

9.3.1 Time step sensitivity analysis

During the hydraulic computations flow over a lateral structure is calculated as constant over a time step. The choice of time step could therefore have impact on the exchange of water between the 1D and 2D domain. Furthermore, if the lateral structures are long, the changes in flow from one time step to the next could become very large. Using too long time steps can therefore cause the model to go unstable (Brunner, 2016a). A time step sensitivity analysis was carried out to investigate how the time step affects the model results when the weir and normal 2D equations are used. All scenarios N-TS1-4 were performed using the diffusive wave form of the 2D equations.

The 1D-2D solver has the option to iterate between the 1D and 2D domains of the model. Using iteration could potentially increase model stability and accuracy, but will much increase computation time. The HEC-RAS user manual recommends to only use 1D-2D iterations for unstable models (Brunner, 2016a). To evaluate the impact of using iterations simulation were performed with and without 1D-2D iterations.

9.3.1.1 Results

Table 9.2: Results from time step sensitivity analysis. No value (-) indicates that the simulation was unstable and crashed before the end of the simulation.

Scenario	Mass Balance Error (3 iterations)	Mass Balance Error (no iterations)	Computation time (3 iterations)	Computation time (no iterations)
W-TS1	1.4 %	1.97 %	49 min	49 min
W-TS2	2.4 %	1.26 %	44 min	26 min
W-TS3	2.1 %	2.7 %	32 min	18 min
W-TS4	2.5 %	2.1 %	25 min	12 min
N-TS1	11.1 %	11.17 %	31 min	21 min
N-TS2	4.9 %	12.4 %	22 min	9 min
N-TS3	15.9 %	-	15 min	-
N-TS4	-	-	-	-

In general, the computation time decreases with increased time steps. If iterations are on the computation time increases significantly for the majority of the simulations.

When the weir equation is used the mass balance errors increase slightly when the time step is increased. Turing of iterations increased the mass balance error for scenario W-TS1 (1s) and W-TS3 (5s), and decreased the error for the two other simulations. The relative differences are however very small.

In general, the model is not very sensitive to the choice of time step when the weir equation is used. No or very small differences in inundation extent between scenarios WTS1-4 could be detected visually, also when comparing simulations with and without iterations. Comparing flow and stage hydrographs in river cross sections, the differences were very small. There were, however, large differences in flow and stage hydrographs over the lateral structures in Önnerupsbäcken. Figure 9.3 (left) shows the flow over the lateral structure connecting Önnerupsbäcken to the golf course (left 2D area in figure 9.2) calculated with and without iterations, and figure 9.3 (right) shows the flow calculated using different time steps. Turning on iterations seems to provide a more smooth flow between the 1D and 2D domain. When longer time steps are used the flow over the lateral structure is slightly oscillating, indicating that the solution is not stable. Using a small time step and allowing 1D-2D iterations seems to be the preferable choice, despite the long computation times.

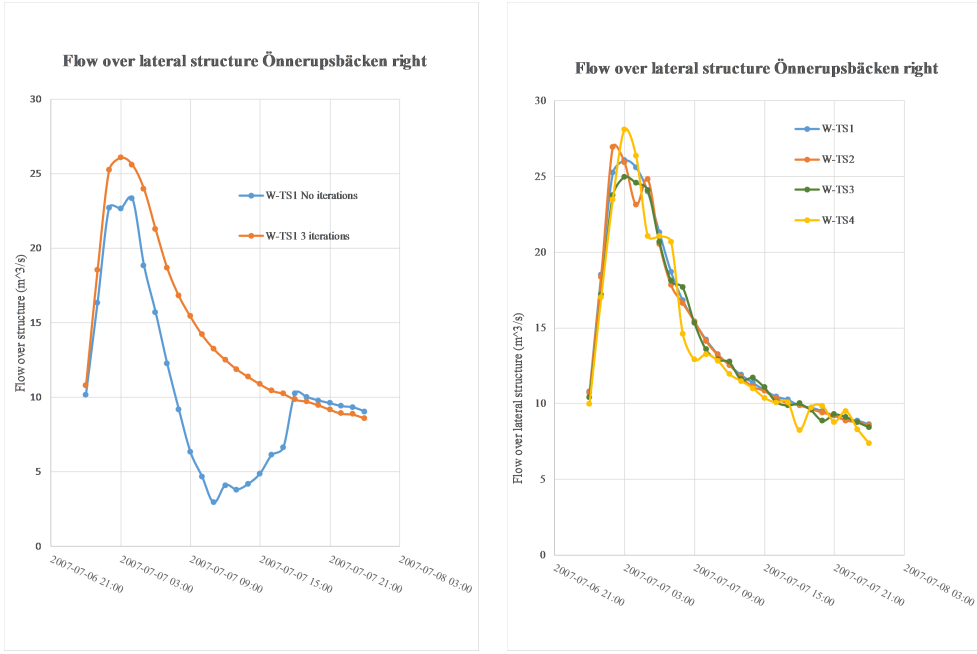

Figure 9.3: Left: Flow over lateral structure connecting Önnerupsbäcken and 2D area 1 , calculated using the weir equation with and without 1D-2D iterations, time step 1s. Right: Flow over lateral structure connecting Önnerupsbäcken and 2D area 1, calculated using the weir equation with iterations and time steps 1-10s.

When the 2D equations are used a time step smaller than 10s was required for the model not to crash. Without iterations, the time step had to be smaller than 5s. The mass balance errors are significantly larger compared to when the weir equation is used. No clear relationship between time step and mass balance error could be detected. However, turning off iterations increased mass balance error for all simulations.

When flow is calculated using the 2D equations the model results are much affected by the choice of time step. Inundation extent increased with increased time step. Flow and stage hydrographs in the river as well as flow over the lateral structure was affected by the choice of model time step and whether or not the program was allowed to iterate. The highest 1D model peak flows were obtained for scenarios N-TS2 (3s) and the lowest for N-TS3 (5s). There was hence no obvious relationship between peak flow and time step.

Figure 9.4 shows flow over the lateral structure connecting Önnerupsbäcken to the golf course calculated using the 2D equations with different time steps, and with/without 1D-2D iterations. All simulations display some flow oscillations, the issue seems to increase with increasing time step. It can be noted that scenario N-TS2, which has the smallest mass balance error still appears less stable compared to scenario N-TS1.

Figure 9.4 (left) shows that the flow oscillations increase when iterations are turned on. However, data is only stored every 10 min, so all peaks might not be captured in the output hydrograph.

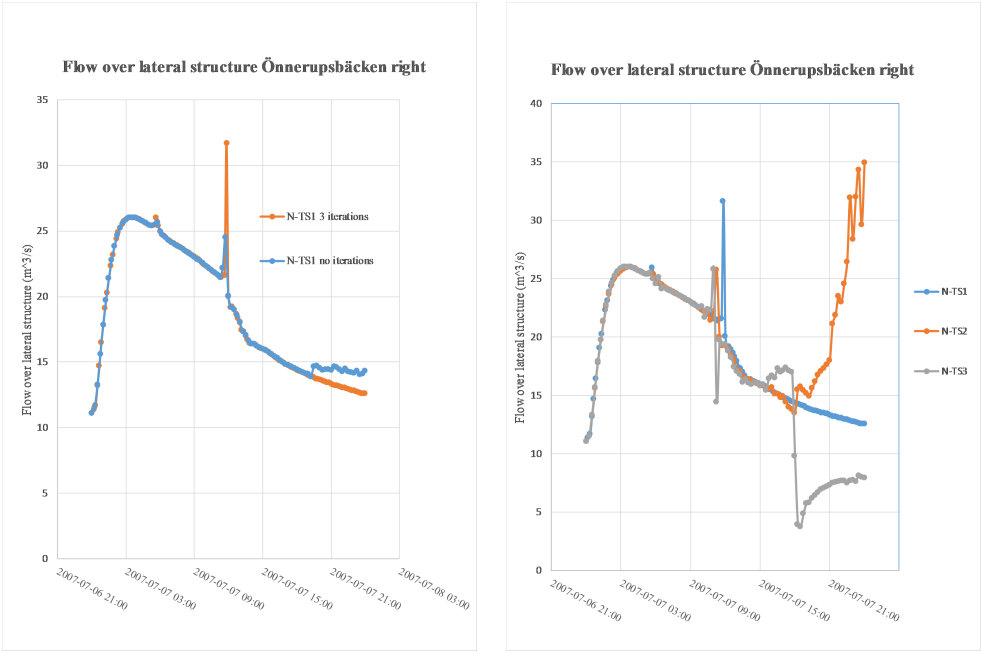

Figure 9.4: Left: Flow over lateral structure calculated using 2D equations with and without 1D-2D iterations, time step 1s. Right: Flow over lateral structure calculated using 2D equations with iterations and time steps 1-10s.

The conclusion from the time step sensitivity analysis is that both the weir equation and the 2D equations are sensitive to time step, and that small time steps and iterations should be used for both methods. The 2D equations are more sensitive to time step choice compared to the weir equation.

9.3.2 Weir coefficient sensitivity analysis

When the weir equation is being used to calculate flow over the structure, the user is required to specify a weir coefficient (C in equation 4.3). The HEC-RAS user manual recommends a weir coefficient between 0.11-0.28 when modelling overland flow escaping the main channel over non-elevated terrain, and between 0.28-0.5 when modelling flow over elevated natural ground (US-ACE, 2015). All simulations were performed using a time step of 1s, since this time step provided the most stable solution. In scenario W-W1 the default weir coefficient is used, this is hence the same scenario as W-TS1.

9.3.2.1 Results

The model is very sensitive to the choice of weir coefficient. A lower weir coefficient results in higher peak flow in the 1D cross sections, and lower flow over the lateral structures. The maximum inundation extent decreased with a decreased weir coefficient. Studying the dynamics of the inundation it could be seen that inundation extent and water levels on the golf course increased faster when a higher weir coefficient was used. Figure 9.5 shows the flow over the lateral structure connecting Önnerupsbäcken to the golf course.

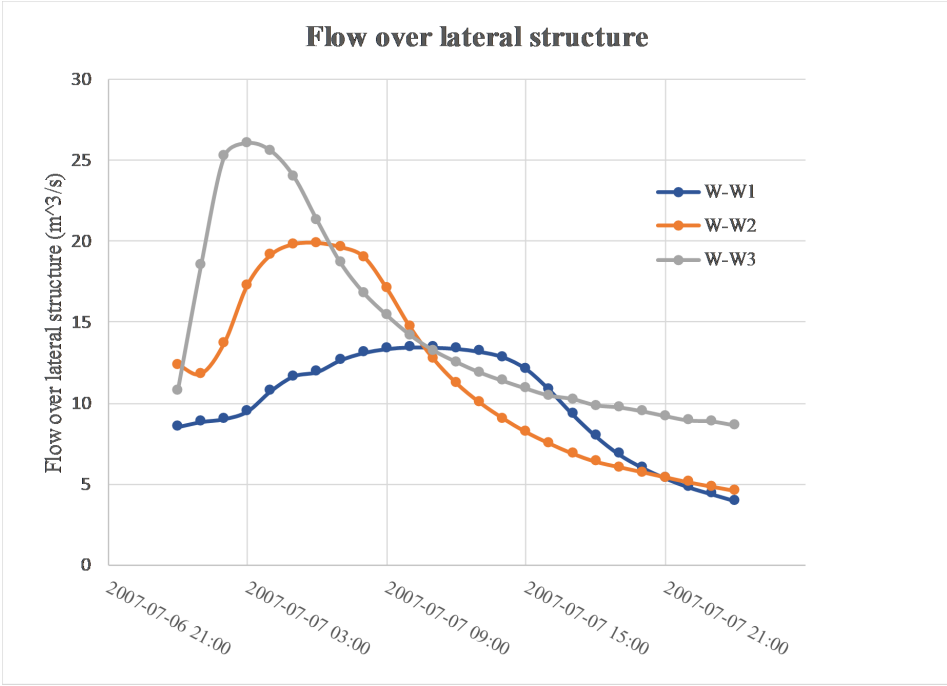

Figure 9.5: Flow over the lateral strucuture connecting Önnerupsbäcken with the golf course calculated using different weir coefficients. (0.1 (W-W1), 0.3 (W-W2) and 1.1 W-W3))

9.3.3 2D calculation method sensitivity analysis

As discussed in the chapter on 2D model results, flow in the 2D domain of the model can be calculated using the full momentum equations or using the diffusive wave approximation. When flow over the structure is calculated using 2D equations, the choice of 2D equations will determine how the flow between the 1D and 2D domain is calculated. When the weir equation is used, the choice of 2D equations will impact the propagation of flow in the 2D domain, which could affect the hydraulic gradient between the 1D and 2D domain. The sensitivity analysis was carried out to determine

how the choice of 2D equations impact model results. The simulations are carried out using time step 1s, allowing 3 1D-2D iterations. Scenario W-DW and N-DW are hence identical to scenarios W-TS1 and N-TS1.

9.3.3.1 Results

Scenario	Computation time	Mass Balance error 2D area left	Mass balance error 2D area right	Mass balance error total
W-DW	32 min	0.015 %	0.005 %	2.2%
W-FM	40 min	0.014 %	0.006 %	2.2 %
N-DW	28 min	11.2 %	0.9 %	11.1%
N-FM	39 min	2 %	0.25 %	2.9 %

Table 9.3: Mass balance errors for scenarios tested in the 2D calculation method sensitivity analysis

The difference between scenario W-FM and W-DW was negligible. Comparing flow over the lateral structure, it could be seen that the hydrographs were almost identical, the boundary conditions provided to the 2D model were hence the same for scenario W-DW and W-FM. When comparing the propagation of flow in the 2D domain very little change was detected. The propagation of flow on the golf course is hence insensitive to the choice of 2D equations. It was concluded that when the weir equation is used to calculate lateral structure flow, the 1D-2D Höje river model is not sensitive to the choice of 2D equations.

Comparing scenario N-DW and N-FM the difference in output was significant. The mass balance error was much reduced when the full momentum equation was used (-11.1% using diffusive wave versus -2.8% using the full momentum equation). The flow over the lateral structures in Önnerupsbäcken was much affected. When the diffusive wave approximation was used the flow over the structure increased, especially towards the end of the simulation period. Looking at the lateral structure in the upper reach of Höje river, little change was detected. Comparing flow hydrographs in the river cross sections it was noted that more water was contained within the 1D domain when the full momentum equation was used.

When looking at inundation extent and water depths in the 2D area, scenario N-FM lead to larger inundation extent compared to N-DW. This contradicts the previous results, which showed that less water enters the 2D domain in scenario N-FM. The answer is found in the continuity balance for the two simulations. The mass balance error for one of the 2D areas in N-DW is high, a lot of water is hence lost during the numerical solution of N-DW, and the results from this simulation are not credible. The mass balance error for N-FM is small, maximum 2% for the 2D flow areas. Likely, increasing the number of 1D-2D iterations will decrease the error in N-DW.

9.4 Calibration

The coupled 1D-2D model was calibrated against the aerial photograph of inundation extent and against stage measurements from Trolleberg.

The 2D full momentum equations were used to calculate flow over the lateral structures to reduce the number of calibration parameters. The calibration was performed through adjusting Manning's n in the cross sections and on the 2D flow areas. Post-calibration values of Manning's n was 0.03 in the main channel cross sections downstream the railway bridge, 0.05 in the main channel of upper Höje river, 0.07 in the cross section floodplain in the upstream reach of Höje river, and 0.05 on the 2D flow areas. Calculating lateral structure flow with the weir equation, using the same values of Manning's n, a good agreement could be obtained with a weir coefficient of 0.15.

During calibration, model stability proved to be affected by changes in Manning's n, and the model was not stable to all tested values of Manning's n. Despite these issues, a good agreement between the aerial photograph and the modeled inundation extent could be obtained, see figure 9.6 for comparison.

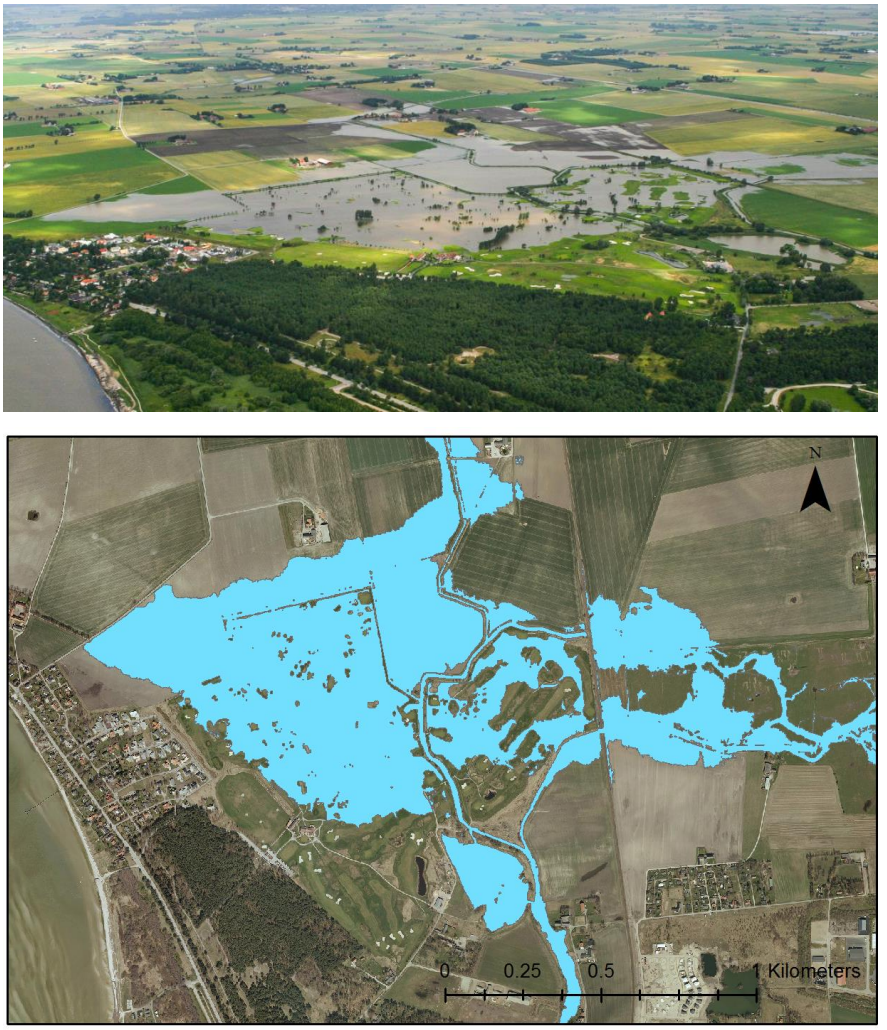

Figure 9.6: Upper: Önnerupsbäcken golf course 8th of July 2007v(Photo: Swedish Coast Guard). Lower: Result from 1D-2D model, inundation extent 8th of July 2007.

Measured and modeled stage in Trollberg can be seen in figure 9.7. The agreement between measured and modeled flow is good, and the peak stage is captured by the model.

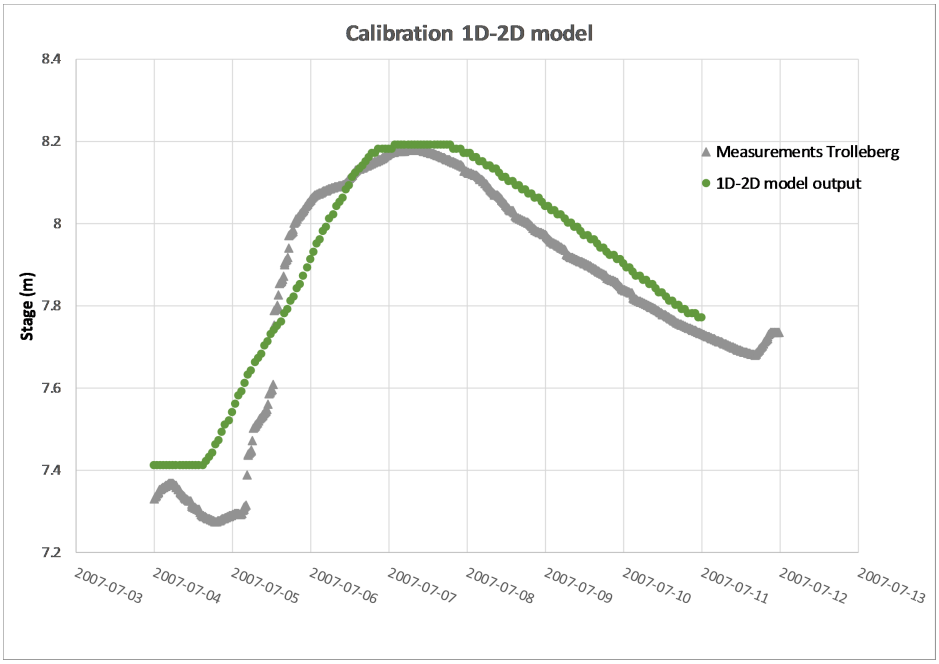

Figure 9.7: Measured flow in Trolleberg and output from 1D-2D model.

9.5 Discussion

9.5.1 Calculation method for 1D-2D exchange flow

The 2D diffusive wave equation was more sensitive to the choice of time step compared to the weir equation. Using the 2D diffusive wave equation also gave rise to significantly larger mass balance errors. However, when the 2D full momentum equations are used to calculate flow over the structure the mass balance errors decrease significantly, although they remain larger compared to when the weir equation is used. Due to the very large mass balance errors it can be concluded that using the 2D diffusive wave equation is not appropriate for the Höje river model.

In Önnerupsbäcken the river is separated from the golf course with a small barrier, when water overtops the lateral structure it will hence flow down a slope. It could be that this slope is too steep to be accurately modeled using diffusive wave simplification, and that the acceleration terms of the full momentum equation are important in this case. This can be compared to the lateral structure in the upper reach of Höje river, where there is no barrier separating the river from the overbank. The flow over this structure is only affected to a very small extent by the choice of diffusive wave or full momentum equations. These results give rise to the hypothesis that when river flow is separated from overbank flow with an elevated barrier, a weir equation or the full momentum 2D equations should be used to calculate flow between the models. When river flow and overland flow is not separated by a barrier, the diffusive wave simplification of the

2D equations seems sufficient to model the exchange flow. However, when there is no clear barrier separating the river from the overbank, it might be difficult to determine a suitable location for the lateral structures. Since the computation time is reduced when the diffusive wave equation is used, this equation is preferable when no change in output between the calculation methods can be detected.

Furthermore, flow calculated using the weir equation is very sensitive to the choice of weir coefficient. Without access to calibration and validation data is can be very difficult to determine an appropriate value of the weir coefficient. This is a disadvantage with using the weir equation, in cases were calibration data is limited, the 2D equations could be a more appropriate choice.

It is difficult to draw general conclusions regarding the appropriate choice of calculation method based on one case study. The results from the sensitivity analysis of the Höje river model showed that the full momentum form of the 2D equations, and the weir equation with appropriate choice of weir coefficient, could model the exchange flow without large mass balance errors. Furthermore, the results indicate that when the terrain is flat and the river is not separated from the 2D area by a levee, the diffusive wave form of the 2D equations are sufficient. Since the weir equations require a weir coefficient to be specified, which have large impact on results, there is a risk of over-parametrization when the weir equation is used. The full momentum 2D equations is therefore the most appropriate choice for the 1D-2D Höje river model.

9.5.2 Set-up and pre-processing

The coupled 1D-2D model with lateral structures is more complex to set up compared to the pure 1D and 2D models, since set-up of both 1D and 2D geometries and coupling between the two models is required. Based on the sensitivity analysis it can be concluded that the coupling parameters will have large impact on model results, and setting up a stable connection that provides accurate model results can be difficult. The 1D-2D model requires more user-specified parameters compared to the pure 1D and 2D models, which leads to more sources of uncertainty.

9.5.3 Advantages and limitations

An advantage with the coupled 1D-2D approach is that the terrain model does not have to be modified to include channel bathymetry. Channel flow is modeled purely in 1D, and the channel is only represented in the cross sections. The coupled 1D-2D approach takes away the issues with representing the channel bathymetry in the 2D mesh, and there is no need to use a finer mesh cell size in the river to accurately model river flow. In areas where flow is mainly 1D, such as the upstream part of Höje river, a pure 1D approach can be applied. This reduces the complexity of the 2D mesh, and the total number of 2D cells, which could reduce the computation time. However, for the Höje river model a very small time step was required for stability, leading to computation times close to those of the pure 2D model.

The boundary conditions to the model can be entered in the same way as in the 1D model. This opens up for the possibility to set-up 1D-2D models on catchment level. However, the lateral structures connecting the 1D-2D domains cannot be too long, both for stability reasons and because they can only contain a maximum of 500 station-elevation points, which limits how much geometric detail the lateral structures can contain. If the modeller has some idea of what areas of the catchment that are likely to be flooded, these areas can be modeled as smaller 2D areas connected to the 1D river. The rest of the model domain, where flow is expected to be mainly contained within the main channel, or where detailed information of inundation dynamics is not of interest, can be modeled purely in 1D.

The main disadvantages with the 1D-2D modeling approach is the instability issues. Finding settings that could provide a stable solution to a simulation of the entire floodwave was very difficult. Changing the boundary conditions will potentially cause new instability issues. The 1D-2D model developed in this project is hence not very versatile.

The stability issues were related to choice of time step and calculation method as well as to the geometry of the lateral connection. The geometry of the lateral structures, and thereby to some extent the stability of the model, are determined based on the terrain data. It was not possible to obtain a stable solution without modifying the geometry of the structure, leading to a poorer representation of the model terrain. The 1D-2D approach appears to be more suitable for modelling areas where the 1D and 2D domains are separated by a clear and smooth levee, and where no tributary streams enters the 1D main channel from the 2D domain. If modeling an area with tributaries, the tributaries should probably either be added as 1D channels, or both tributaries and main channel should be modeled in 2D.

If another river reach was to be modeled using the 1D-2D approach it is very possible that the above-mentioned stability issues would not arise. It can be concluded that the coupled 1D-2D approach is not appropriate for the Höje river model.

Another drawback of the 1D-2D approach is the fact that parameters describing the coupling have such large impact on model results. This increases the uncertainty, and the number of calibration parameters, which might lead to over-parameterization.

When flow leaves the 1D domain it will be added as a boundary condition to the 2D domain. Although not mentioned explicitly in the HEC-RAS documentation, it appears as momentum is not transferred between the 1D and 2D domain. The 1D domain of the model cannot model any momentum in the lateral direction, if the river is highly meandering, the lack of lateral momentum in the channel and the lack of momentum transfer between the 1D and 2D domain might lead to inaccurate results.

10 Model comparison

In this study, important differences between 1D, 2D and 1D-2D modelling have been explored and will be highlighted in the following chapters. In addition, the applicability of the different models are discussed based on areal characteristics and desired level of complexity.

10.1 Model set-up and results

In the following chapters, the models are compared with respect to input data and pre-processing, geometry set-up, boundary conditions, computations and result (calibration).

10.1.1 Input data and pre-processing

Input data is essential for both 1D, 2D and 1D-2D models. If a pure 1D model is to be constructed, topography data only has to be available at the cross sections, whereas 2D and 1D-2D models require elevation data covering the entire domain, such as a DEM. In Sweden, DEM with resolutions of 2m are available for many areas.

Bathymetry measurements are often provided along transects of the river, a format suitable for 1D (or 1D-2D) applications since data can be extracted and directly used as cross sections. If a pure 2D model is set-up, some pre-processing of the elevation model is typically required to incorporate the bathymetry measurements. This is the case when using elevation data from the Swedish Land Survey (Lantmäteriet). HEC-RAS has a built in tool for interpolating river bathymetry from cross section. In the current available versions of HEC-RAS (up to 5.0.3) a bug is causing the interpolation routine to work poorly around meanders. The interpolation results also seem to be sensitive to where the user has specified the bank stations of the cross sections. Overall, there is a lack of description of the method used for the interpolation in HEC-RAS. Due to the highlighted importance of correct representation of river bathymetry (e.g. (Cook and Merwade, 2009)), important uncertainties may lie within the method of interpolation.

10.1.2 Geometry set-up

The models differ substantially when it comes to geometric set-up. 1D models consists of cross sections which represent the topography of the river and floodplain at cross sections only. 2D and coupled 1D-2D models, on the other hand, use a computational mesh to capture additional terrain detail on the floodplain. Both the 2D and 1D-2D model make use of the cross sections constructed in the 1D model, but need additional work.

In the 2D and 1D-2D model, a mesh has to be digitized. Computational cells have to be aligned along important barriers to prevent leakage. Finding a suitable mesh

structure might take large amounts of time since the result might be very sensitive to careful placement of breaklines and choice of suitable cell sizes. More time is needed to find a suitable river representation in the pure 2D model than in the coupled 1D-2D coupled. However, the structure separating the 1D-2D model might take considerable amount of time to set-up when long and complex river barriers are present.

Representation of river structures is developed for 1D modelling and thus induce uncertainties when applied to pure 2D-models. For instance, Bridges must be presented using culverts, gates or by carefully modifying the terrain. The last option however, cannot incorporate situations where the water level impacts the bridge deck. Using gates or culverts on the other hand, it may be hard to match the elevation-area curve representing the opening (US-ACE, 2016). In addition, different benchmark loss values are likely needed in order to prevent overestimation of energy losses (Babister et al., 2012).

10.1.3 Boundary conditions

The adding of boundary conditions differ between the 1D and 2D models. In 1D, upstream boundary conditions in form of stage or flow hydrographs can be added at the uppermost cross section of a the modeled river reach. Internal boundary conditions can be added as lateral inflow hydrographs, either to a single cross section, or uniformly distributed over several cross sections.

In 2D, boundary conditions can only be added at the outer edge of the computation mesh. This is problematic when modeling rivers with lateral inflows from tributaries or downstream sub-catchments.

In 2D, rainfall can be added as a boundary condition, enabling simple rainfall-runoff simulations. However, it is not possible to add spatially distributed rainfall. In addition, infiltration/evaporation cannot be currently modeled in HEC-RAS.

10.1.4 Computations

Computation times
The computation times vary dramatically between the 1D, 2D and 1D-2D models. In this study, the 1D solver can simulate the whole model area over a month-long period in less than 1 minute, whereas the 2D and 1D-2D solvers take several hours to simulate a period of a couple of days. The computation times of the 2D and 1D-2D models are similar. The 1D-2D model has a less complicated mesh, with fewer cells and larger minimum cell size. However, a very small time step is required for the 1D-2D model to remain stable. In this study, the 2D model can be run with time step around 5s, whereas the 1D-2D model requires a time step of 1s. Choice of time step is however, case specific.

Stability
Stability was problematic for all models. By far, the 1D-2D model had the largest stability issues. During the set-up and sensitivity analysis of the 1D-2D model it was

concluded that the model was sensitive to all kinds of changes in flow dynamics. The fact that the model was so sensitive makes is less versatile than the other models. If the boundary conditions are changed, for instance if different scenarios are to be modeled, a lot of time would potentially have to be spent stabilizing the model.

The stability issues with the 1D Höje river model were related to cross sectional spacing. For some scenarios, low flows also caused stability issues. Due to the extensive documentation on 1D model stability, and the many options available in HEC-RAS to aid debugging, the stability issues were relatively easy to overcome.

The 2D model had overall less issues with stability than the 1D and 1D-2D models, although the diff. wave simplification was mostly used for the pure 2D modelling. When using the full momentum equation, the model was much more sensitive that when using the diff. wave simplification. Results from the sensitivity analysis indicate that the sensitivities are mainly caused inside the river. The diffusive wave simplification was not free from issues, becoming unstable when incorporating the railway bridge.

10.1.5 Calibration

All models were able to produce a satisfactory calibration result. Similar Manning's n values were used for all the three models. Thus, no significant increase in Manning's n had to be used for the 1D compared to the 2D representations, as has been observed in many previous studies (Tayefi et al., 2007). Meanwhile, due to the lack of available calibration data, studying this effect has not been a focus of the report.

Full momentum 2D equations were used in the floodplain of the 1D-2D model. In the pure 2D mode, however, the diffusive wave equation was used due to the issues with large energy losses inside the river channel, highlighted in section 8.2.2.

Mass balance errors of 1.3%, 3.2% and 0.001% were generated by the 1D, 1D-2D and 2D models respectively. Non of the models reached maximum number of iterations during the simulations, meaning that the numerical solutions were converging for all these simulations. The 1D solver has a larger water surface calculation tolerance compared with the 2D solver (0.006 m vs 0.003 m) which could partly explain the difference in mass balance error. Furthermore, the 2D solver has a specified computation volume tolerance, which is not the case for the 1D model.

The differences in dynamics is illustrated in 10.1, showing the water surface elevation over time at a point on the golf course (location shown in figure C.1 in the Appendix).

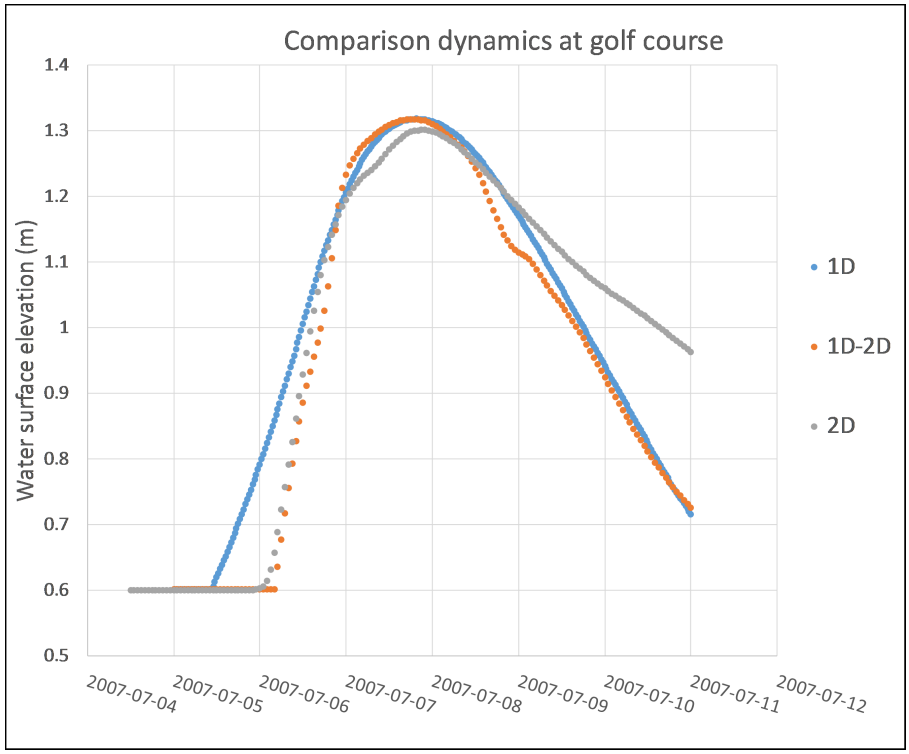

Figure 10.1: Computed water surface elevations at a point on the golf course, generated by the 1D,2D and 1D-2D calibrated models respectively.

As expected, the water levels start to rise earlier in the 1D simulation due to the incorrect representation of flow in the floodplain. The recession of the peak is interestingly similar for the 1D and 1D-2D models. It was expected that the 1D model would produce the steepest recession, since water cannot be "trapped" behind barriers when water is withdrawing. The reason for the similarity between the 1D and 1D-2D model remains unclear.

10.1.6 Summary

In the following table is a summary of this chapter, highlighting the most important differences between model set-up that were faces in this study.

Table 10.1: Summary of differences between models

Data requirements and pre-processing needs	1D	1D-2D	2D
XS-data	YES	YES	YES*
Digital elevation model	NO	YES	YES
River bathymetry interpolation	NO	NO	YES
Geometry set-up			
Terrain representated by	XS	XS+Mesh	Mesh
Set-up time	⏱	⏱⏱⏱	⏱⏱
Representation of complex river structures	Suitable	Suitable	Questionable
Representation of lateral inflow	Good	Good	Bad
Computations			
Computation times	Short	Long	Long
Stability problems	☹	☹☹☹	☹☹
Instability source	XS placement	Lateral structures	Full momentum in river, bridges (Culvert)

*Unless available topographical data is sufficient to represent the river bathymetry.

10.2 Model applications

Depending the desired level of detail and the complexity of the area that is to be modeled, different models will be more or less suitable. This section will consider the findings from the case study and the literature review, and based on this present some guidelines regarding what models that could be suitable for different applications.

In table 10.2, suitable models are picked out depending on application critera. More detail regarding model choice will be discussed in the following sections.

Table 10.2: Summary of what models that can be used for different applications

Required level of detail	
Maximum inundated areas	1D, 2D or 1D-2D
Dynamics and velocities important (e.g. Hazard assessment)	2D or 1D-2D
Structures	
Few, simple (weirs)	1D,1D-2D or 2D
Many, complex (dams, gates, bridges,culverts)	1D or 1D-2D
Floodplain characteristics	
Floodplain behind levee	2D or 1D-2D
V-shaped terrain	1D or 2D
Simple/rural	1D, 2D or 1D-2D
Urban	2D or 1D-2D

10.2.1 Required level of detail of model output

This case study has highlighted many differences between 1D, 2D and 1D-2D models both in terms of model output and in terms of time and effort that is required to set up and run the models. Depending what the project aim is, different models will be more or less suitable.

If the aim of the project is to find the maximum inundation extent, a 1D model could be sufficient, as in the Höje river case. However, the applicability of the 1D approach will depend on the characteristics of the area that is modeled. In more complex areas, where the inundation extent will be determined by how flow propagates around barriers on the floodplain, a 1D model will likely not be able to accurately determine the maximum inundation extent. 2D or 1D-2D models can be used to estimate maximum inundation extent. These models will, as discussed earlier, require longer set-up and computation times compared to the 1D approach, but might be necessary in more complex areas.

If flooding dynamics and detailed information regarding velocities on the floodplain is of interest, a 2D or 1D-2D model is required. This is due to the inherent limitations of 1D modeling that has been discussed previously.

10.2.2 Hydraulic structures

When modelling a river with many bridges and hydraulic structures, it is important to represent the structures in the hydraulic model to be able to accurately simulate the effect of different scenarios. Modeling of bridges and structures is not studied in detail in this project, however, the basic bridge modeling conducted in this case study highlighted that the 1D and 2D approaches differ very much in the way that hydraulic structures are represented. In 1D, the modelling of hydraulic structures is well studied, there exists a variety of calculation methods that can be used, and the models can provide detailed output data on flow around structures. This makes 1D models more suitable for modelling rivers where there are many and complex structures

interacting with the river flow. If details regarding flow around bridges and structures is important, a 1D approach is preferable due to the many limitations in modelling hydraulic structures in 2D. In 2D, it is possible to model simpler structures, such as weirs or culverts. If the modeled river only includes a few, rather simple, structures, a 2D model can be used. Energy losses caused by hydraulic structures could also be represented though local adjustment of the friction parameters, although this is not considered as an ideal solution (Babister et al., 2012).

10.2.3 Floodplain characteristics

The shape of the floodplain will have large impact regarding which model that should be used, and how this model should be constructed. This section will consider different types of floodplain and discuss how the model should be set up to model this type of floodplain as accurately as possible.

10.2.3.1 Floodplain behind levee or barrier

Modelling flow in a river where the main channel is confined by a levee is problematic using the 1D approach, as has been highlighted in the 1D chapter. In contrast to 1D models, both 1D-2D and 2D models can be used to model channel-floodplain interaction when floodplain and river are by a levee or some other barrier.

Using a pure 2D model, the results will likely be very sensitive to the capturing of the barriers using breaklines, as was discussed in chapter 8 concerning 2D modelling. In the 1D-2D case the banks are explicitly represented in the lateral structures, and there is no risk for leakage due to misalignment of the 2D cells, as is the case in pure 2D models. However, the case study showed that the parameters describing the lateral structures will have large impact on both model stability and results.

10.2.3.2 V-shaped terrain or valley

If the terrain is v-shaped, meaning that the terrain surrounding the river is sloping downwards in the direction of the river, and no barrier separates the floodplain from the river, a less complex model is likely required.

One of the drawbacks that has been highlighted with 1D modelling is the simplification that a single water surface is calculated for each cross section. If the floodplain is v-shaped, this simplification will be closer to reality compared to when the floodplain is confined by a levee. A 1D modelling approach is hence more suitable for modelling v-shaped floodplains.

A pure 2D model can also be used. If there are no barriers separating the river from the floodplain, there is no need to use breaklines or smaller cell sizes to capture the bank elevations. In those cases, large computational mesh sizes can probably be used thanks to the sub-grid approach, and result in realistic computation times, even on catchment scale.

Using a 1D-2D approach for a v-shaped catchment can be problematic, as there will be no clear separation between the main channel, which should be modeled in 1D, and the floodplain. Therefor it will be difficult to determine suitable locations for the lateral structures. In a v-shaped valley flow will likely be mainly in the direction of the stream, and a combined 1D-2D approach will not be necessary to describe this type of area.

10.2.3.3 Simple/rural floodplain

When modelling a simple, rural floodplain without many barriers limiting the flow, this case study suggests that a 2D or 1D-2D model with a rather large cell size (>20 m) can be used, if combined with breaklines defining important topograhical features.

A pure 1D model could also be used if the dynamics of the inundation is not of interest. This case study showed that the 1D model could accurately reproduce the inundation on the golf course, which is considered as a simple floodplain. If the barriers limiting flow are few, a 1D model can be sufficient, and the barriers can be represented implicitly though the friction coefficient.

10.2.3.4 Complex/urban floodplain

In a complex floodplain, such as an urban area, there are many barriers that will limit flow and affect flood propagation. Fluvial flooding of urban areas has not been studied in this project. The case study has highlighted the general limitations of the 1D approach when modelling floodplain flow. These issues are likely to be more important when modelling urban floodplain, as has been shown in literature (Vojinovic and Tutulic (2008); Costabile et al. (2015)). A 2D or 1D-2D approach is hence preferable when modeling flow on complex floodplains.

In literature it is suggested that 2D model of urban floodplains are very sensitive to mesh resolution, and that using larger cell sizes might decrease model accuracy as barriers cannot be fully represented (Yu and Lane, 2006a). Studies have also showed that using sub-grid terrain representation can allow larger cell sizes to be used (Yu and Lane, 2011, 2006b). It remains to be investigated whether similar result would be obtained using the HEC-RAS sub-grid model.

11 Uncertainties

This section will discuss and summarize the uncertainties related to all models used in this project.

One of the major uncertainties is the flow data that is used as boundary conditions to all models. Flow data was collected from the hydrological model S-HYPE, and were rescaled to capture the measured peak flow in Trolleberg. As discussed in section 6.4, there is a lot of uncertainty related to the flow and stage measurements from Trolleberg. There is also some uncertainty regarding the magnitude of the flow in Önnerupsbäcken. Önnerupsbäcken is regulated by a culvert some kilometers upstream the model domain, which may reduce the maximum flows in Önnerupsbäcken at high flow events. It is hence possible that flow in Trolleberg has been underestimated and flow in Önnerupsbäcken has been overestimated. If the boundary flows are wrong, the friction parameters determined during model calibration will also be incorrect, decreasing the chance of producing accurate results when modeling other scenarios.

The lack of validation data is another source of uncertainty. None of the models have been validated against other events than that of July 2007. This reduces the confidence in the calibration parameters.

All models were calibrated against a major flooding event. The fact that the models could reproduce this large event indicates that they will probably be able to simulate other larger flooding events with some level of confidence. Recorded data from large flooding events is not always available. If the models would have been calibrated against low flow scenarios, the confidence in the calibration parameters would be lower. An interesting study would be to calibrate the 1D, 2D and 1D-2D models against high and low flow scenarios, and study the robustness of the calibration for the different models.

For all models, there is also some uncertainty regarding the hydraulic computations. The governing equations are based on a series of assumptions that must be considered. In the 1D case, the assumption that flow is purely 1D is a major simplification of reality. In the 2D case, the assumption that the vertical velocities are negligible might be inaccurate, at least when modelling channel flow. The diffusive wave simplification has been used in many of the simulations performed in this project. Using this simplification all acceleration and turbulence terms are neglected, which might not be accurate when modeling flow in channels or on complex floodplains. In addition to the uncertainties regarding the applicability of the governing equations, there is some additional uncertainty related to the numerical solution of the equations. The numerical solvers all has some tolerance to errors, and the solution does not always converge, which might cause mass balance errors.

12 Conclusions

This study has highlighted some of the most important differences between the construction of 1D, coupled 1D-2D and pure 2D hydraulic models in HEC-RAS. In addition, important design considerations and uncertainties regarding 2D-and coupled 1D-2D modelling have been highlighted. In the following sections, the conclusions are presented.

12.1 Model comparison

Suitable choice of model depends on the detail of input data, area characteristics, desired level of complexity in the output data and project time (and money). Based on this case study and literature search, a rough guide for choosing a suitable model has been presented and discussed (see chapter 10). For the Höje river, all models could provide a good estimate of inundation extent. The 1D-2D model was not suitable for the application due to the many stability issues. Depending on what information that is of interest, a 1D or 2D model would be the preferable choice for the Höje river.

12.2 Model specific considerations

The results from the 2D mesh analysis show that model result is very sensitive to mesh alignment along barriers using so called "breaklines". In rural floodplains with clear barriers, correct use of breaklines is more important than computational cell size, and will enable considerable reductions in computation time.

The 2D urban study suggest that using the diffusive wave simplification may overestimate flood propagation and underestimate maximum depths when modelling rapid events in Lomma. The sub-grid approach has potential when modelling rapid events in urban areas, but needs to be further investigated in areas where validation data is available.

The results from the 1D-2D sensitivity analysis showed that the parameters describing the coupling will have large impact on model stability and model results, and that these parameters should be chosen with care. Furthermore, it was concluded that the 1D-2D model easily becomes unstable when the water surface elevation is approximately the same as the elevation of lateral structure.

13 Recommendations

Based on this case study, some recommendations regarding the set-up of 2D and 1D-2D models in HEC-RAS have been formulated.

13.1 2D modelling in HEC-RAS

Based on the 2D sensitivity analysis, the following recommendations are provided for future modelling.

In rivers surrounded by protective barriers, the following criteria should be fulfilled when constructing the computational mesh around a river: (i) Cell faces should be aligned with the highest elevation of the barriers at all locations. (ii) Cell faces should be perpendicular to the main river flow direction. (iii) Cell sizes should be small enough to allow criteria (i) and (ii) to be fulfilled, i.e. no interference between different alignments. The impact of criteria (ii) remains to be investigated.

Until further studies regarding the effect of using the full momentum equations in rivers have been conducted, using the diffusive wave equation currently seems to be a better option for pure 2D modelling, as the use of the 2D full momentum equations seem to highly overestimate energy losses in channels using HEC-RAS.

Pluvial modelling is not currently suitable in HEC-RAS. The interaction roof-ground induce large uncertainties when houses are incorporated into the DEM. The potential of the "precipitation" boundary conditions in rural areas remain to be explored.

13.2 1D-2D modelling in HEC-RAS

The following recommendations are based on the results from the set-up and sensitivity analysis of the 1D-2D model. It should be emphasized that these recommendations might not be valid for all model application.

If the main channel is separated from the floodplain with a barrier, the weir equation or the full momentum 2D equations should be used to calculate lateral structure flow. If no barrier is present, the diffusive wave form of the 2D equations is sufficient.

The weir equation should only be used to calculate lateral structure flow if calibration data is available, as this option requires a weir coefficient to be specified, which will have large impact on model results.

Rivers with tributaries entering the main river from the 2D domain might be problematic to model using a 1D-2D approach, as stability issues may arise due to the interaction between the tributary and the main channel.

13.3 Future studies

This project has compared potentials and limitations of 1D, 2D and 1D-2D modelling in HEC-RAS. This section will present aspects that should be investigated more in detail, and suggest some future studies that might contribute to the understanding of when and how different hydraulic models should be used.

When it comes to the sub-grid approach, the 2D sensitivity analysis highlighted several areas of uncertainty that still needs investigation. First of all, river representation in 2D has to be further studied. The importance and effect of varying computational cell size (and the number of cells within the river) should be investigated in a river where the effect of barriers can be minimized. Preferably, the study should be conducted in an artificially constructed V-shaped river without significant barriers. In connection, the effects of using the full momentum equation for 2D river flow should be explored, as this study indicate that it may overestimate energy losses. The influence of computational cell size on the result generated by the full momentum equation should be investigated. Results are preferably compared with results from corresponding diffusive wave approach and a 1D representation. In a completely straight river where energy losses are considered well represented by the 1D case, such a study may be able to quantify potential over-estimation of energy losses generated by the full momentum approach.

A similar study could also be conducted comparing river flow modelling using different types of 2D models. A study comparing the HEC-RAS sub-grid technique with non sub-grid 2D models for modelling river flow could provide some insight in how river flow is best modelled in 2D, and could further enhance the understanding of when and how the sub-grid technique should be used.

The importance of computational cell alignment in relation to the main river flow direction should also be investigated, using a similar areas as discussed above.

With regards to pluvial events. The potentials of sub-grid techniques should be further investigated. In many urban areas of Sweden, DEM resolutions of 0.5-1m can be generated by LIDAR data from Lantmäteriet (Lantmäteriet, 2015) or LIDAR measurement conducted by muncipalities. In such cases, sub-grid approaches enable better use of the highly detailed data than non-sub grid approaches. Studies may for example compare a non sub-grid model with a computational mesh of 4m with a 4m sub-grid approach, including a comparison of computation times. Furthermore, the use of the diffusive wave simplification for urban events should be further investigated in an area where validation data is available.

The difference between 1D-2D and pure 2D models when modeling highly meandering rivers should be investigated more in detail. The exchange of flow and momentum between the main channel and floodplain should be addressed, as well as the effect of lateral momentum within the river.

The effect of river bathymetry interpolation should be further investigated, preferably in highly meandering rivers.

Future studies regarding Lomma are suggested to target combined effect of pluvial and

fluvial events. An important aspect is to find out what flows and stages in Höje river that restrict outflow from stormwater pipes. Such effects might significantly increase the damage from pluvial events similar to those that have caused damage in Lomma over the last years. When modelling such an event, a software that may incorporate stormwater systems is thus preferable.

References

Andersson, M. and Bates, P. (1993). A Two-Dimensional Finite-Element Model for River Flow Inundation. *Proceedings: Mathematical and Physical Sciences*, 440(1909):481–491.

Arcement, G. J. J. and Schneider, V. R. (1989). Guide for Selecting Manning ' s Roughness Coefficients for Natural Channels and Flood Plains United States Geological Survey Water-supply Paper 2339. 2339(2339):39.

Babister, M., Ball, J., Barton, C., Bishop, W., Gray, S., Jones, R. H., McCowan, A., Murtagh, J., Peirson, B., Phillips, B., Rigby, T., Retallick, M., Smith, G., Syme, B., Szylkarski, S., Thompson, R., and Weeks, B. (2012). *Australian Rainfall & Runoff Revision Project 15: Two dimensional Modelling in Urban and Rural Floodplains.* Number November.

Brunner, G. W. (2014). Combined 1D and 2D Modeling with HEC RAS.

Brunner, G. W. (2016a). HEC-RAS River Analysis System : Hydraulic Reference Manual. (February).

Brunner, G. W. (2016b). HEC-RAS River Analysis System : User's Manual. (February).

Casulli, V. (2008). A high-resolution wetting and drying algorithm for free-surface hydrodynamics. (August 2008):391–408.

Chaudhry, M. H. (2008). *Open-Channel Flow.* Springer Science + Business Media, Boston.

Chow, V. T. (1959). Open Channel Hydraulics.

Church, J., Clark, P., Cazenave, a., Gregory, J., Jevrejeva, S., Levermann, a., Merrifield, M., Milne, G., Nerem, R., Nunn, P., a.J. Payne, Pfeffer, W., Stammer, D., and a.S. Unnikrishnan (2013). Sea level change. *Climate Change 2013: The Physical Science Basis. Contribution of Working Group I to the Fifth Assessment Report of the Intergovernmental Panel on Climate Change*, pages 1137–1216.

Coles, S. G. (2001). *An introduction to Statistical Modeling of Extreme Values.*

Cook, A. and Merwade, V. (2009). Effect of topographic data, geometric configuration and modeling approach on flood inundation mapping. *Journal of Hydrology*, 377(1-2):131–142.

Costabile, P. and Macchione, F. (2015). Enhancing river model set-up for 2-D dynamic flood modelling. *Environmental Modelling and Software*, 67:89–107.

Costabile, P., Macchione, F., Natale, L., and Petaccia, G. (2015). Flood mapping using LIDAR DEM. Limitations of the 1-D modeling highlighted by the 2-D approach. *Natural Hazards*, 77(1):181–204.

Dahlström, B. (2010). Regnintensitet–en molnfysikalisk betraktelse. *SVU Rapport*, page 46.

Engman, E. T. (1986). Rougness Coefficients for Routing Surface Runoff. *Journal of Irrigation and Drainage*, 112(1):39–53.

European Environment Agency (2010). *Mapping the impacts of recent natural disasters and technological accidents in Europe - An overview of the last decade*. Number No. 13/2010.

Höje Å Vattenråd (2016). Höje Å avrinningsområde.

Horritt, M. and Bates, P. (2002). Evaluation of 1D and 2D numerical models for predicting river flood inundation. *Journal of Hydrology*, 268(1-4):87–99.

Horritt, M. S. and Bates, P. D. (2001). Effects of spatial resolution on a raster based model of flood flow. *Journal of Hydrology*, 253(1-4):239–249.

Horritt, M. S., Bates, P. D., and Mattinson, M. J. (2006). Effects of mesh resolution and topographic representation in 2D finite volume models of shallow water fluvial flow. *Journal of Hydrology*, 329(1-2):306–314.

Lantmäteriet (2015). GSD-Elevation data , Grid 2 +.

McMillan, H. K. and Brasington, J. (2007). Reduced complexity strategies for modelling urban floodplain inundation. *Geomorphology*, 90(3-4):226–243.

Morales-Hernández, M., Petaccia, G., Brufau, P., and García-Navarro, P. (2016). Conservative 1D-2D coupled numerical strategies applied to river flooding: The Tiber (Rome). *Applied Mathematical Modelling*, 40(3):2087–2105.

MSB (2014). *Kartläggning av skyfalls påverkan på samhälls- viktig verksamhet*.

Neal, J., Schumann, G., and Bates, P. (2012a). A subgrid channel model for simulating river hydraulics and floodplain inundation over large and data sparse areas. *Water Resources Research*, 48(11):1–16.

Neal, J., Villanueva, I., Wright, N., Willis, T., Fewtrell, T., and Bates, P. (2012b). How much physical complexity is needed to model flood inundation? *Hydrological Processes*, 26(15):2264–2282.

Olsson, J. and Josefsson, W. (2015). Skyfallsuppdraget. (37).

Persson, G., Sjökvist, E., Åström, S., Eklund, D., Andréasson, J., and Johnell, A. (2011). Klimatanalys för Skåne län. *SMHI*.

Salvadore, E., Bronders, J., and Batelaan, O. (2015). Hydrological modelling of urbanized catchments: A review and future directions. *Journal of Hydrology*, 529(P1):62–81.

SMHI (2014). Tidsserier från S-HYPE.

Svenskt Vatten (2011). *Publikation P104 - Nederbördsdata för dimensionering och analys av avloppssystem.*

Sweco Environment AB (2009). Översvämningskartering av Höje Å genom Lomma kommun samt analys av stigande havsnivå.

Sweco Environment AB (2010). Höje Å genom Lomma, Lund och Staffanstorp. Technical report.

Tayefi, V., Lane, S., Hardy, R., and Yu, D. (2007). A comparison of one- and two-dimensional approaches to modelling flood inundation over complex upland floodplain. *Hydrological Processes*, 21(May 2007):3190–3202.

Trafikverket BaTMan (2016). Konstruktion 3500-1368-1 (1).

US-ACE (2015). HEC-RAS River Analysis System 2D Modeling User ' s Manual. (April).

US-ACE (2016). HEC-RAS 5.0.3 Release Notes.

Vojinovic, Z. and Tutulic, D. (2008). On the use of 1D and coupled 1D-2D modelling approaches for assessment of flood damage in urban areas. *Urban Water Journal*, 6(3, September 2009):183–199.

Yu, D. (2005). Diffusion-based modelling of flood inundation over complex floodplains.

Yu, D. and Lane, S. N. (2006a). Urban fluvial flood modelling using a two-dimensional diffusion-wave treatment, part 1: Mesh resolution effects. *Hydrological Processes*, 20(7):1541–1565.

Yu, D. and Lane, S. N. (2006b). Urban fluvial flood modelling using a two-dimensional diffusion-wave treatment, part 2: Development of a sub-grid-scale treatment. *Hydrological Processes*, 20(7):1567–1583.

Yu, D. and Lane, S. N. (2011). Interactions between subgrid-scale resolution, feature representation and grid-scale resolution in flood inundation modelling. *Hydrological Processes*, 25(1):36–53.

Appendices

A Distribution of boundary conditions

A.1 Distribution of flow data in 1D and 1D-2D model

Figure A.1 shows a graphical overview of how the flow data is distributed in the 1D-model and 1D-2D model.

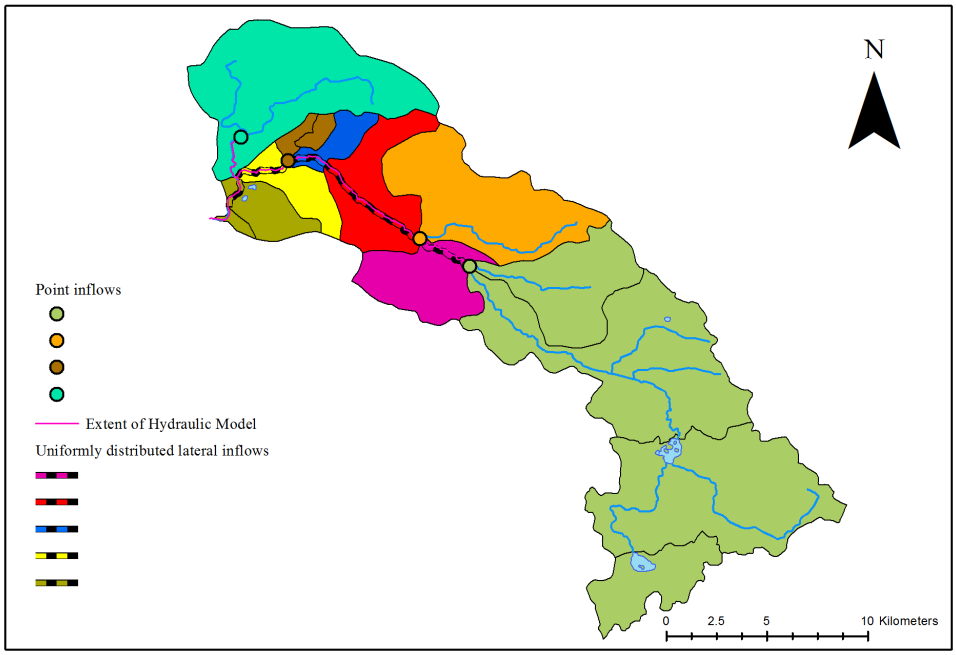

Figure A.1: Distribution of inflow hydrographs from contributing sub-catchments. Points represents inflow into a single cross section, lines represents flow distributed over several cross sections. The map is colour coded, an input line/point has the same colour as the sub-catchment(s) from which the flow is originating.

A.2 Distribution of flow data in 2D model

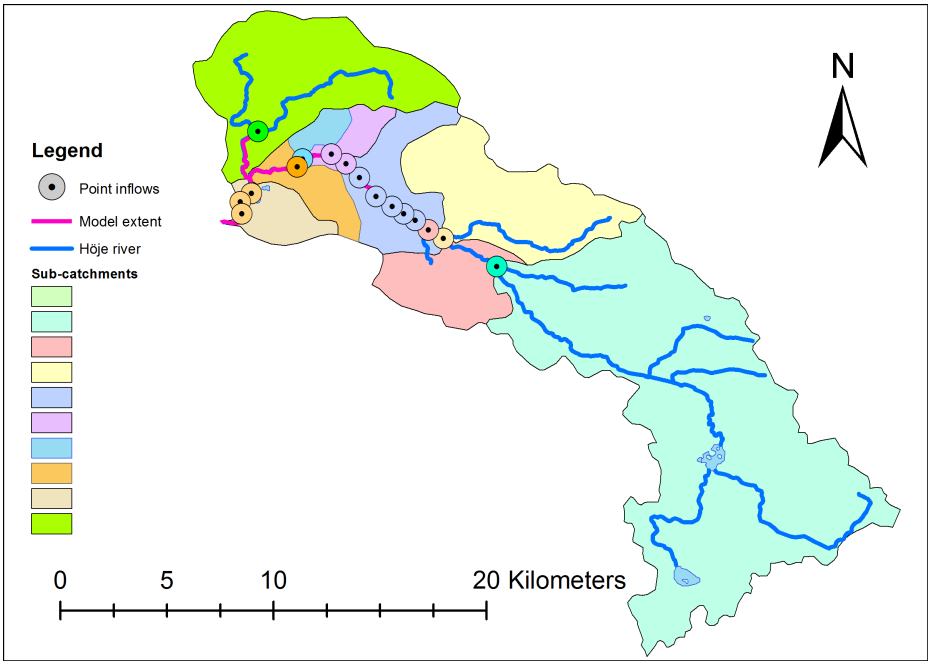

Figure A.2: Map showing the connection between point inflow boundaries and the sub-catchments. The color of the points indicates from which sub-catchment (same color) the flow originates.

B Frequency analysis

To estimate extreme flows and extreme sea water levels frequency analyses of flow measurement from Trolleberg and sea water level measurements from Barsebäck were carried out. The results from these analyses are presented under sections 6.4 and 6.5. This section will briefly introduce the methodology for carrying out a frequency analysis.

Annual maxima were extracted from the two dataseries: Gumbel distributions and Generalized Extreme Value distributions(GEV) were fitted to the maxima. The following model was adopted:

X_i = Daily average flow or water level during year i

M_n is the annual maximum flow

$$M_n = max(X_1, X_2, ...X_n)$$

If yearly maxima is assumed to independent it can be modeled using a GEV, where the distribution function G is given by

$$G(z) = exp\Big\{ - \Big[1 + \xi\Big(\frac{z-\mu}{\sigma}\Big)\Big]^{-1/\xi}\Big\} \tag{B.1}$$

Where μ is a location parameter, σ is a scale parameter and ξ is a shape parameter. (Coles, 2001).

Taking the limit of the GEV-distribution given by equation B.1 as the shape parameter $\xi \to \infty$ gives a special case of the GEV referred to as the Gumbel distribution. Its distribution function is given by:

$$G(z) = exp\Big[- exp\Big\{ - \Big(\frac{z-\mu}{\sigma}\Big)\Big\}\Big] \tag{B.2}$$

Flow and sea water levels with given return periods were calculated through extracting the corresponding quantiles from the fitted distributions.

B.1 Flow data from Trolleberg

Yearly maxima were extracted from a flow date series containing average daily from from 1973-2016. GEV and Gumbel distributions were fitted to the recorded annual maximum flow using MATLAB (version 2015a), and flow with return periods of 500, 100, 50, 10 and years were calculated. The figure below shows the empirical distribution function of annual maximum flow, and the fitted Gumbel and GEV distribution functions.

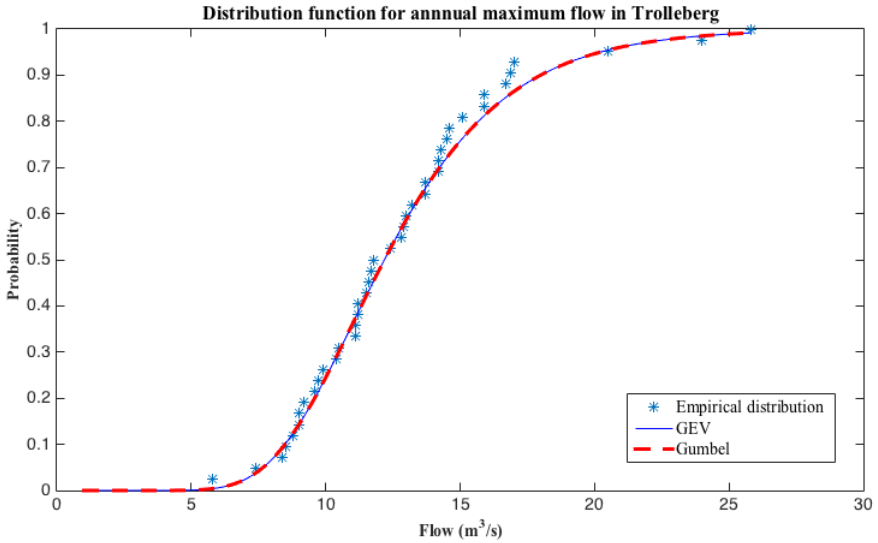

Figure B.1: Empirical distribution function and GEV and Gumbel distribution functions fitted to annual maximum flow data from Trolleberg 1973-2016.

Both distributions seem to fit well with data. Return period flows were calulated from both the Gumbel and the GEV distribution. The return period flows are presented in table B.1 below. The calculated return period flows were the same down to two decimals accuracy, therefore, only one result column is presented.

Table B.1: Results from frequency analysis of flow data from Trolleberg station.

Return Period (years)	Flow (m^3/s)
5	15.7
10	18.0
50	23.2
100	25.2
200	27.4

B.2 Sea level data from Barsebäck

Sea water level data recorded at Barsebäck from 1992-2016 was analysed. Yeary maxima was extracted and Gumbel and GEV distributions were fitted to the data series using MATLAB (version 2015a). The figure below shows empirical and fitted distribution functions.

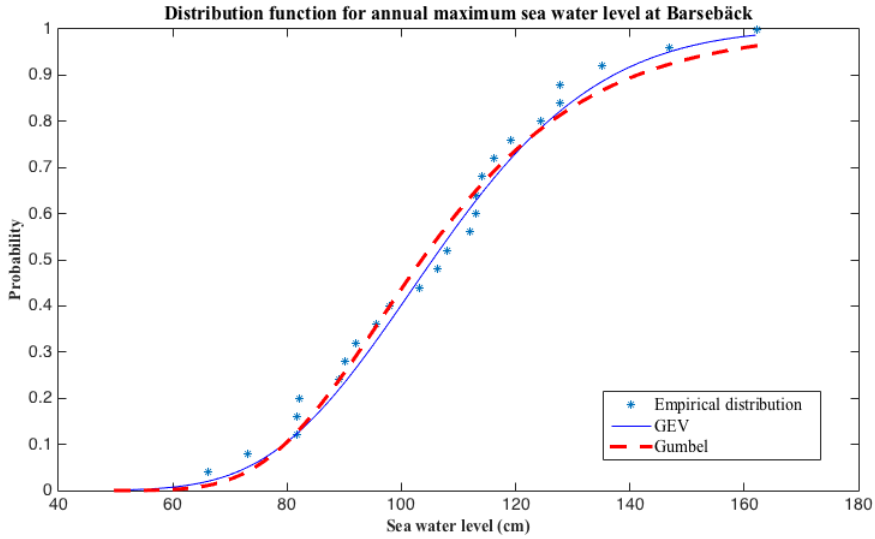

Figure B.2: Empirical distribution and GEV and Gumbel distribution functions adjusted to annual maximum sea water level in Barsebäck 1992-2016

The GEV distribution was considered to best describe the data, however return period water levels were calculated using both distributions for comparison. Water levels with return periods of 5, 10, 50 100 and 200 years were calculated, the results are presented in table, B.2. Water levels are given in reference system RH2000.

Table B.2: Results from frequency analysis of sea water level data from Barsebäck

Return Period (years)	Sea water level (cm) GEV	Sea water level (cm) Gumbel
5	126	126
10	137	141
50	158	174
100	165	188
200	171	202

B.3 Design rain

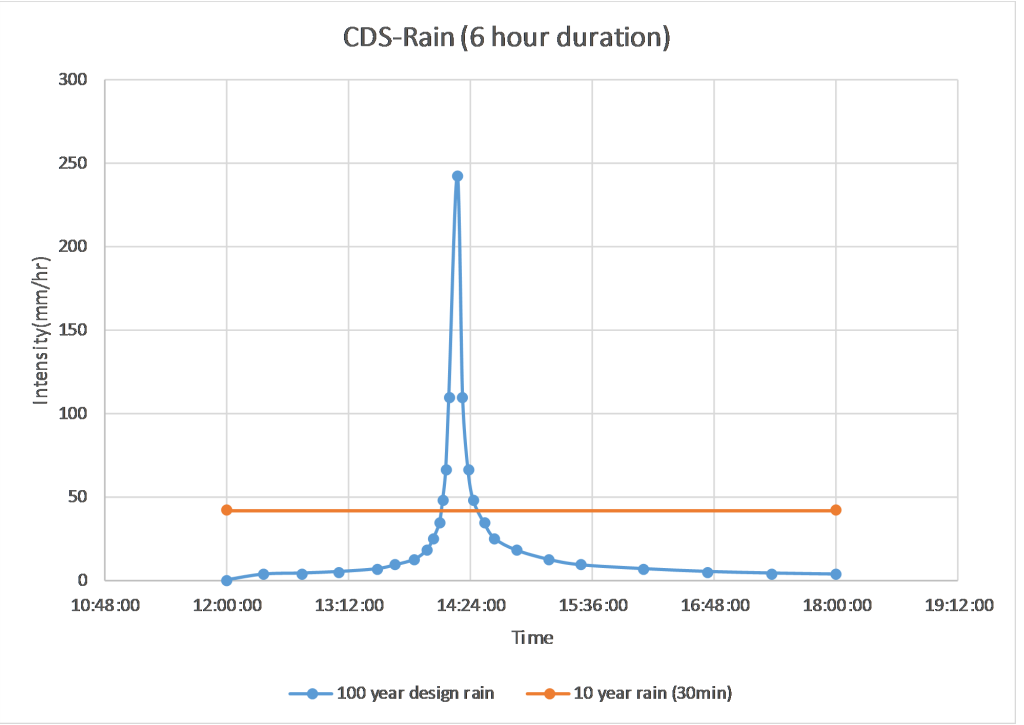

Figure B.3: 6 hour CDS-rain where the capacity of a 10year rain with 30min duration is removed to compensate for the capacity of the stormwater system.

C Calibration

The figure shows the location of the point where the model results were extracted and compared.

Figure C.1: Location of comparison between calibrated models